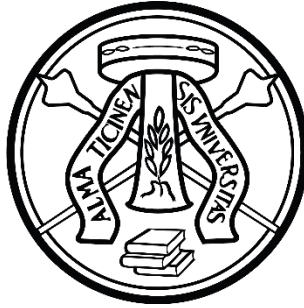


University of Pavia

Brain and Behavioral Sciences Department



Metric biases in body and object representations

Doctoral thesis for the degree of Doctor of Philosophy

Ph.D program in Psychology, Neuroscience and Medical Statistics

XXXII Cycle 2016-2019

Doctoral Candidate: **Valeria Carmen Peviani**

Under the supervision of: **Prof. Gabriella Bottini**

Pavia, September 2019

Table of contents

Abstract	4
General Introduction	6
Chapter 1: Biased body representations and movement	12
<i>Study 1: The biased representation of the hand serves perception and action</i>	12
Introduction	12
Method	13
Participants	13
Tasks and Procedure	14
Analysis	16
Results	18
Interim discussion	24
<i>Study 2: The motor system (partially) deceives body representation biases in absence of visual correcting cues</i>	26
Introduction	26
Method	28
Participants	28
Tasks and Procedure	29
Analysis	29
Results	31
Interim discussion	34
Biased body representations and movement: general discussion	37
Chapter 2: Factors modulating metric biases in body and objects representations	38
<i>Study 3: Visual and somatosensory information contribute to biases in body representation</i>	38
Introduction	38
Method	39
Participants	39
Tasks and Procedure	39
Analysis	41
Results	43
Interim discussion	46
<i>Study 4: Biases in body representation: are they body specific?</i>	50
Introduction	50
Method	52
Experiment 1: Hand, owned Mobile phone	52
Experiment 2: Hand and owned Mobile phone, Fake Hand and unfamiliar Mobile phone	54
Experiment 3: Hand, Fake Hand, Mug	56

Experiment 4: Fake Hand and Hand before and after the Rubber Hand Illusion	58
Experiment 5 and 6: the role of object affordances	63
Analysis on the pooled data	66
Interim discussion	68
<i>Study 5: Exploring the direct electrophysiological correlates of hand and object size estimation: an sEEG study</i>	70
Introduction	70
Method	71
Patients	71
Task and procedure	71
Behavioural results	72
sEEG coverage and acquisition	74
Cortical reconstruction	74
sEEG analysis	74
Results	77
Interim discussion	82
Factors modulating metric biases in body and objects representations: general discussion	87
<hr/>	
Metric biases in body representations: Conclusions	88
Supplementary materials	91
References	110
Acknowledgements	116

Abstract

Metric biases in body and object representations

The dimensions and proportion of our body parts are typically misestimated. For instance, the hand is perceived as distorted, with its width overrepresented compared to its length. Even though we misperceive its shape and dimensions, our hand is the protagonist of extremely accurate fine movements, as well as the means by which we sense the world.

This thesis is organised into two chapters. The first one describes two studies aimed at investigating the role of the biased representation of the hand in motor planning and execution. In Study 1, we provided evidence in support of the hypothesis that our motor system makes use of the distorted hand representation when movements are performed in absence of visual guidance: we observed that the pattern of errors in a proprioceptive matching task was compatible with biases affecting the hand representation. However, we also found that the error's magnitude was reduced compared to what predicted by that hypothesis. Results of Study 2 suggest that the motor system refines the movement trajectories, partially overcoming the misestimation of the hand dimensions, by integrating current somatosensory inflow and motor outflow. Our results highlight the role of these systematic biases, as an important source of error, in movement driven by proprioception only, and prompt to shift the focus from the body as an isolated system, to the body as integrated and active into the environment.

In this vein, the second chapter enters the debate regarding the specificity of the metric biases affecting body representations, by testing whether these biases extend to the surrounding environment, and which sensorial information and higher-order factors modulate them. Study 3 addresses the role of visual and somatosensory information in estimating the size of our body, by comparing the perceived dimensions of body parts affording different degrees of tactile acuity and visual accessibility. We found that both visual and somatosensory factors are likely to shape biases affecting body representations, and that somatosensory factors come into play mostly when visual cues are poor, ambiguous or unavailable. In Study 4, we investigated whether the metric biases are specific to the size estimation of the body, or whether they generalise to the size estimation of objects, too. We reasoned that, from an ecological perspective, the selective misestimation of our body dimensions may not be functional to an efficient interaction with the environment. An extensive investigation of the perceived dimensions of the hand and several objects showed that metric biases indeed extended to objects, were stable over time and were unrelated to the degree of familiarity or sense of ownership for the object. Yet, the pattern of the distortions might depend, at least to a degree, on the manipulability of the object, since objects which do not afford manipulation and interaction were differently represented.

Finally, Study 5 sought to elucidate the neural underpinnings associated with these last results. We recruited six patients with refractory epilepsy undergoing stereo-EEG recordings for diagnostic reasons, to study the electrophysiological responses elicited during the size estimation of the participant's hand and of a highly familiar and manipulable object (participant's mobile phone). The similar behavioural pattern of distortions affecting those two targets was reflected by similar activity in the high- γ band, spreading over occipito-temporal, posterior parietal and frontal areas, consistent with the involvement of the visual imagery network. In two patients, we also registered a higher activity over the precentral area during the size estimation of the hand compared to that of the mobile phone, possibly supporting the additional role of the sensorimotor cortex in hand metric representation.

Together, our results speak for a multisensory origin of the metric biases affecting body representations and for their involvement in motor planning and execution. Furthermore, these biases are mirrored in the representations of external objects, especially when objects afford action-oriented behaviour, i.e., interaction and manipulation. The fact that both the effector and the object of our actions are affected by metric biases, highlights the importance of considering and addressing the interaction between body representation and perception of the surrounding environment.

General Introduction

Metric biases in body and object representations

The body is our primary interface with the world: it allows us to gather inputs from the outside, to build a representation of the world, to act and directly manipulate the environment. In order to accomplish this, our brain needs to represent the configuration of our body segments in space. This mental representation of the body, also named “body schema” is the result of the integration of multisensory inputs coming from the visual, proprioceptive, tactile, vestibular and motor systems (de Vignemont, 2010; Dijkerman & de Haan, 2007; Paillard, 1999), with implicit information about body dimensions. The information about body dimensions is stored by a specific component of the body representation, conceptualised as the “body model” (Longo, 2015a; Longo & Haggard, 2010), which has recently been the object of a growing attention.

Surprisingly, metric information about the body is not as accurate as one may expect. As a matter of fact, we show poor accuracy in judging our body proportion and dimensions (Linkenauger et al., 2015; Longo, 2015a; Sadibolova, Ferrè, Linkenauger, & Longo, 2019). The bulk of evidence for a distorted body representation comes from studies investigating the perceived dimensions of the hand. In a seminal study, Longo and Haggard (2010) used the Localisation Task to measure the perceived hand shape. They asked participants to point to the perceived location of different landmarks (tips and knuckles) of their own occluded hand. The perceived position of tips and knuckles of the hand was biased, resulting in a distorted hand representation, shorter and wider compared to the actual hand shape (i.e. the finger length was underestimated, whereas the hand width was overestimated). The biased hand representation measured through the Localisation Task has since been documented by a number of studies (e.g. Cocchini, Galligan, Mora, & Kuhn, 2018; Coelho & Gonzalez, 2018; Ganea & Longo, 2017; Longo & Haggard, 2012b), and turned out to be fairly robust to different experimental manipulations (e.g. tactile cues instead of verbal instructions [Mattioni & Longo, 2014]; the absence of non-informative vision [Longo, 2014]; different hand postures [Longo, 2015c]). Other studies showed that these biases vary in magnitude depending on the task used. Biases are reduced in magnitude when participants are asked to compare the length of a line with that of their own hand in a Line Length Judgment Task (e.g. Longo & Haggard, 2012b; Peviani, Melloni & Bottini, 2019). This difference has been attributed to the retrieval of a more implicit hand representation during the Localisation Task compared to the Line Length Judgment Task (Longo & Haggard, 2012b). However, other studies demonstrated that the distortions resulting from the Localisation Task are partially biased by a mislocalisation of the knuckles, perceived as closer to the fingertips than they actually are. Specifically, when participants were asked to explicitly locate their knuckles on their palm, either with or without visual feedback, they made a systematic distal error

(Longo, 2015c). A similar distal error was detected when participants were asked to localise the knuckles on a hand silhouette, or on someone else's hand (Longo, Mattioni, & Ganea, 2015). Importantly, once the mislocalisation of the knuckles was measured and regressed out, the hand metric biases were significantly reduced, and comparable to those arising from the Line Length Judgment Task (Saulton, Bühlhoff, & de la Rosa, 2017).

Even though we misperceive its shape and dimensions, our hand is the protagonist of extremely accurate fine movements, as well as the means of sensing the world. Each movement is based on the computation of a motor vector, which is defined by a certain amplitude and direction. The motor vector links the represented starting point with the represented ending point of the movement (Soechting & Flanders, 1992). When visual guidance is present, the starting point is computed through the integration of visual and proprioceptive information (Desmurget & Grafton, 2000). It can be hypothesised that, in absence of visual inputs, proprioceptive information is integrated with the hand representation, distorted in shape and dimensions, in order to provide the starting point of a motor vector.

The **first chapter** of this thesis describes two studies which aimed at testing this hypothesis, i.e., that in absence of visual inputs, proprioceptive information is integrated with the distorted hand representation in order to provide the starting point of a motor vector. More generally, the first chapter aimed at investigating the role of the biased representation of the hand in motor planning and execution. Concretely, we developed a dynamic version of the Localisation Task, named Proprioceptive Matching Task, in which participants were asked to match the tips and knuckles of their concealed hand with a visual target, by performing simple hand shifts. We then administered with both the tasks 21 healthy participants and compared the resulting maps.

To preview, we found that the hand maps resulting from the Localisation Task and the Proprioceptive Matching Task are qualitatively similar, suggesting that the starting points of the motor vectors lay on the biased metric representation (Peviani & Bottini, 2018). Such finding also speaks against the need of a conceptual distinction between the body schema, as the body representation emerging from the integration of multisensory inputs (de Vignemont, 2010; Dijkerman & de Haan, 2007; Paillard, 1999), and the body model, which stores information about the size and shape of our body (Longo, 2015a; Longo & Haggard, 2010). Indeed, we demonstrated that the distorted hand representation subserves motor control, which is coherent with the definition of body schema (Medina & Coslett, 2010). So far, there is no empirical evidence of a dissociation between the body schema and the body model.

Interestingly, the maps measured by means of the Localisation Task and of the Proprioceptive Matching Task presented a quantitative difference. In detail, the perceived hand shape in the dynamic condition was significantly more proportionated. A follow-up study (Peviani, Liotta & Bottini, submitted) aimed at gaining further insights on such phenomenon by testing the role of recent sensorimotor

information gained through the Proprioceptive Matching Task on the hand metric representation measured by means of the Localisation Task. If the gain of sensorimotor information can directly influence the perceived locations of the hand landmarks (i.e. the starting points of the motor vectors) it follows that the hand representation would be more accurate after the Proprioceptive Matching Task compared to after a rest period. Alternatively, if receiving sensorimotor input does not directly affect the hand representation, rather it refines the trajectory of the motor vectors, the Localisation Task should not detect any change in such representation after the Proprioceptive Matching Task. Our data on 24 healthy subjects suggest that the apparent adjustment of the hand representation observed during the Proprioceptive Matching Task does not reflect an actual change in how the hand is represented. Instead, it is likely to reflect the refinement of the movement trajectory, providing interesting insights about how the motor system partially overcomes metric biases in body representations.

With the purpose to continue extending the focus of the investigation from the body as an isolated system to the body as active in and interactive with environment, the **second chapter** of this thesis enters the debate regarding the nature and specificity of the biases affecting body representations. We ran three studies aimed at investigating to which extent the metric biases are body-specific, or they extend to objects in the environment. In these studies we assessed the metric representation of several targets (either objects or body parts) using the Line Length Judgment Task, adapted from Longo & Haggard (2012), in which participants were required to compare the perceived dimensions of the unseen target with the length of a line displayed on the computer screen.

In the first study (Peviani, Melloni & Bottini, 2019), we addressed the role of visual and somatosensory factors in determining the perceived dimensions of our body parts. We hypothesised that, if an unspecific bias generally shapes our mental representations (e.g. a bias related to visual perception and/or visual imagery), different body parts should be similarly misrepresented. It has been argued that the biases affecting the body representation are a consequence of the massively distorted somatotopic representation, also known as the homunculus (Linkenauger et al., 2015; Longo, 2015a; Sadibolova et al., 2019). This hypothesis developed from two pieces of evidence. Firstly, the anisotropy of the hand representation, characterised by a higher underestimation of the vertical dimension (the finger length) compared to the horizontal one (the hand width) has been associated (Longo, 2015a) to the presence of oval-shaped receptive fields in the hairy portions of the skin, whose axes are more often oriented along the length of the limbs (Cody, Garside, Lloyd, & Poliakoff, 2008; Schady & Torebjörk, 1983; Stevens & Choo, 1996). Secondly, distortions of length estimates of body parts scale with the respective body part's tactile acuity. Tactile acuity can be defined as the ability to discriminate two tactile stimuli on the skin, and it is often measured in terms of two-points discrimination threshold, which is the minimum distance at which two tactile stimuli are discerned. The tactile acuity depends on the receptive field's density in a

certain portion of the skin, and it is proportional to the cortical representation of that body part (Penfield, & Rasmussen, 1950; Weinstein, 1968). Previous studies reported that less sensitive body parts (e.g., arm, leg and torso) are perceived as longer than more sensitive body parts (the hand and the foot), suggesting the existence of a compensatory mechanism, for which body parts that are underrepresented at the cortical level are overrepresented at the cognitive level (Linkenauger et al., 2015; Sadibolova et al., 2019).

However, recent investigations have highlighted the need to address the influence of non-somatosensory factors (e.g. conceptual and visual) which are not specific to the body. We already mentioned that once the visual mislocalisation of the finger knuckles was controlled, hand representation biases were reduced (Saulton, Bühlhoff, & de la Rosa, 2017). Critically, the same pattern of distortions was observed when participants were required to recall the dimensions of a fake hand, a hand-shaped rake and an inverted T-shaped object (Saulton, Dodds, Bühlhoff, & de la Rosa, 2015; Saulton, Longo, Wong, Bühlhoff, & de la Rosa, 2016). This last result suggests that the bias affecting body representations might be unspecific instead of body-specific; thus it might generally affect our mental representations, regardless of whether the representation relates to the body or to the surrounding environment. Vision research established that the perception of visual size is not accurate. The perceived size of a visual stimulus varies substantially across observers and across the visual field, and it is likely to be represented at very early stages of visual processing (Schwarzkopf, 2014). For instance, cortical idiosyncrasies in V1 predict inter-individual variability in size estimations, suggesting that individual differences in size estimation could be explained by cortical architectural features (Moutsiana et al., 2016). Furthermore, the eccentricity of a stimulus influences its perceived size: size underestimation increases with stimulus eccentricity (e.g. Bedell & Johnson, 1984). Three-dimensional objects are also affected by visual biases (e.g. Ganel & Goodale, 2003; Ganel, Chajut & Algom, 2008). It is conceivable that these biases underlie metric distortions affecting body and object mental representations.

Therefore, the first study, involving 37 healthy participants over two experiments, compared the metric representations across body parts affording different tactile acuity but also different degrees of visual accessibility. We found that both visual and somatosensory factors are likely to shape biases affecting body representations. Interestingly, we found that somatosensory factors come into play mostly when visual cues are poor, ambiguous or unavailable (i.e. when participants judged the dimensions of the dorsal portion of their neck).

In the second study instead, we tested whether these biases are specific to the size estimation of the body, or generalise to the size estimation of external physical entities. We reasoned that, from an ecological perspective, the selective misestimation of our body dimensions may not be functional for an efficient interaction with the environment. For instance, hand-object interaction is likely to be affected by the size misestimation of our hand (Peviani & Bottini, 2018). Under this perspective, it is reasonable to

hypothesise that these biases are not specific to the body, but extend to objects as well. However, we have little (and contrasting) evidence about how objects are represented compared to the hand (see for instance Saulton et al., 2017, 2015), and it is unknown whether objects' representations are modulated by different factors, such as familiarity with the object, the sense of ownership over it, and its manipulability. Therefore, in the second study, which involved 152 participants over six experiments, we compared the perceived dimensions of several objects, across different conditions (Peviani, Magnani, Bottini & Melloni, in preparation). If the pattern of distortions described for the hand is body-specific, we would expect to find differences between its representation and the representations of objects. Instead, it turned out that the pattern of distortions extends to several daily-life objects, such as a mobile phone and a coffee mug, independently of how familiar we are with them. On the contrary, a fake hand was systematically perceived as different compared to the participant's hand, even after the induction of a temporary feeling of ownership toward it, indicating that factors other than the hand-like shape and the feeling of ownership modulate the pattern of distortions of a hand-like object. For instance, intrinsic properties of the fake hand, such as its texture, rigidity and size, as well as the emotions that it possibly elicits and the actions that it possibly afford, may influence its size estimation. In line with the hypothesis that perception is action-specific (Witt, 2011), we reasoned that the affordances of an object, representing the possibility to act on such object (Gibson, 1979), might play a role in its perceived dimensions. To test this proposal, we compared the perceived dimensions of objects which either elicit or inhibit interaction with them. We found that objects that are potentially harmful (cactus) or disgusting (dirty soap) were differently perceived from the manipulable ones. Our data therefore suggest that the metric biases that affect the representation of the hand extend to the representation of real objects that are more likely to afford manipulation and interaction. This indicates that both the effector and the object of the action are not accurately perceived, providing a new perspective on the hand-object interaction problem and how this could be addressed in future work. For instance, it can be argued that, if we misperceive the dimensions of our hand, misperceiving the dimensions of objects we are likely to interact with would facilitate hand-object interaction.

In the third study (Peviani, Mariani, Tassi, Lo Russo, Melloni & Bottini, in preparation), we extended our investigation to the neural level. Despite the rich behavioural evidence attesting the similarity between the perceived dimensions of the hand and of manipulable objects, we cannot exclude that different neurocognitive mechanisms underlie the size estimation of one's own hand compared to an object. We therefore chose to compare the brain activity triggered by the size estimation of one's own unseen hand and one's own unseen mobile phone. Specifically, we analysed the direct electrophysiological responses recorded from intracranial electrodes in six patients with refractory epilepsy undergoing stereo-EEG recordings for diagnostic purposes. In short, we did not find evidence of

a differential neural activation across conditions. Instead, in both the conditions we observed an increased high- γ activity, which represents a reliable electrophysiological index of average neuronal population firing (Miller et al., 2007; Ray & Maunsell, 2011; Suffczynski, Crone, & Franaszczuk, 2014), spreading in occipito-temporal, posterior parietal and frontal areas, consistent with the involvement of the visual imagery network (Winlove et al., 2018). In addition, for two patients we recorded a difference in the β response over the precentral gyrus between Hand and Mobile conditions, which needs to be further addressed in order to establish whether, besides visual imagery, sensorimotor processing has an additional role in hand metric representation.

To summarise, this thesis aimed at contributing to a better understanding of the body representation, with a focus on the metric biases characterising it. While most of the research addressing biases in metric representations studied the body as the object of our perception, we tried to re-discover its role as the effector of our actions. In detail, we investigated whether the motor system makes use of a distorted body representation and we shed the light on how it partially corrects for its biases. We showed that, along with the contribution of visual inputs, the estimation of our body metrics is likely to rely also on sensorimotor cues, especially when visual information is poor or ambiguous, in line with the notion that body representations are built from the integration of multiple sensory inputs available in a particular moment (de Vignemont, 2010). Furthermore, our behavioural and electrophysiological data suggest that the pattern of distortions ascribed to the hand representation extends to objects that afford manipulation, indicating that both the effector and the object of our actions are misperceived in their dimensions. Together, our results highlight the importance of considering and addressing the interaction between body representation and perception of the surrounding environment.

Chapter 1: Biased body representations and movement

Study 1: The biased representation of the hand serves perception and action ¹

Introduction

As described above, it has been shown that we systematically misperceive the dimensions of our hand, as we tend to underestimate finger length compared to hand width (Longo, 2015a; Longo & Haggard, 2010). However, even though we implicitly represent our hand as distorted, we are generally able to perform accurate fine movements. This discrepancy might be explained by the fact that visual feedback partially offsets the body representation distortions while moving. Indeed, movement accuracy decreases without visual guidance (e.g. Kuling, Brenner, & Smeets, 2013). However, no systematic error pattern attributable to body model distortions was documented in Proprioceptive Matching Tasks performed in absence of sight. For instance, in a recent study (Kuling, van der Graaff, Brenner, & Smeets, 2017), authors asked participants to perform pointing movements at visual targets with the left or the right unseen hand in different postures (palm facing up or down). The matching errors were too inconsistent across subjects and across experimental conditions to be read as the result of systematic misjudgements of the finger positions. Nevertheless, since both the hand posture and the fingers configuration have shown to influence the hand perceived shape (Longo, 2015c; Longo & Haggard, 2012a) we argue that it is crucial to accurately handle those factors in order to reduce the noise of the results and allow to draw conclusion about the role of the distorted hand representation in motor programming.

Therefore, Study 1 (Peviani & Bottini, 2018) was set out to investigate whether, in absence of visual guidance, movement planning is based on the distorted hand representation. Each movement is based on the computation of a motor vector, which links the starting point with the ending point of the movement (Soechting & Flanders, 1992). Generally, the starting point, which is the representation of the initial position of the body part involved in the movement, is computed through the integration of visual and proprioceptive information (Desmurget & Grafton, 2000). We aimed at exploring whether, in absence of visual guidance, the starting point of the motor vectors is based on the biased hand representation.

To achieve this goal, we developed a dynamic version of the Localisation Task, LT (Longo & Haggard, 2010): the Proprioceptive Matching Task (PMT), designed to study the role of the distorted hand representation in simple motor performance. Indeed, this task aimed at reducing the noise level, which may come from changes in posture and fingers configurations, and at isolating, if involved, the distorted hand representation in a motor performance. While in the LT participants were asked to indicate the perceived location of tips and knuckles of their hidden hand, in the PMT participants were asked to

¹ The following sections (introduction, method, analysis and discussion relative to Study 1) have been largely extracted and adapted from Peviani & Bottini (2018).

match tips and knuckles of their concealed hand with a visual target, by performing simple hand shifts. Each PMT item requires a motor vector to be computed from the perceived position of that specific landmark (starting point) to the perceived position of the visual target (ending point). The starting points of the motor vectors were charted to obtain the PMT map.

If the distorted hand representation provides the motor system with the movement starting points, the PMT map would resemble the LT map. Alternatively, such representation could only subserve body perception, yet not action. So far indeed, the metric body representation has been investigated in body perception tasks such as the Localisation Task (Longo & Haggard, 2010), tasks involving judgments of body size (Linkenauger et al., 2015; Longo & Haggard, 2012a), and judgments of tactile size (Longo & Haggard, 2011). A dissociation between action-oriented and perception-oriented body representations has been proposed (Dijkerman & de Haan, 2007). Different processes and representations might be involved when a body part has to be localised rather than a motor vector being computed. The study by Sittig and colleagues (1985) elegantly showed that the movement performance can be independent from the perceived position of a certain body part. The authors induced a shift in the position of the participant's forearm by applying a vibration on the biceps tendon. This technique prompts a shift of the forearm, unnoticed by the subject. Although the subjects misperceived the forearm position after the involuntary shift, in the absence of visual guidance, the movements toward an external target were quite accurate. This outcome suggests that the representation of the forearm position used by the motor system may dissociate from the subject's conscious representation of its position.

To summarise, Study 1 aimed at investigating if motor programs are primarily based on the perceived position of a body part, achieved by the integration of the (distorted) body representation with incoming sensory information. To this purpose, both the LT and the PMT were administered in a within-subject counterbalanced design, and the resulting hand maps were compared.

Method

Participants

Twenty-one (6 males) healthy participants were enrolled and received university credits for participating in the study. They all were right-handed as assessed by the Edinburgh Handedness Inventory (Oldfield, 1971). They were aged between 20 and 39 (mean 23.90 ± 4.36 years). All the participants gave their Informed Consent to participate in the study. The study was designed according to the ethical standards of the Declaration of Helsinki and approved by the Ethical Committee of the University of Pavia.

Tasks and Procedure

Prior to the experiment, participants were required to point out both the tip and knuckle of each finger on a 2D hand model, to prevent conceptual misunderstanding. Participants were instructed to consider the tip of each finger as the central point of the nail and the knuckle as the protruding part of the metacarpophalangeal bone.

In the PMT (**Figure 1.1a** and **Figure 1.1b**) participants sat in front of a desk. They were asked to place the right hand inside a freely supported cardboard white box (35 x 35 x 6 cm), while blindfolded. The box had an upper removable lid and an emery paper bottom, whose friction, along with the use of double-sided tape, would prevent the participant's finger from sliding from the initial position during the task. Furthermore, participants were instructed to retain the fingers from moving for the entire test. In addition, to enable the conversion from pixels to centimeters during the off-line data processing, a 5 cm ruler was fastened to the bottom. A baseline photograph (1280 x 960 pixels) was taken to the participant's hand, in position, before closing the box, by a camera (Microsoft LifeCam VX-2000) orthogonally located over the apparatus at 50 cm height. The baseline photograph was then compared with the hand position at the end of the experiment to make sure that no remarkable changes in finger configurations occurred during the task. The blindfolding was removed from the participant's eyes once the box lid was closed, to allow a full visual feedback of the box, of the targets and of the participant's matching movements during the entire task duration. In the starting position participants had the right hand aligned with their body midline and the left hand under the desk. Marks were previously drawn on the table in order to help participants to return to the initial position after each trial was completed.

Each item consisted of a vocal instruction read by the experimenter providing one of the ten hand landmarks (tips and knuckles of the hand) and one of the four visual targets (e.g. "Tip of the index finger, target A"). Participants were instructed to slide the right hand, consequently the box, onto which the hand was fixed, in order to align the perceived position of that specific landmark with that of the visual target. The four visual targets were printed on a Plexiglas board (80 x 20 cm), placed over the box. The targets corresponded to the square of a rectangle (17 x 13 cm). The PMT comprised 400 randomised items (40 for each of the ten landmarks equally distributed for the four visual targets), split into two consecutive blocks interspersed by a 3-minute break. No time limit was given, although participants were required to perform a direct, straight movement and to halt as soon as they felt the landmark to be aligned with the target. After each movement, a picture was taken for the off-line data processing. The participant was then instructed to return to the starting position.

The LT consisted of a slightly modified paradigm by Longo & Haggard (2010). While in the PMT the white box was free to move, in the LT it was fastened to the table. As in the PMT, prior to sealing the box and the participant's eyes being unblindfolded, a photograph of the hand was taken. The

participants had a full visual feedback of the box, of the stick and of their Localisation movements during the entire task duration. Each item (**Figure 1.1a**) consisted of a vocal instruction read by the experimenter providing one of the ten hand landmarks (e.g. “tip of the index finger”). Participants were asked to point with the right hand at the perceived location of that landmark by means of a stick over the box surface. The LT was composed of 400 randomised items split into two consecutive blocks. After each pointing, a picture was taken for the off-line data processing.

Each participant performed both the tasks during two consecutive sessions, in a within-subject counterbalanced design. In order to maximise accuracy in both tasks, movements were accomplished by the right dominant hand. Consequently, in the LT participants localised landmarks using the right hand, while in the PMT they moved their right hand toward the visual targets. Therefore, for each subject we obtained a right hand map by the PMT and a left hand map by the LT. As a research on 633 healthy subjects (mean age 22.11 ± 2.07) showed, the asymmetry of human right and left hands is very subtle (Barut, Sevinc, & Sumbuloglu, 2011). Moreover, previous studies provided evidence about the similarity between the body model of the dominant and non-dominant hand (Longo & Haggard, 2010). Hence, we applied a symmetrical transformation to the right hands’ maps in order to compare them to the left hands’ ones.

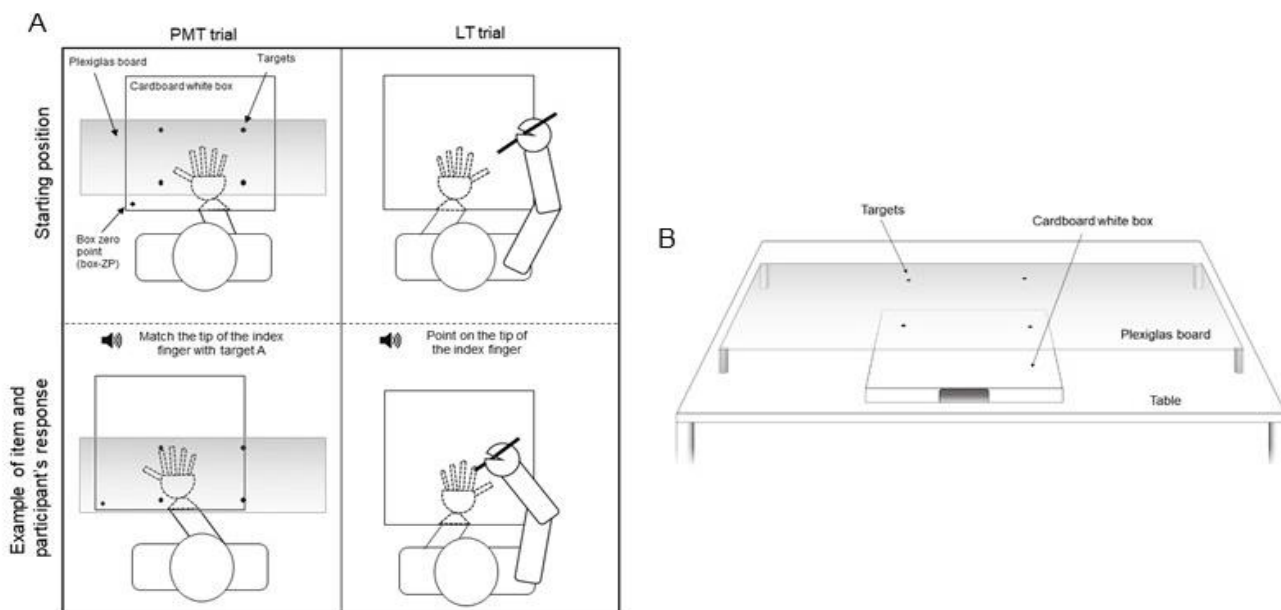


Figure 1.1 (a) The starting positions for the PMT (top-left) and LT (top-right) are depicted. Bottom-left, an example of item and a plausible response for the PMT is represented: the participant has slid the cardboard white box in which his/her hand is fixed to align the perceived position of his/her index fingertip with one of the targets. Bottom-right, an example of item and a plausible response for the LT is depicted: the participant has pinpointed the perceived position of his/her index fingertip by putting a stick on the cardboard white box in which his/her hand is fixed. (b) The experimental setup for the PMT is depicted in 3D from the participant's side. Participants were asked to sit at the table and insert the hand in the box through the designated hole on its side.

Analysis

All the XY coordinates were manually extracted from the pictures using ImageJ (Abràmoff, Magalhães, & Ram, 2004) and all centered on a fixed point marked on the desk surface (zero point, ZP). More specifically, the XY coordinates of the ten landmarks (central points of each nail and of each knuckle) belonging to the left and right hands were extracted from baseline pictures taken before each task. For each LT's item, the XY coordinates of the stick tip pointing at the board were extracted for each picture. Regarding the PMT, for each participant, XY coordinates of the four visual targets and those of a square mark on the left lower box surface corner (box-ZP) were coded in the starting position. For each item, the coordinates of the box-ZP position after movement were extrapolated from each picture. The motor vector for each item was computed as the difference between the XY coordinates of the box-ZP after movement and those of the box-ZP in starting position. For each item, the perceived position of the landmark was computed by subtracting the item's motor vector from the item's visual target coordinates.

Consequently, mean XY coordinates were computed for each perceived landmark position for the PMT and the LT, obtaining the perceived PMT and LT maps for each subject. A symmetrical transformation across a vertical straight line was applied on the PMT map. For each map, estimated finger lengths (distance between each tip-knuckle pair), estimated mean finger length (average of finger lengths), estimated hand width (distance between index and little finger's knuckles) and the shape index (SI: $100 \times \text{hand width} / \text{middle finger length}$) were computed in pixels. For each participant, actual finger length, actual hand width and SI were computed as the mean of the left and right actual measurements. All the measurements were converted in centimeters. In order to allow comparisons across subjects, ratios between perceived and actual measurements were computed for each participant (estimation ratio, ER). When $ER = 1$, the perceived distance is accurate, when $ER < 1$ the perceived distance is underestimated compared to the actual one, whereas when $ER > 1$, the perceived distance is overestimated. ERs were computed for each finger length, mean finger length, knuckle spacing and hand width.

At first, we used the software MorphoJ (Klingenberg, 2011) to compute morphometric analyses. Previously, we removed the differences in terms of finger postures across tasks and subjects, following the same procedure reported by Longo & Haggard (2010). In detail, for each map, the XY coordinates of each fingertip were twisted to match the template posture used by Longo & Haggard (2010). Later, we used Generalized Procrustes Alignment to perform Procrustes superimpositions aligning by the principal axes for LT, PMT and the actual maps separately in order to adjust object size, location and orientation (Bookstein, 1997). In so doing, we obtained a new set of shape variables and coordinates in Bookstein Units (BU). We used the Procrustes Analysis of Variance (ANOVA) to test for differences in shape,

quantified by the Procrustes distance (sum of the distances between corresponding landmarks of two shapes) among conditions (Goodall, 1991).

As a second step, we compared the SIs and ERs across conditions. In particular, we ran paired t-tests and repeated measures ANOVAs with statistical package SPSS (IBM Corp. Released 2010). Normality assumptions were previously checked. In each analysis, the condition (LT, PMT or actual measures) was the independent variable whereas the ER was the dependent variable.

Finally, we adopted a different approach (Lag-1 analysis) recently developed (Medina & Duckett, 2017) to further examine our data. The authors argued that averaging among trials may mask potential biases that could contribute to explain the hand representational distortions. They administered the LT selectively on the hand knuckles and found that biases in spatial localisation of memorised targets were more likely to explain the body model distortions. We performed the Lag-1 analyses on the LT and PMT data considering all the ten hand's landmarks. The first analysis was set out to explore whether the participants used the n-1 trial perceived location to make a Localisation judgment on trial n. Firstly, for each task, we computed the actual lag-1 vector (vector between the actual position on trial n-1 and the actual position on trial n), the perceived lag-1 vector (vector between the perceived position on trial n-1 and the perceived position on trial n). Then, we computed the perceived origin error (POE) (difference between the actual lag-1 vector and the perceived lag-1 vector in terms of both the Euclidean distance and Euclidean angle) and the actual origin error (AOE) (difference between the actual lag-1 vector and the vector between the actual position on trial n-1 to the perceived position on trial n in terms of both the Euclidean distance and Euclidean angle). As the distributions of all the four variables were skewed, we decided to use the medians as measures of their central tendency. We analysed the effects of Task (LT, PMT), Error Origin (POE, AOE) and Shift (between two knuckles (kk), between two fingertips (tt), between a fingertip and the relative knuckle (fkt) or a different finger's knuckle (kt)) through a 2x2x2 repeated-measures GLM for each vector's feature (Euclidean distance and angle) using SPSS (IBM Corp. Released 2010).

In the second set of analyses, we explored whether the perceived displacement is higher than the actual displacement on the medio-lateral shifts and lower than the actual displacement on the proximo-distal shifts. Firstly, we computed a model for each task and displacement component (medial, lateral, proximal and distal), for a total of 8 models, using the “nlme” package in R (Pinheiro, Bates, DebRoy, Sarkar, & R Core Team, 2018). We did not include in the models the displacements with no shift (e.g. in which the distance between the perceived location on trial n-1 and n is equal to zero in the medial dimension). In each model, we entered the actual displacement as a predictor and the perceived displacement as a dependent variable, controlling for the within-subjects differences by including the random effect of Subject. To compare the two tasks, we fitted a model for each dimension with the Actual

displacement, the Task and their interaction as fixed effects and the Subject as a random effect. The slope of each factor is a measure of the overestimation/underestimation of the perceived displacement compared to the actual displacement. Concretely, a slope > 1 represents an overestimation, whereas a slope < 1 represents an underestimation. The intercept instead is a measure of a possible constant bias in Localisation judgments.

Results

Procrustes fits revealed well-organised spatial maps for both LT and PMT. Procrustes ANOVAs detected a difference in mean shape between LT and actual maps (Goodall's $F(16,640)=33.20$, $p<.001$), as well as between PMT and actual maps (Goodall's $F(16,640)=18.17$, $p<.001$). The LT and PMT maps revealed different mean shapes (Goodall's $F(16,640)=18.80$, $p<.001$) as well. **Figure 1.2a** illustrates the shape differences among the three maps.

Differences in shape were confirmed by a repeated measures ANOVA comparing SIs in LT, PMT and actual maps ($F(2,20)=251.42$, $p<.001$, partial $\eta^2=.93$). In particular, the LT's SI revealed bigger distortions compared to the PMT's one (SIs: LT 141.90 ± 22.59 vs PMT: 120.94 ± 23.92 , $p=.005$), and they were both significantly different from the actual SI (Actual SI: 65.29 ± 4.21 , both $ps<.001$), as it is showed in **Figure 1.2a**. The difference in shape may represent a reduction of the distortions, as the estimation of LT and PMT SIs were significantly correlated ($r(19)=.52$, $p=.015$).

In order to better examine shape differences among the three maps we aimed at comparing the PMT and LT perceived dimensions with the actual ones. As actual ERs (Baseline, B) are equal to one by definition, one-sample t-tests against one were computed to for each PMT and LT's ER distribution.

Mean finger length was underestimated in both LT (ER = 0.56 ± 0.11 , 43.21% underestimation) and PMT maps (ER= 0.61 ± 0.10 , 39.15% underestimation), with $t_{LTvsB}(20)=-42.04$, $p<.001$; $t_{PMTvsB}(20)=-38.22$, $p<.001$ (**Figure 1.3a**). One-sample t-tests confirmed the underestimation of each finger length (**Figure 1.3b and Table 1.1**). Hand width was overestimated in both LT (ER= 1.23 ± 0.15 , 22.93% overestimation) and PMT (ER= 1.15 ± 0.16 , 14.97% overestimation), with $t_{LTvsB}(20)=12.64$, $p<.001$; $t_{PMTvsB}(20)=8.393$, $p<.001$ (**Figure 1.4a**). Paired t-test analyses showed a similar overestimation of each knuckle spacing between the index and little finger in LT and PMT. A distinct pattern was observed for the thumb-index knuckle spacing, which was accurately estimated in LT and underestimated in PMT (**Figure 1.4b and Table 1.2**). No significant differences resulted between LT and PMT maps in both mean finger length ERs ($t(20)=-1.908$, $p=.212$) and hand width ERs ($t(20)=2.12$, $p=.139$) (**Figure 1.3a and Figure 1.4a**). Differences in individual finger length ERs between LT and PMT are reported in **Table 1.1**. Bonferroni corrections were applied within each analysis to reduce the probability of a type-1 error.

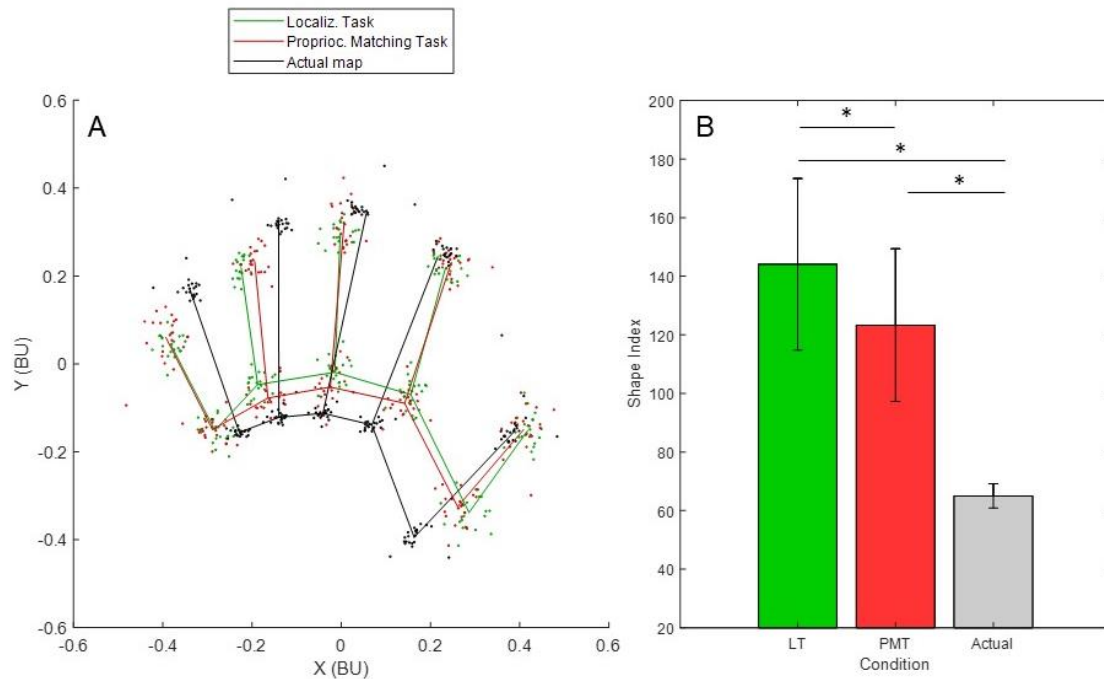


Figure 1.2 (a) Representations of the Proprioceptive Matching Task (PMT), Localisation Task (LT) and Actual hand maps were obtained by plotting the results of the Procrustes fits in Bookstein units (BU). For each participant, the BU coordinates have been averaged across trials separately for each landmark. Lines connect the averaged BU coordinates across participants. (b) Shape indexes (hand width * 100 / middle finger length) resulting from PMT, LT and Actual hand measures are displayed. Asterisks represent significant differences ($p < .05$, Bonferroni corrected).

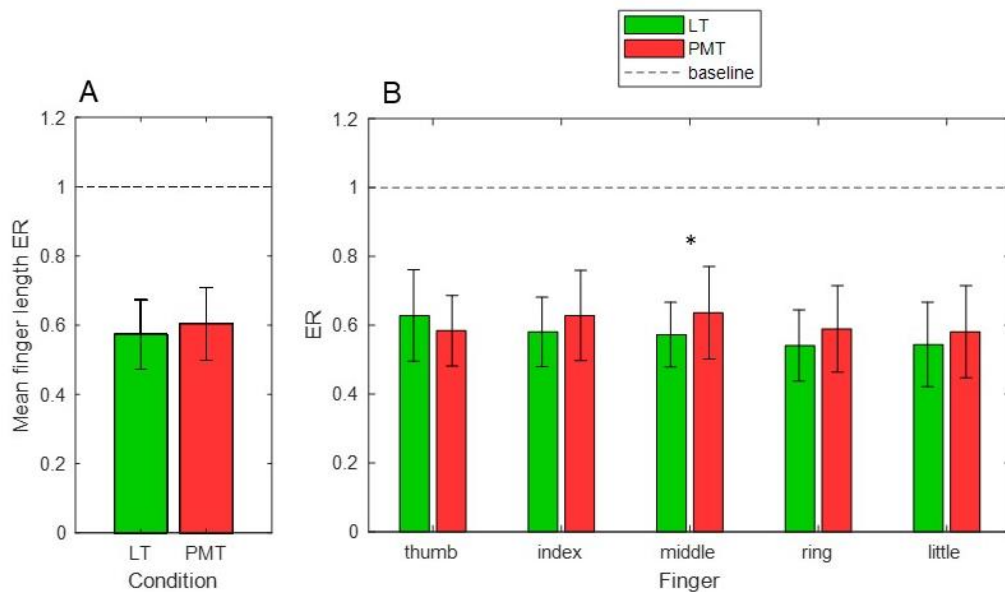


Figure 1.3 (a) Mean finger length ERs are represented for the LT and PMT. A significant ($p < .001$) underestimation of both ERs compared to the baseline (dashed line) was detected. (b) ERs for each finger length are represented for LT and PMT. All ERs significantly differed ($p < .001$, Bonferroni corrected) from the baseline. The asterisk represents a significant difference ($p < .05$, Bonferroni corrected) between LT and PMT perceived length of the middle finger.

			Thumb	Index	Middle	Ring	Little
A Descriptive statistics (Finger length ERs)							
LT	$M \pm SD$		0.62 ± 0.14	0.58 ± 0.09	0.57 ± 0.09	0.53 ± 0.12	0.54 ± 0.12
PMT	$M \pm SD$		0.60 ± 0.08	0.63 ± 0.12	0.64 ± 0.13	0.59 ± 0.11	0.58 ± 0.14
B Paired t-test (Finger Length ERs), 20 df							
LT vs baseline	t value Sig.		-24.59 $p < .001^*$	-38.22 $p < .001^*$	-31.11 $p < .001^*$	-31.03 $p < .001^*$	-33.83 $p < .001^*$
PMT vs baseline	t value Sig.		-35.64 $p < .001^*$	-38.39 $p < .001^*$	-25.47 $p < .001^*$	-31.85 $p < .001^*$	-28.86 $p < .001^*$
LT vs PMT	t value Sig.		0.44 $p = 1.000$	-2.30 $p = .097$	-3.18 $p = .014^*$	-2.28 $p = 0.101$	-1.12 $p = .823$

Table 1.1 (a) Means (M) and standard deviations (SD) of each finger length ER in both conditions. (b) Results of one-sample t -tests comparing the finger length ERs of LT and PMT against 1 (baseline) and paired t -test analysis comparing finger length ERs across conditions. Asterisks represent statistical significance with $p < .05$ (Bonferroni corrected).

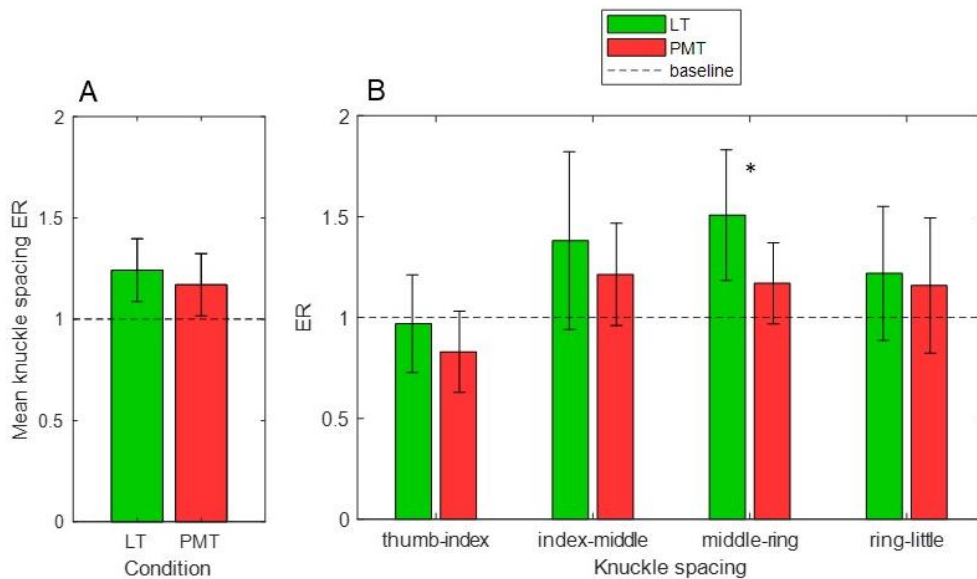


Figure 1.4 (a) Hand width ERs are represented for the LT and PMT. A significant ($p < .001$) overestimation of both ERs compared to the baseline (dashed line) was detected. (b) ERs for each knuckles spacing are represented for LT and PMT. All ERs significantly differed ($p < .05$, Bonferroni corrected) from the baseline, except for the LT thumb-index knuckles spacing. The asterisk represents a significant difference ($p < .001$, Bonferroni corrected) between LT and PMT representations middle-ring knuckles spacing.

		Thumb-index	Index-middle	Middle-ring	Ring-little
A Descriptive statistics (knuckle spacing ERs)					
LT	<i>M</i> ± <i>SD</i>	0.95 ± 0.25	1.32 ± 0.25	1.48 ± 0.30	1.17 ± 0.25
PMT	<i>M</i> ± <i>SD</i>	0.83 ± 0.20	1.21 ± 0.26	1.17 ± 0.18	1.14 ± 0.31
B Paired t-test (knuckle spacing ERs), 20 <i>df</i>					
LT vs baseline	<i>t</i> value Sig.	-1.47 <i>p</i> =0.473	9.55 <i>p</i> <0.001*	14.75 <i>p</i> <0.001*	4.13 <i>p</i> =0.002*
PMT vs baseline	<i>t</i> value Sig.	-5.29 <i>p</i> <0.001*	5.94 <i>p</i> <0.001*	5.65 <i>p</i> <0.001*	3.38 <i>p</i> =0.009*
LT vs PMT	<i>t</i> value Sig.	1.91 <i>p</i> =0.212	1.81 <i>p</i> =0.258	4.54 <i>p</i> =0.001*	0.38 <i>p</i> =1.000

*Table 1.2 (a) Means (M) and standard deviations (SD) of each knuckles spacing ER in both conditions. (b) Results of one-sample t-tests comparing the knuckles spacing ERs of LT and PMT against 1 (baseline) and paired t-test analysis comparing knuckles spacing ERs across conditions. Asterisks represent statistical significance with *p*<.05 (Bonferroni corrected).*

From the first set of Lag-1 analyses we found similar effects on both the dependent variables considered (Euclidean distance and error). Regarding the Euclidean distance, the main effects of Shift and Error Origin were significant, meaning that, on average, the Euclidean distance was different based on the landmarks involved ($\text{mean}_{\text{fkt}}=.117\pm.004$; $\text{mean}_{\text{kt}}=.128\pm.004$; $\text{mean}_{\text{fkt}}=.097\pm.002$; $\text{mean}_{\text{kt}}=.094\pm.003$; $F(3,60)=51.170$, $p<.001$), and was bigger for vectors with the *n*-1 perceived location as an origin (POE) and those with the *n*-1 actual location as an origins (AOE) ($\text{mean}_{\text{POE}}=.124\pm.003$; $\text{mean}_{\text{AOE}}=.094\pm.003$; $F(1,20)=1047.688$, $p<.001$). On the contrary, the main effect of Task was not significant ($F(1,20) = 1.984$, $p=.174$). More interestingly, all the interactions were significant (Task*Shift: $F(3,60)=16.833$, $p<.001$; Task*Error Origin: $F(1,20)=26.232$, $p<.001$; Shift*Error Origin: $F(3,60)=96.569$, $p<.001$; Shift*Error Origin*Task: $F(3,60)=26.988$, $p<.001$). The post-hoc comparisons on the three-way interaction revealed different patterns of results across shifts and tasks. Precisely, we found that in the LT the Euclidean distance was bigger for POE than for AOE only when the judgments involved a *kt* shift ($\text{mean}_{\text{POE-kt}}=.167\pm.007$; $\text{mean}_{\text{AOE-kt}}=.095\pm.003$; $p<.001$) or a *fkt* shift ($\text{mean}_{\text{POE-fkt}}=.145\pm.007$; $\text{mean}_{\text{AOE-fkt}}=.093\pm.004$; $p<.001$), whereas the distance was bigger for the AOE compared to the POE when the judgments involved a *tt* shift ($\text{mean}_{\text{POE-tt}}=.078\pm.003$; $\text{mean}_{\text{AOE-tt}}=.091\pm.004$; $p=.002$) or a *kk* shift ($\text{mean}_{\text{POE-kk}}=.089\pm.003$; $\text{mean}_{\text{AOE-kk}}=.098\pm.004$; $p=.044$). For the MT task instead, the Euclidean judgment was always higher for the POE than for AOE ($\text{mean}_{\text{POE-fkt}}=.138\pm.006$ vs $\text{mean}_{\text{AOE-fkt}}=.093\pm.003$, $p<.001$; $\text{mean}_{\text{POE-kt}}=.156\pm.007$ vs $\text{mean}_{\text{AOE-kt}}=.094\pm.003$, $p<.001$; $\text{mean}_{\text{POE-tt}}=.113\pm.004$ vs $\text{mean}_{\text{AOE-tt}}=.096\pm.003$, $p<.001$; $\text{mean}_{\text{POE-kk}}=.108\pm.003$ vs $\text{mean}_{\text{AOE-kk}}=.092\pm.003$; $p<.001$). Expectedly, significant differences

between the two tasks were found only for the POE vectors involving the kk shifts ($p < .001$) and the tt shifts ($p < .001$).

When the Euclidean angle was considered, we found a main effect of Shift ($\text{mean}_{\text{fkt}} = 8.948 \pm .291$; $\text{mean}_{\text{kt}} = 10.280 \pm .443$; $\text{mean}_{\text{kk}} = 11.907 \pm .381$; $\text{mean}_{\text{tt}} = 6.985 \pm .182$; $F(1,20) = 45.313$, $p < .001$), and of Origin Error ($\text{mean}_{\text{POE}} = 10.218 \pm .216$; $\text{mean}_{\text{AOE}} = 8.841 \pm .264$; $F(3,60) = 30.783$, $p < .001$), whereas the main effect of Task was not significant ($F(1,20) = 3.049$, $p = .096$). All the interactions were significant (Task*Shift: $F(3,60) = 13.688$, $p < .001$; Task*Error Origin: $F(1,20) = 27.627$, $p < .001$; Shift*Error Origin: $F(3,60) = 73.533$, $p < .001$; Shift*Error Origin*Task: $F(3,60) = 19.156$, $p < .001$). The post-hoc comparisons highlighted the same pattern of differences found for the Euclidean distance, with the only exception that the angle separating vectors involving the kk Shift was similar for POE and AOE vectors in the PMT ($\text{mean}_{\text{POE-kk}} = 12.169 \pm .680$ vs $\text{mean}_{\text{AOE-kk}} = 12.791 \pm .651$; $p = .338$). Moreover, significant differences between the two tasks were found not only for the POE vectors involving the tt shifts ($\text{mean}_{\text{LT-POE-tt}} = 5.421 \pm .255$ vs $\text{mean}_{\text{PMT-POE-tt}} = 8.321 \pm .369$, $p < .001$) and kk shifts ($\text{mean}_{\text{LT-POE-kk}} = 8.088 \pm .318$ vs $\text{mean}_{\text{PMT-POE-kk}} = 12.161 \pm .680$, $p < .001$), but also for those involving the fkt shifts ($\text{mean}_{\text{LT-POE-fkt}} = 8.965 \pm .527$ vs $\text{mean}_{\text{PMT-POE-fkt}} = 12.093 \pm .729$, $p = .003$) and kt shifts ($\text{mean}_{\text{LT-POE-kt}} = 14.688 \pm .719$ vs $\text{mean}_{\text{PMT-POE-kt}} = 12.000 \pm .703$, $p = .001$), with the latter having an opposite trend of difference.

From the second set of analyses, depicted in **Figure 1.5**, we confirmed the existence of an overestimation on the medio-lateral axis and an underestimation on the proximo-distal axis, which were more accentuated in the LT compared to the PMT. In particular, when the medio-lateral dimension in the LT was considered, we found a significant main effect of Actual displacement for both the medial ($\beta = 1.068$, $t(3856) = 70.027$, $p < .001$) and lateral ($\beta = 1.067$, $t(3827) = 70.841$, $p < .001$) directions. The intercepts in both the medial ($\alpha = .001$, $t(3856) = 0.279$, $p = .780$) and lateral ($\alpha = -.0003$, $t(3827) = -.082$, $p = .934$) models were not significant. Similarly, in the MT the effect of the Actual displacement was significant for the medial direction ($\beta = 1.018$, $t(3851) = 79.390$, $p < .001$) and for the lateral direction ($\beta = 1.030$, $t(3813) = 84.982$, $p < .001$) as well. The intercepts were both not significant (medial: $\alpha = .007$, $t(3851) = 1.733$, $p = .083$; lateral: $\alpha = -.004$, $t(3813) = -.956$, $p = .331$).

When the proximo-distal dimension in the LT was considered, we found a significant main effect of Actual displacement for both the proximal ($\beta = 0.816$, $t(3795) = 57.043$, $p < .001$) and distal ($\beta = 0.824$, $t(3888) = 58.064$, $p < .001$) directions. The intercepts in both the proximal ($\alpha = .0005$, $t(3795) = 0.136$, $p = .892$) and distal ($\alpha = -.003$, $t(3888) = -1.065$, $p = .934$) models were not significant. Similarly in the PMT, the effect of the Actual displacement was significant for the proximal direction ($\beta = 0.874$, $t(3822) = 50.467$, $p < .001$) and for the distal direction ($\beta = .873$, $t(3842) = 55.727$, $p < .001$) as well. The intercepts were both not significant (proximal: $\alpha = .004$, $t(3822) = -0.833$, $p = .405$; distal: $\alpha = -.003$, $t(3842) = .878$, $p = .380$). In order to compare the two tasks, we fitted a model for each dimension with the Actual displacement, the Task and

their interaction as fixed effects and the Subject as a random effect. Regarding the medio-lateral displacements, we found a significant main effect of Actual displacement (medial: $\beta=1.068$, $t(7277)=69.903$, $p<.001$; lateral: $\beta=1.068$, $t(7660)=70.033$, $p<.001$) as well as a significant interaction between the Actual displacement and the Task for both the medial and the lateral direction (medial: $\beta_{\text{ACTDISP*LT}}=1.068$, $\beta_{\text{ACTDISP*PMT}}=1.019$, $t(7727)=-2.734$, $p=.006$; lateral: $\beta_{\text{ACTDISP*LT}}=1.068$, $\beta_{\text{ACTDISP*PMT}}=1.030$, $t(7660)=-2.277$, $p=.023$). The main effect of Task was not significant (medial: $\beta_{\text{LT}}=1.068$, $\beta_{\text{PMT}}=1.101$, $t(7727)=$, $p=.271$; lateral: $\beta_{\text{LT}}=1.068$, $\beta_{\text{PMT}}=1.064$, $t(7660)=-.673$, $p=.501$). As the previous models, the intercepts were not significant. Similarly, for the proximo-distal displacements we found a significant main effect of Actual displacement (proximal: $\beta=.817$, $t(7637)=56.864$, $p<.001$; distal: $\beta=.824$, $t(7750)=57.733$, $p<.001$), as well as a significant interaction between the Actual displacement and the Task for both the proximal and the distal direction (proximal: $\beta_{\text{ACTDISP*LT}}=.817$, $\beta_{\text{ACTDISP*PMT}}=.874$, $t(7637)=2.891$, $p=.004$; distal: $\beta_{\text{ACTDISP*LT}}=.824$, $\beta_{\text{ACTDISP*PMT}}=.873$, $t(7750)=2.741$, $p=.006$). The main effect of Task was not significant (proximal: $\beta_{\text{LT}}=.817$, $\beta_{\text{PMT}}=.813$, $t(7660)=-.673$, $p=.501$; distal: $\beta_{\text{LT}}=.824$, $\beta_{\text{PMT}}=.831$, $t(7637)=-.749$, $p=.454$). The intercepts were not significant.

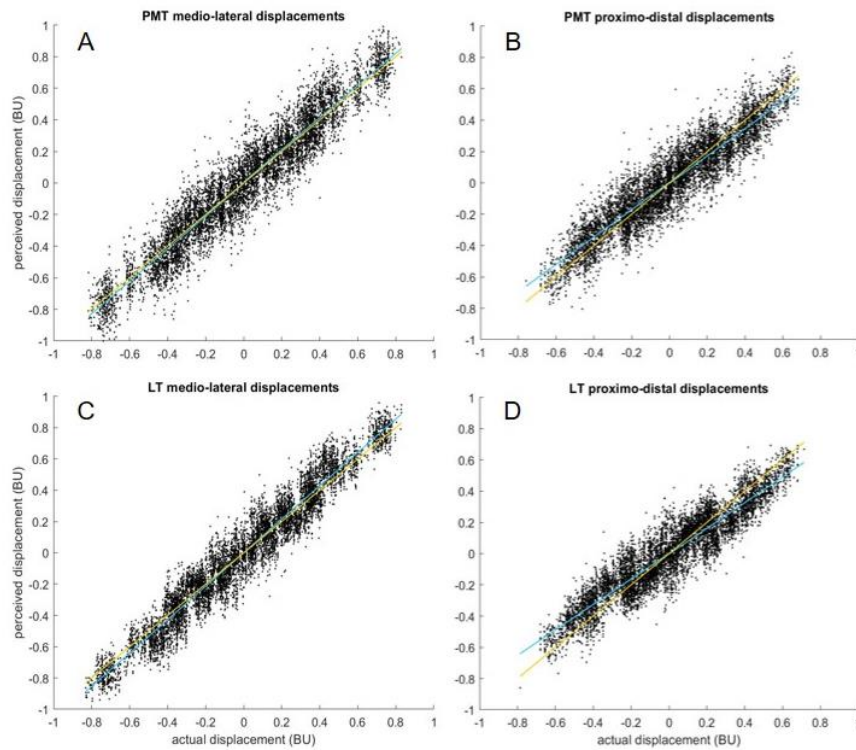


Figure 1.5 The relationship between the actual displacement and the perceived displacement, both in Bookstein Units (BU), is represented for each trial for the PMT, separately considering the displacements on the medio-lateral (a) and the proximo-distal (b) axes. Similarly, the same relationship is represented for the LT separately for the displacements on the medio-lateral (c) and the proximo-distal (d) axes. In each scatterplot the regression line fitted through a Linear Mixed-Effects Model is in light blue, whereas the orange line represents a one-to-one relationship between the actual and perceived displacements.

Interim discussion

Although the perceived hand shape has been shown to be highly distorted in healthy subjects (Longo & Haggard, 2010), our motor fine movements do not seem to be affected by these distortions. Visual incoming inputs could mainly be responsible for movement adjustments. Study 1 aimed at exploring whether, in absence of visual inputs, movement starting points are computed on the basis of the distorted hand representation. To achieve our goal, we required the participants to perform simple hand movements in order to match the perceived position of the tips and knuckles of their own concealed hand by a visual target. The starting points of the motor vectors were mapped and compared to the body representation obtained through the traditional LT (Longo & Haggard, 2010).

As a major finding, using morphometric analyses and repeated-measures analyses on the average perceived distances, we demonstrated that similar distortions, albeit with slightly different magnitudes, characterise both the LT and the PMT maps compared to the actual hand shape. Both LT and PMT maps undeniably exhibited an underestimation of the finger lengths as well as an overestimation of the hand width. It is worth noting that the magnitude of the hand width overestimation in both the LT (23%) and the PMT (15%) is less accentuated than in most of the previous studies, which reported overestimation indexes between 52.2% (Mattioni & Longo, 2014) and 86.4% (Longo, 2015c). Other works, instead, reported lower overestimation indexes, ranging between 18.67% to 37.40% (Medina & Duckett, 2017; Saulton et al., 2015). Similarly to what Saulton and colleagues have hypothesised, it is possible that in our task the participant's hand was positioned with the fingers closer to each other compared to the other studies. It has been shown that the maps obtained are less overestimated in terms of width when the fingers are not splayed (Longo, 2015c).

It has been recently suggested that averaging among trials may mask potential biases that could contribute to explain the hand representational distortions (Medina & Duckett, 2017). Therefore, we adopted the Lag-1 approach on LT and PMT data. Regarding the LT, our results support the hypothesis of Medina and Duckett (2017) that participants use the $n-1$ trial perceived location to make a Localisation judgment on trial n . However, this occurred only when the shift between trial $n-1$ and n has a higher medio-lateral component (knuckle to knuckle or fingertip to fingertip). On the contrary, when the shift involved a fingertip and a knuckle, participants seem to rely more on the actual locations in their localisation judgments.

Interestingly, in the PMT we did not observe such an effect, neither for the shifts with a high proximo-distal component (knuckle to fingertip) nor for the shifts with a high medio-lateral component, meaning that the perceived position on trial $n-1$ is not used to make a localisation judgment on trial n . Since in the PMT the hand changes position in the space at each trial to match four different visual

targets, once the perceived location of the landmark on trial n-1 is defined, it should be mentally “shifted” toward the target of the consecutive trial to be used as the basis of the trial n localisation judgment. This implicit strategy seems to require more effort rather than to make the localisation easier. It is more plausible that the participants actually relied on the perceived position of the landmark addressed by each trial.

Moreover, in line with the conventional analyses, we found a significant overestimation of the medio-lateral displacements along with a significant underestimation of the proximo-distal displacements for both the LT and the PMT, and no effects of constant bias in any of the tasks and displacement directions, in contrast with what Medina and Duckett (2017) reported. This discrepancy could be attributed to the fact that in our task participants were asked to localise both the fingertips and the knuckles whereas their task involved only the knuckles. In addition, we used a higher number of trials per each landmark (40 vs 12), increasing the precision of the measurement. Finally, the PMT dimensions along the proximo-distal axis are less underestimated than in the LT, whereas dimensions along the medio-lateral axis are less overestimated than in the LT. These results are in line with the morphometric and repeated-measures analyses which found that the PMT map is less distorted than the LT map.

In general, our results suggest that the distorted hand representation, in absence of visual information, is primarily used to draw motor vectors’ starting points. Indeed, in the PMT, simple matching movements were affected by the biases characterising the hand metric representation. In other words, such representation does not subserve only body perception, instead, it covers a pivotal role in motor planning. Although we studied the involvement of the hand metric representation during a very simple motor task, we argue that this representation is always integrated with sensory inputs in order to plan and perform a movement. It is conceivable that, when less simple movements are considered, errors which are clearly explained by body representation distortions would be harder to detect, since richer sensorimotor and proprioceptive feedback loops are elicited.

Interestingly, our analyses showed that, while the mean length and the width estimations are similar in PMT and LT maps, the overall map proportions measured through the SIs and Procrustes fits differ between the two maps. Namely, the PMT map’s shape is closer to the actual one, compared to the LT map. However, looking at the results reported in **Table 1.1** and **Table 1.2**, displayed in **Figures 1.3** and **Figure 1.4**, it can be observed that the PMT ERs seem to be generally more accurate in comparison the LT ones. While only the differences between middle finger ERs and middle-ring spacing ERs survived multiple comparisons, this modest trend might have been well detected from the overall proportion analyses. In all, these results suggest that in the PMT task, an adjustment of the hand representation biases occurred. The second study of the present chapter aimed at shedding light on this result.

Study 2: The motor system (partially) deceives body representation biases in absence of visual correcting cues ²

Introduction

We put forward three hypothesis to explain the difference between the hand maps measured by means of the Localisation Task (LT) and the Proprioceptive Matching Task (PMT) described in Study 1 of the present chapter.

First, the higher accuracy could reflect an adjustment at the representational level. In other words, engaging the participant in a dynamic task might result in an updated hand representation. As for the potential mechanism underlying this possible representational change, we argue that gaining specific sensorimotor information by performing hand movements could modulate the perceived hand size. Changes in body representations after experimental manipulations involving multisensory inputs (e.g. after tool-use: Cardinali, Brozzoli, & Farnè, 2009; illusory hand magnification: Linkenauger, Witt, & Proffitt, 2011), intensive sensorimotor training (Cocchini et al., 2018), or simply physical and cognitive development (Brownell, Nichols, Svetlova, Zerwas, & Ramani, 2010; Brownell, Zerwas, & Ramani, 2007) have been reported by previous studies. This suggests that body representations are relatively malleable and can be modulated by afferent and motor information, facilitating our adaptation to the environment. The mental representation of our body is indeed the result of multisensory inputs coming from the visual, proprioceptive, tactile, vestibular and motor systems (de Vignemont, 2010; Medina & Branch Coslett, 2016), and is therefore sensitive to changes involving the sensory inflow and motor outflow. During the PMT, participants are required to perform matching movements that provide additional sensorimotor information, which might contribute to updating their hand representation. Under this hypothesis, the difference between the perceived hand map probed by the dynamic, compared to the static task, would reflect a partial correction of the hand representation biases, with the motor plan being drawn from a more veridical hand map.

As a second hypothesis, the higher accuracy in a dynamic compared to a static body representation task might reflect an adjustment at the motor level. Specifically, during the PMT, the matching movements might have been fine-tuned by the internal forward models, which operate during motor performance. One of the most influential models of motor control (Desmurget & Grafton, 2000) theorises that, when we have to perform a goal-directed movement, a raw motor plan is sketched on the basis of the hand and the target locations. The raw motor vector is then adjusted by internal forward models which integrate motor outflow with current sensory inflow and generate kinematic and sensory

² The following sections (introduction, method, analysis and discussion relative to Study 2) have been largely extracted and adapted from Peviani, Liotta & Bottini (submitted).

predictions of the implemented motor command (Miall & Wolpert, 1996). Forward models are built through sensorimotor learning processes, combining information about an individual's own body properties and the external world (Karniel, 2011; Wolpert, Diedrichsen, & Flanagan, 2011). It could be hypothesised that, when a movement has to be performed in normal circumstances, at first, the motor vector is roughly computed starting from the distorted body representation; afterwards, the incoming visual and sensorimotor inputs contribute to increasingly fine-tune the motor plan. In simpler words, the matching movements may have been partially guided by our implicit hand motor experience, which is usually enriched by visual feedback. In this case, the difference between the LT and PMT maps would reflect a refinement of the motor vectors' trajectory, rather than of the hand representation itself.

Third, the difference found between PMT and LT maps could reflect a difference in the representation of participants' left and right (dominant) hands. Indeed, Study 1 was designed so that both tasks required participants to perform movements with their dominant hand, with the consequence that the right hand was mapped during the PMT, whereas the left hand was mapped during the LT. Although a previous study did not find any differences between the body model of the left and the right hand (Longo & Haggard, 2010), we cannot rule out the possibility that a right-left difference may arise when a task involving movement is used.

For the purpose of this investigation, we recruited twenty-four healthy participants to perform the PMT with the left hand and assessed the resulting changes in terms of perceived hand dimensions by means of the LT, which was administered on the same hand before and after the PMT. We included two further experimental conditions in our within-subject design (**Figure 1.6**). The first one aimed at evaluating the combined effect of recent visual and sensorimotor information on the perceived hand maps. Participants performed a non-blind version of the PMT (i.e. the visuo-proprioceptive matching task, vPMT) between the two LT administrations. The second one aimed at controlling for the effect of learning, therefore participants rested for 20 minutes between the two LT. The order of the experimental condition was counterbalanced across subjects.

If gaining specific sensorimotor information can directly alter the perceived locations of the hand landmarks, it follows that the hand representation should be more accurate after the PMT compared to after a rest period. Following such logic, it could be hypothesised that providing an extensive multisensory feedback, as in the visuo-proprioceptive condition, might result in a greater improvement of the LT performance. Alternatively, if gaining sensorimotor information does not directly affect the hand representation, the LT should not detect any change in such representation after any of the experimental manipulations. In other words, the sensorimotor integration occurring during the PMT does not affect the starting point of the motor vectors, rather contributes to refine their trajectory. Finally, if the difference between the LT and PMT maps described in Study 1 of the present chapter reflects a difference between

the right hand and left hand maps, it should be minimised once the LT and PMT are administered on the same hand.

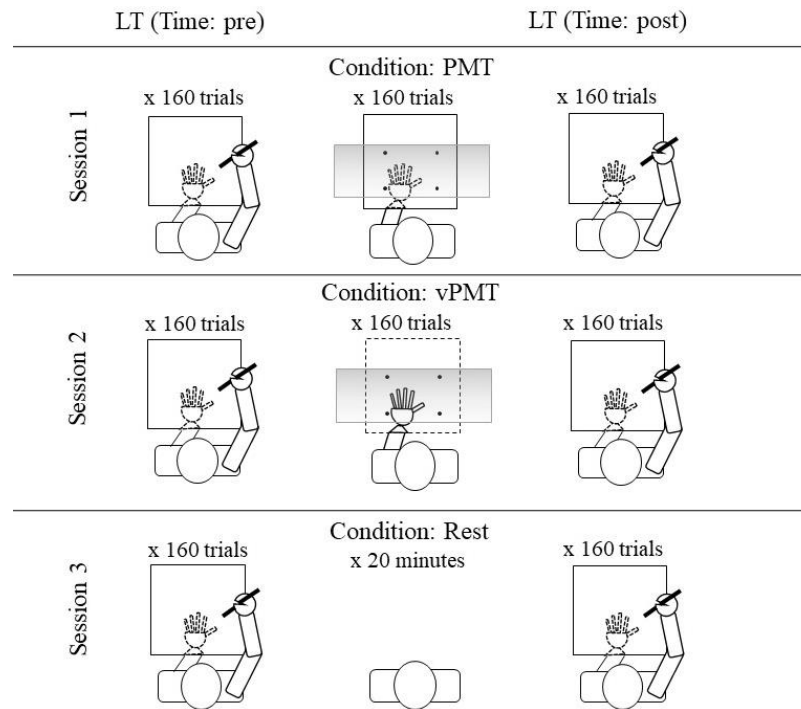


Figure 1.6 Experimental design: we used a 3x2 within-subject design to test the effect of Condition and Time on the perceived hand dimension measured by means of the Localisation Task (LT). Each participant underwent three experimental sessions. In each session, the Localisation Task (LT) was administered twice, before and after the experimental manipulation, which consisted of the Proprioceptive Matching Task (PMT), the visuo-Proprioceptive Matching Task (vPMT) or the control condition (Rest). The order of the sessions was counterbalanced across participants.

Method

Participants

Twenty-four (eighteen females) healthy participants were recruited for the present study and received university credits in return. Participants were university students (mean education 14.62 ± 2.33 years) aged between 20 and 33 years old (mean age 22.54 ± 3.12 years). All participants were right-handed as assessed by the Edinburgh Handedness Inventory (Oldfield, 1971). The study received approval from the

local ethical committee (University of Pavia) and adhered to the ethical standards of the Declaration of Helsinki.

Tasks and procedure

Each participant took part to three experimental sessions within four weeks, with an interval of two weeks between an experimental session and the following one. Informed consent was obtained from each participant prior to the first session. The order of the sessions was counterbalanced across participants. During each experimental session, participants were administered with the Localisation Task (LT) twice, in order to assess their hand metric representation right before and right after the experimental manipulation, which consisted of one out of two tasks, namely the Proprioceptive Matching Task (PMT) and the visuo-Proprioceptive Matching Task (vPMT), or a Rest period (**Figure 1.6**).

The administration of the LT and PMT followed the same procedure described in Study 1 of the present chapter. The procedure relative to the vPMT overlaps with that described for the PMT, except for the fact that, in the former, a box without the lid was used. Therefore, participants had complete visual feedback of their hand while performing the matching movements. During the rest period, participants seated quietly, with their hands under the table for 20 minutes. In each session, each Localisation Task included 160 trials, as well as each PMT and vPMT. The order of the trials was randomised.

Analysis

For each trial of the LT, the XY coordinates in pixels relative to the perceived position of the hand's landmarks were extracted by means of ImageJ (Abràmoff et al., 2004) and MATLAB (The MathWorks, version R2017b). Analogously to what described in Study 1 of the present chapter, the XY coordinates of the stick tip pointing at the board was extracted from each picture. Mean XY coordinates of each perceived landmark position were computed for each participant, condition and time, resulting in six perceived maps per participant. In order to minimise differences in the hand posture each finger of each hand map was rotated to match a standard posture, defined as the angle resulting from the intersection of that finger with the horizontal line binding the little and index knuckles, following the procedure described by Longo & Haggard (2010).

For each map, the perceived finger lengths (distances between each fingertip and its relative knuckle), mean finger length, hand width (distance between the knuckle of the little and index fingers) and shape index ($100 \times \text{hand width} / \text{middle finger length}$) were computed in pixels and converted in centimeters. Following a similar procedure, XY coordinates in pixels relative to the actual position of the hand's landmarks have been extracted from the baseline photographs taken at the beginning of each LT

administration. For each participant, the actual hand map was obtained by averaging the six measurements together. After finger rotation, the actual hand dimensions were calculated in pixels and converted in centimeters.

The perceived hand dimensions (five finger lengths, mean finger length, hand width and shape index) were normalised by dividing them by their relative actual dimensions (e.g. perceived thumb length / actual thumb length) to obtain the Estimation Ratios (ERs), which were the dependent variables of most of our analysis. The distributions of the ERs for each of the three sessions (corresponding to the three experimental manipulations: PMT, vPMT and Rest) and times (pre and post), were explored through box-and-whiskers plots to detect outliers. Two participants were excluded from the analysis due to the presence of outlier observations (higher than the third quartile plus three times the third interquartile, or lower than the first quartile minus three times the first interquartile) in more than 50% of the distributions. Before running statistics we checked whether the ERs were normally distributed by performing a Shapiro-Wilk test on each dimension's distribution for each condition. The following distributions did not meet the normality assumption: index finger ERs for the Rest condition ($W(44) = .941$, $p=.025$), the middle finger ERs for the PMT condition ($W(44) = .939$, $p=.022$) as well as for the vPMT condition ($W(44) = .893$, $p=.001$), the little finger ERs for the PMT ($W(44) = .939$, $p=.022$) and the mean length ERs for the Rest condition, although borderline ($W(44) = .950$, $p = .057$). In the case of such variables, non-parametric statistics were used.

In order to investigate whether the ERs were significantly different from 1 and thus to attest the presence of finger length underestimation and hand width overestimation, previously reported in the literature (Longo & Haggard, 2010), we ran one-sample t-tests and one-sample Wilcoxon Signed Rank tests against 1 for each dimension. Subsequently, we aimed at testing whether the distortions characterising the implicit hand representation benefit from performing a vPMT or a PMT compared to the rest condition. To do that, we fitted a General Linear Model or a Generalized Linear Model with Tweedie distribution and log-link, investigating the effects of Condition (PMT, vPMT and Rest) and Time (pre, post), as long as their interaction, on each dimension ERs.

Next, we adopted a morphometric approach to further investigate the differences in shape between the perceived and actual maps, as well as across conditions and time. Similarly to what described in Study 1, we used the Generalized Procrustes Alignment to perform the Procrustes superimposition for each condition (including the actual maps) and time. In so doing, we obtained coordinates in Bookstein Units (BU). Next, we performed the Procrustes Analysis of Variance (ANOVA) to test for differences in shape (Goodall, 1991), quantified by the Procrustes distance (sum of the distances between corresponding landmarks of two shapes) to test the effect of Condition and Time.

Furthermore, we aimed at comparing the implicit maps averaged across the six LT measurements with the implicit maps resulting from the PMT (for the data extraction we followed the same procedure described in Study 1. We used paired sample t-tests and Wilcoxon Signed Ranks tests to compare the ERs for each dimension, and the Procrustes ANOVA to test for differences in shape.

All the statistical analyses were computed with SPSS (IBM Corp. Released 2010) and MATLAB (The MathWorks, version R2017b).

Results

Firstly, the one-sample t-tests and Wilcoxon Signed Rank tests comparing each dimension ER against 1 confirmed the presence of a significant underestimation of the finger lengths and an overestimation of the hand width, resulting in a disproportioned shape index, as measured by the LT for each condition and time (all p s < .001, see **Supplementary materials**).

Morphometric analyses further confirmed a difference in terms of shape between the perceived maps obtained by administering the LT and the actual hand map in each condition, clearly visible in **Figure 1.7**. Here, we report the results concerning the comparisons between the perceived LT map and actual hand map for each experimental manipulation (PMT, vPMT, Rest), averaged across times (pre, post): PMT condition vs actual: $F(16,736)=104.82$, $p<.001$; vPMT condition vs actual: $F(16,736)=90.97$, $p<.001$; Rest condition vs actual: $F(16,736)=104.82$, $p<.001$.

Importantly, our analyses showed that inaccurate perceived hand dimensions were not adjusted by performing neither a Proprioceptive Matching Task nor a visuo-proprioceptive one, compared to the rest condition. Indeed, the effect of Condition, Time, as well as their interaction were not significant for any of the dimensions considered (**Table 1.3**). Coherently, we did not find any significant change in terms of shape by running a Procrustes ANOVA investigating the effect of Condition and Time (Condition: $F(32,1632) = .59$, $p=.966$; Time: $F(16,1632) = 1.21$, $p=.258$). In order to explore possible interactions, we ran a comparison between the maps referred to the pre- and post- experimental manipulation within each condition (PMT condition: $F(16, 544) = 1.03$, $p=.432$; vPMT condition: $F(16, 544) = .62$, $p=.862$), Rest condition: $F(16, 544) = .23$, $p=.999$).

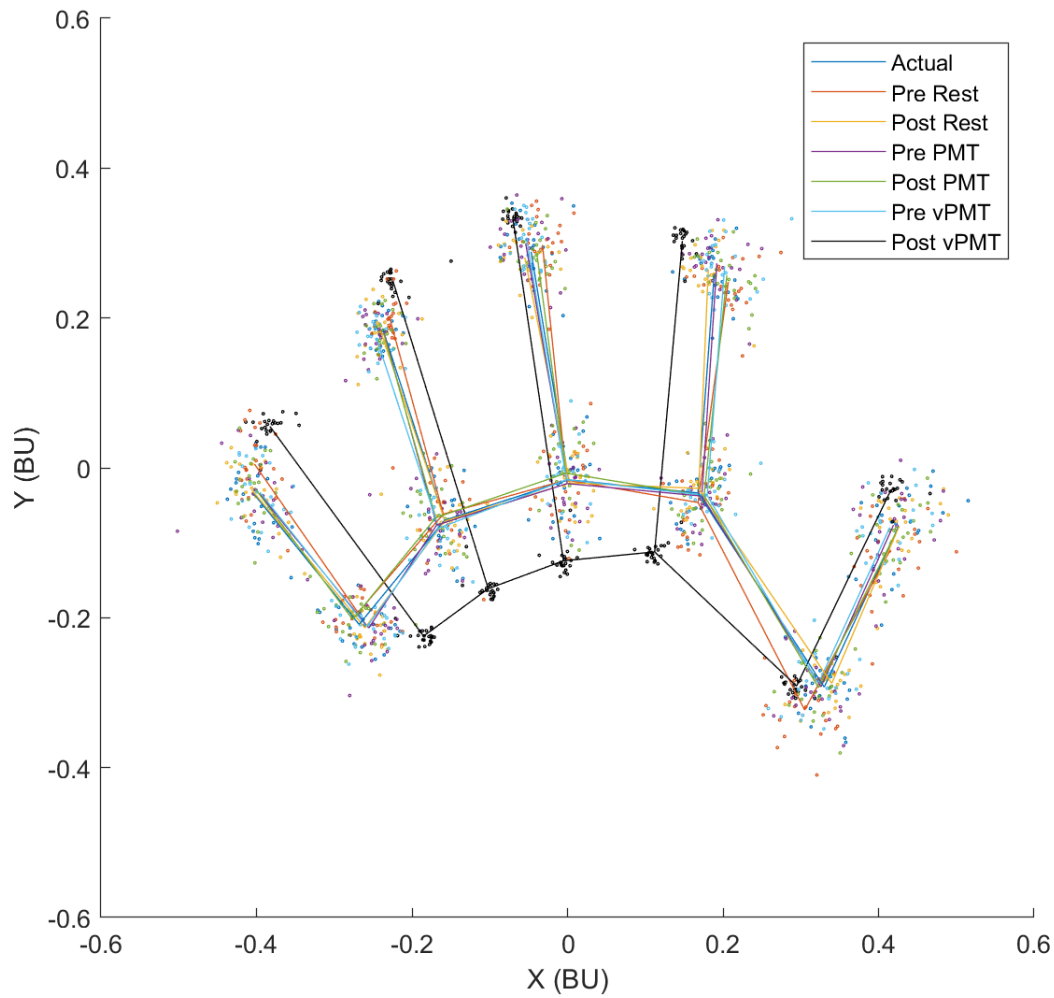


Figure 1.7 - The average perceived hand map measured by means of the Localisation Task before (pre) and after (post) each experimental manipulation (Proprioceptive Matching Task (PMT), visuo-Proprioceptive Matching Task (vPMT) and Rest), is represented. The average actual hand shape is depicted in black. The map coordinates, expressed in Bookstein Units (BU), were obtained by performing the Procrustes superimposition on the raw data.

Dimension	Effect	Test Statistic (df)		p
Thumb length	Condition	F (2,42)	1.041	.362
	Time	F (1,42)	.262	.614
	Condition * Time	F (2,42)	.455	.637
Index finger length	Condition	W (2)	1.951	.377
	Time	W (1)	2.311	.128
	Condition * Time	W (2)	.355	.837
Middle finger length	Condition	W (2)	.227	.893
	Time	W (1)	4.006	.045
	Condition * Time	W (2)	1.008	.604
Ring finger length	Condition	F (2,42)	1.916	.160
	Time	F (1,42)	.821	.375
	Condition * Time	F (2,42)	.038	.963
Little finger length	Condition	W (2)	.152	.927
	Time	W (1)	1.003	.316
	Condition * Time	W (2)	1.155	.561
Mean finger length	Condition	W (2)	.132	.936
	Time	W (1)	1.889	.169
	Condition * Time	W (2)	.322	.851
Hand width	Condition	F (2,42)	1.546	.225
	Time	F (1,42)	.438	.515
	Condition * Time	F (2,42)	1.870	.167
Shape index	Condition	F (2,42)	1.668	.201
	Time	F (1,42)	1.496	.235
	Condition * Time	F (2,42)	2.031	.144

Table 1.3 - Results of the 3x2 repeated-measures analyses on the Estimation Ratios (ERs) are reported for each dimension considered. In detail, a general or generalized linear model has been applied to investigate the effect of Condition (visuo-proprioceptive, proprioceptive or rest), Time (pre, post) and their interaction on the ERs for each hand dimension, measured through the Localisation Task.

Finally, we compared the perceived hand dimensions measured by means of the LT (averaged across times and conditions) and those measured by means of the PMT. Importantly, our data showed that the perceived hand map obtained from the PMT is more proportionated compared to the Localisation Task one and closer to the actual hand map, replicating the results of Study 1 (Peviani & Bottini, 2018). In detail, we found a significant adjustment for the middle finger length (LT: $0.530 \pm .102$ vs PMT: $0.607 \pm .149$; $Z(21) = -3.036$, $p = .002$), for the mean finger length (LT: $0.571 \pm .086$ vs PMT: $0.623 \pm .094$; $t(21) = -2.294$, $p = .032$) and a marginal trend of adjustment for the hand width (LT: $1.198 \pm .293$ vs PMT: $1.119 \pm .263$; $Z(21) = -1.899$, $p = .058$), which resulted in an overall adjustment of the map proportions, reflected by the shape index (LT: $2.425 \pm .528$ vs PMT: $1.953 \pm .440$; $t(21) = 5.577$, $p < .001$), see **Figure 1.8a**. Only the differences regarding the middle finger length and the SI ERs survived Bonferroni

correction ($p = .014$ and $p = .003$, respectively), similarly to what reported in Study 1. The remaining dimensions did not differ between the tasks (Thumb length: LT: $0.671 \pm .104$ vs PMT: $0.682 \pm .190$; $t(21) = -.274$, $p = .787$; Index finger length: LT: $0.5966 \pm .091$ vs PMT: $0.635 \pm .127$; $t(21) = -1.301$, $p = .207$; Ring finger length: LT: $0.516 \pm .096$ vs PMT: $0.559 \pm .136$; $t(21) = -1.422$, $p = .170$; Little finger length: LT: $0.549 \pm .104$ vs PMT: $0.617 \pm .173$; $t(21) = -1.904$, $p = .071$). Means and standard deviations or medians and interquartile ranges have been reported for each comparison. The Procrustes ANOVA confirmed the difference in shape between the tasks ($F(36,672) = 2.070$, $p = .016$), see **Figure 1.8b**.

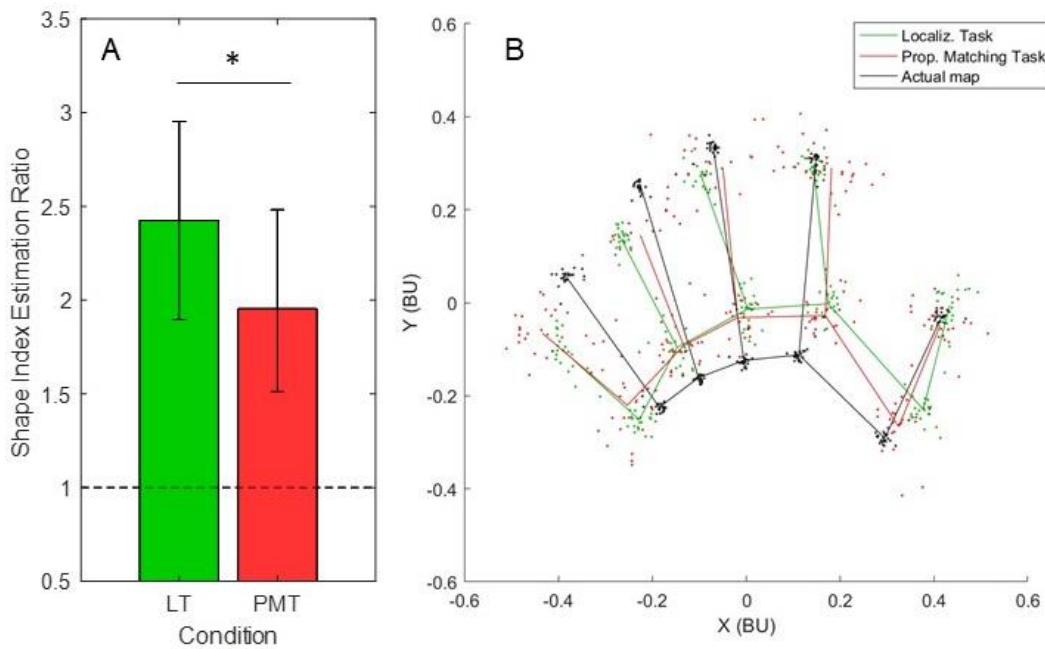


Figure 1.8 (a) The average shape index Estimation Ratios (ER) measured by means of the Localisation Task (LT) and Proprioceptive Matching Task (PMT) are represented. Error bars indicate standard deviations. The dashed black line represents the real shape index. (b) The average perceived hand maps measured by means of the LT and through the PMT are represented, along with the average actual hand map. The map coordinates, expressed in Bookstein Units (BU), have been obtained by performing the Procrustes superimposition on the raw data.

Interim discussion

Our data suggest that gaining hand-specific sensorimotor information via PMT administration does not modulate the represented hand size, as measured by a static offline task. Indeed, the hand perceived dimension assessed through the LT was unaltered after the PMT or its non-blind version, the vPMT, compared to the rest condition. As expected, the hand width, measured by the distance between the knuckles of the index and little fingers was overestimated and the finger length was underestimated, resulting in a perceived short and flat hand, in line with previous evidence (Longo, 2015a; Longo &

Haggard, 2010). These distortions were present before and after each experimental manipulation, as revealed by both repeated-measures analyses on the perceived dimensions and morphometric analyses on the perceived hand shape.

Crucially, while we did not find a significant change of the hand representation following the gain of specific somatosensory information, our data showed that the perceived hand dimension emerging from the PMT was more veridical, replicating the findings described in Study 1 (Peviani & Bottini, 2018). This result rules out the possibility that the difference observed between the LT and PMT maps reflects a difference between the right and left hand maps, since in the present study the representation of the same hand (the left) was mapped in both the tasks. Instead, our data suggest that the motor system refines the movement trajectory, possibly as the result of the integration of current somatosensory inflow and motor outflow. We argue that, during the PMT, a feedback-forward system involving the somatosensory and motor systems is activated, allowing a re-adjustment of the trajectory of the motor vector.

Our data are in line with previous findings showing that the misestimation of the hand dimension can be modulated in magnitude by providing additional sensory information during the task (“online”), as in the case of the PMT. For instance, the distortions were attenuated when tactile (Mattioni & Longo, 2014) or visual - albeit non-informative - (Longo, 2014) cues were provided “online”. On the contrary, the perceived distortions are robust to additional sensorimotor cues when those are provided “offline”. Nevertheless, long-term plasticity in body representations can be achieved by intensive practice, as suggested by the comparison between the hand representations of skilled baseball players (Coelho, Schacher, Scammel, Doan, & Gonzalez, 2019) and of magicians (Cocchini et al., 2018) with those of non-experts.

With Study 1 and 2 we showed and replicated that the performance in a dynamic hand representation task is more accurate than in a static hand representation task. Results of Study 2 suggest that this difference might be explained by the online integration of sensorimotor information in the internal forward models, active during motor planning and execution. However, there are at least two alternative explanations that would potentially fit our findings, and that would merit the attention of future studies.

First, the LT and the PMT may differ in terms of cognitive demands. Specifically, each PMT item requires to retain and process two bits of information (hand landmark to be localised and visual target to be reached), in contrast to each LT item, which requires to retain and process one bit of information (hand landmark to be localised). A higher working memory load might have triggered an overall higher level of sustained attention, which might have positively affected the accuracy in the hand landmark localisation. In future research, it would be interesting to investigate whether the attentional level has a modulatory effect on the LT performance.

Second, the results of the first set of Lag-1 analyses performed in Study 1 suggest that the landmark localisation in the two tasks is likely to be underlined by partially different mechanisms. In the LT, participants relied more on the localization judgment on trial $n-1$ to perform the localization judgment on trial n . On the contrary, and coherently with the task demands, in the PMT the localization on trial $n-1$ did not have a significant influence on the localization on trial n , suggesting that participants relied more on the landmark perceived position in the PMT. Further studies would be needed to investigate whether the higher accuracy in the PMT is the result of less biased localisation judgments.

Biased body representations and movement: general discussion

Study 1 was set out to explore the involvement of the (biased) hand representation in motor planning and execution. We showed that our motor system makes use of the distorted hand representation when a movement is performed in absence of visual guidance. Indeed, the motor performance is biased in a way that reflects the hand representation distortions. However, we also found that the motor performance in the Proprioceptive Matching Task is more accurate compared to what expected by considering the distorted hand map as the starting point of the motor vectors. In other words, we move as grounding on a more proportionated hand representation. Study 2 further investigated this phenomenon. We concluded that the motor system does rely on the distorted hand representation to draw the starting points of the motor vectors, and it refines the movement trajectories by integrating current somatosensory inflow and motor outflow in the forward models, partially overcoming the misestimation of the hand dimensions.

Together with previous research, our studies contribute to solve the mismatch between our fine motor performance and effective interaction with the environment (even in absence of visual cues) on one side, and the pronounced distortions characterising our hand representation on the other side. Furthermore, by showing that the starting points of the motor vectors lay on the biased metric representation (Peviani & Bottini, 2018), we provided evidence against the distinction between the body schema and the body model. Indeed, we demonstrated that the distorted hand representation subserves motor control, which is coherent with the definition of body schema as “a highly plastic representation of the body parts, in terms of posture, shape, and size, that can be used to execute or imagine executing movements” (Medina & Coslett, 2010).

Chapter 2: Factors modulating metric biases in body and objects representations

Study 3: Visual and somatosensory information contribute to biases in body representation ³

Introduction

As previously stated, Study 3 aimed at providing evidence about the nature of the distortions of the body representation, by addressing the role of visual and somatosensory factors on body representation biases. While authors proposed that these biases are originated from the distorted somatotopic cortical maps (Longo, 2015a), recent studies have called into question whether these biases are (solely) of somatosensory origin.

We compared the metric representations across body parts affording different degrees of tactile acuity but also different degree of visual accessibility. We hypothesised that, if the same visual-based pattern of distortions shapes our mental representations, it follows that different body parts should be similarly misrepresented. In contrast, if other factors, such as the tactile acuity of a body part, have an additional impact on its metric representation, we should be able to detect different patterns of distortions across body parts.

We thus investigated absolute differences across the representations of two orthogonal dimensions, i.e., width and length, of several body parts (**Figure 2.1**). In the first experiment, we compared the hand dorsum with that of the foot, as they are characterised by a similar tactile acuity (Mancini et al., 2014) but have a different aspect ratio. In the second experiment, we compared the representations of the lips, as they are highly sensitive (Chen et al., 1995; Costas, Heatley, & Seckel, 1994; Lass, Kotchek, & Deem, 1972; Rath & Essick, 1990) and coupled with the hand during motor planning and interaction with the environment (Gentilucci, Benuzzi, Gangitano, & Grimaldi, 2001; Gentilucci & Campione, 2011); of the nose, for which we have roughly a similar degree of visual access; and of the dorsal portion of the neck, as it has poor tactile acuity (Nolan, 1985) and visual accessibility. To evaluate the metric representation across those different body parts we used the Line Length Judgment (LLJ) Task (**Figure 2.2b and c**). In detail, participants were asked to compare the dimensions of horizontal and vertical lines displayed on a computer screen with the vertical and horizontal dimensions of a certain target, which needed to be recalled from memory. The lines presented were shortened or lengthened compared to each target's actual dimensions and participants were asked to decide whether each line was shorter or longer in a two-alternative forced choice task by pressing a button.

³ The following sections (introduction, method, results and discussion relative to Study 3) have been largely extracted and adapted from Peviani, Melloni & Bottini (2019).

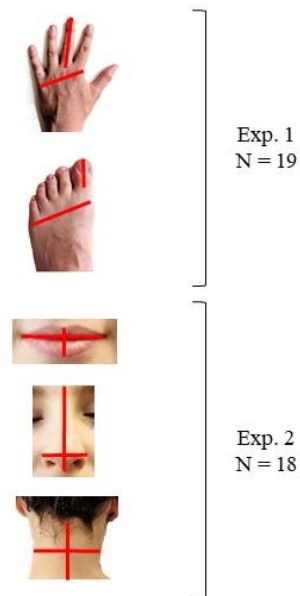


Figure 2.1 Experiments, sample sizes and targets are represented.

Method

Participants

Nineteen (17 females) participants took part in experiment 1 (mean age: 23.70 ± 6.03). Eighteen female participants took part in experiment 2 (mean age 24.00 ± 5.98). All participants were right-handed according to the Edinburgh Handedness Inventory (Oldfield, 1971), with a mean laterality index of 92.27 ± 6.20 in the first experiment and of 95.11 ± 7.12 in the second experiment. Participants received university credits or monetary compensation (10 Euros per hour) for their participation. Informed consent was obtained prior to each study. Both studies received approval from the local ethical committees (University of Pavia and Ethics Council of the Max Planck Society) and adhered to the ethical standards of the Declaration of Helsinki.

Task and procedure

We evaluated the metric representation of five different body parts (**Figure 2.1**) by means of the LLJ Task (**Figure 2.2b and 2.2c**). Participants were asked to determine whether the length of vertically or horizontally oriented lines was shorter or longer compared to a specific body part serving as a reference. In experiment 1, the reference was either the left hand or the left foot of the participant. In experiment 2,

the reference was either the nose, the lips or the dorsal portion of the neck. For each body part, participants had to compare the lines to either the width (medio-lateral dimension) or the length (rostral-caudal dimension) of that body part.

Before the beginning of the first experiment, we measured the width of the subject's left hand and length of the middle finger, as well as the width of the subjects' left foot and the length of the big toe. Measurements were processed with the subjects' eyes closed. The hand width and length were $8.383 \pm .764$ and $7.700 \pm .622$ cm, respectively. The foot width and length were $4.577 \pm .590$ and $8.733 \pm .723$ cm. The experiment consisted of 4 blocks, each containing 80 trials. Line length ranged from -30% to +10% of the actual length of the participant's body part with an interval of 1%. For each interval, two lines were presented. These ranges were chosen from a pilot study where we observed that both the width and the length of the hand were systematically underestimated i.e., participants' responses were asymmetrically distributed, with a higher frequency of judgments for underestimation than for overestimation (**Supplementary materials**). We evaluated whether introducing an asymmetry in the range of the lines presented as stimuli could alter the underlying estimation (e.g. by yielding a greater underestimation), by comparing the magnitude of the misestimation of the hand dimensions measured in a pilot study (N=17) using a symmetrical range (-30 to +30%) with the non-symmetrical range used in the present study. The paired t-tests on the hand length EE (previous experiment mean EE = $-.766 \pm .651$ vs current experiment mean EE = $-.996 \pm .651$; $t(29) = -.827$, $p = .415$, $BF_{10} = 0.443$) and on the hand width EE (previous experiment mean EE = $-.380$ vs current experiment mean EE = $-.593$; $t(29) = -.785$, $p = .439$, $BF_{10} = 0.432$) were both not significant. As no differences were observed across studies we used the non-symmetrical range in order to increase sensitivity by increasing the number of trials per condition.

Before the beginning of the second experiment, length and width of each body part (lips, nose and dorsal portion of the neck) were measured while the participants' eyes were closed. Dimensions of the lips were measured while asking subject to relax them. The lips width was measured from the right to the left commissures, its length was measured from the upper to the lower vermilion's borders at the body midline. The width of the nose was measured at the naris level; its length was measured from the tip to the nasion. The width of the dorsal portion of the neck was measured from the right to the left boundary to the height of its midpoint; its length was measured as the distance between the hair line and the shoulder line. The length and width dimensions were $1.362 \pm .230$ and $4.793 \pm .274$ cm for the lips, $5.062 \pm .396$ and $3.237 \pm .444$ cm for the nose, and 8.256 ± 1.106 and 8.631 ± 0.626 cm for the dorsal portion of the neck, respectively. The second experiment consisted of 6 blocks, each containing 120 lines, ranging from -30% to +30% of the actual length of the participant's body part with an interval of 1%.

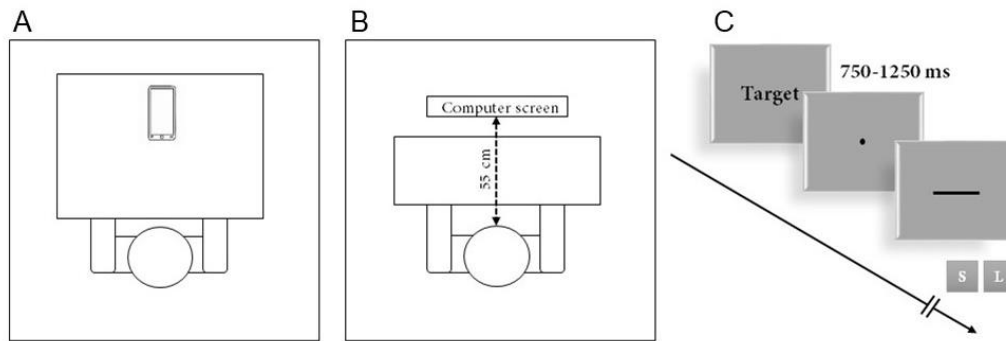


Figure 2.1 The experimental procedure and the experimental paradigm for the Line Length Judgment (LLJ) Task are depicted for Study 3 (B+C) and Study 4 (A+B+C). (a) Only in Study 4, after the target was measured, the participant was required to observe it (unless the target was the participant's own hand or own mobile phone) for a period of time lasting 60 to 120 seconds (depending on the experiment). (b) In both Study 3 and Study 4, participants were seated at 55 cm from the screen and an opaque panel covered their hands while responding. (c) In both Study 3 and Study 4, after the initial instructions (e.g. "Think about the length of your left hand") a certain number of trials were presented in sequence. Each trial consisted of a horizontal or vertical line and the participant was instructed to respond with the left key for 'shorter' (S) and with the down key for 'longer' (L).

Analysis

Experiment 2 confirmed the general tendency to systematically underestimate the target's dimension (**Supplementary materials**). We thus selected for both experiments trials with lines distortions in the range of -30 to 10%. Similarly to what we described above, we grouped the responses of the LLJ Task in four ranges: i) -30 to -21%, ii) -20 to -11%, iii) -10 to -1%, iv) 1 to 10%, and labels -2, -1, 0 and 1 were assigned to each range respectively. Similarly to what we did in Study 3, we fitted psychometric functions to estimate the Point of Subjective Equality (PSE) separately per participant, body part and dimension. Psychometric functions were fitted using the Palamedes Toolbox (Prins & Kingdom, 2018) in MATLAB (The MathWorks, version R2017b). Subsequently, we computed the EEs, meant as the percentage of underestimation (negative sign) or overestimation (positive sign) of a certain body part and dimension. The EEs distributions were inspected for normality (Kolmogorov-Smirnov normality test) and outliers (box-and-whiskers plots). Extreme outliers were removed (higher than the third quartile plus three times the third interquartile, or lower than the first quartile minus three times the first interquartile). Seven out of 37 observations were excluded from the analyses as extreme outliers. None of the distributions violated the normality assumptions (all p s > .05), except for the distribution of the EEs relative to the hand width ($D(14) = .293$, $p = .002$).

To study the distortions both for the length and width of each body part separately we conducted one-sample t-tests on the EE values against zero. To study the differential effect for each dimension we also conducted repeated-measures ANOVA on the EEs with factors body part and dimension (length/width) in SPSS (IBM Corp. Released 2010). In addition, we report Bayes factors – BF_{10} – (Rouder, Speckman, Sun, Morey, & Iverson, 2009) which represent the likelihood of the presence of the effect (H1) to the likelihood of the absence of such effect (H0), given the data. BF_{10} values larger than 1 represent evidence for the alternative hypothesis (H1). Bayesian analyses were performed in JASP (JASP Team, 2018).

To directly compare across the different body parts tested across the two studies i.e., hand, foot, lips, nose and the neck we pooled all the EEs data in a Linear Mixed-Effects Model in SPSS, with body parts and dimensions as fixed effects, including random intercepts and slopes to account for inter-subject variability.

As a further step, we aimed at comparing body parts as a whole, collapsing over the width and length dimensions. To this purpose, we used a multidimensional scaling approach: given a matrix of interpoint distances, multidimensional scaling allows to summarise the distances (or dissimilarities) among different instances and to represent them in an N-dimensional space. Specifically, we applied multidimensional scaling in MATLAB (The MathWorks, version R2017b) on the Euclidean distances computed among the EEs referred to the length, the width, the shape (width/length*100) and the size (length*width) of the hand, foot, lips, nose and the neck, to obtain a 2D configuration matrix.

Finally, on the pooled dataset we investigated the effect of the tactile acuity and the actual size of each body part on the EE for each dimension separately. To this end, we extracted the two-point discrimination threshold from studies investigating tactile acuity by means of a two-point discrimination task (Chen et al., 1995; Gentilucci et al., 2001; Gentilucci & Campione, 2011; Mancini et al., 2014; Nolan, 1985). We also explored the modulation of the effect of tactile acuity by that of the actual size, following previous reports (Linkenauger et al., 2015; Sadibolova et al., 2019). For each dependent variable (length EE and width EE) we fitted four different models: 1) a null Linear Mixed-Effects Model including random intercepts; 2) a model including the actual dimension as fixed effect and random intercepts and slopes; 3) a model with the tactile acuity as fixed effect including random intercepts and slopes, 4) a model with the tactile acuity, the actual dimensions as well as their interaction as fixed effects including random intercepts and slopes. We used the likelihood ratio test to detect a significant difference in the residual sum of squares between each pair of nested models. This last set of analyses was computed in R (R Development Core Team, 2008).

Results

We first investigated the perceived length and width of the hand and the foot. We found that both those measures are underestimated i.e., they are perceived as shorter and thinner than their actual dimension (HAND length EE = -10.07 ± 6.45 %, $t(13) = -5.727$, $p < .001$, $BF_{10} = 349.928$; width EE = -5.28 ± 7.72 %, $t(13) = -2.676$, $p = .019$, $BF_{10} = 3.367$; FOOT length EE = -9.37 ± 9.99 %, $t(13) = -4.780$, $p < .001$, $BF_{10} = 94.385$; width EE = -5.23 ± 7.47 %, $t(13) = -3.525$, $p = .004$, $BF_{10} = 12.846$). Despite the differences in actual size across the hand and the foot, both body parts appear to be similarly distorted (main effect of body part: $F(1,13) = .317$, $p = .583$, $BF_{10} = 0.247$, dimension: $F(1,13) = 3.603$, $p = .080$, $BF_{10} = 1.329$, and interaction: $F(1,13) = .008$, $p = .930$, $BF_{10} = 0.200$).

We next investigated the perceived dimensions of the lips, the nose and the neck, which vary in tactile acuity and visual accessibility. The lips and the nose were underestimated in their length (LIPS, EE = -7.56 ± 8.52 %, $t(15) = -3.321$, $p = .005$, $BF_{10} = 10.340$; NOSE, EE = -5.57 ± 8.88 %, $t(15) = -3.94$, $p = .001$, $BF_{10} = 33.345$) and also in their width (LIPS, EE = -3.20 ± 6.95 %, $t(15) = -2.243$, $p = .040$, $BF_{10} = 1.773$; NOSE EE = -14.45 ± 8.02 %, $t(15) = -10.410$, $p < .001$, $BF_{10} = 440e+6$). In contrast, the length and width of the neck were accurately perceived (length EE = $.79\% \pm 9.80$, $t(15) = .323$, $p = .751$, $BF_{10} = 0.268$; width EE = -3.06 ± 7.80 %, $t(15) = -1.571$, $p = .137$, $BF_{10} = 0.709$). We evaluated the effect of body part and dimension on the EE in a 2x3 within-subject analysis of variance (ANOVA). We found a main effect of dimension ($F(1,15) = 5.272$, $p = .037$, $BF_{10} = 10.73$), reflecting a bigger underestimation of the perceived length compared to the perceived width, a significant main effect of body part ($F(1,15) = 4.594$, $p = .049$, $BF_{10} = 17.023e+4$) and a significant interaction ($F(1,15) = 4.755$, $p = .046$, $BF_{10} = 24.950$). Post-hoc test revealed that the perceived length of the lips and nose were underestimated more compared to the neck (lips vs neck length EE: $p = .049$, $BF_{10} = 3.681$; nose vs neck length EE: $p = .034$, $BF_{10} = 4.993$). In contrast, the perceived width of the nose was more underestimated than those of the lips and the neck (nose vs lips width EE: $p < .001$, $BF_{10} = 1414.796$; nose vs neck width EE: $p = .001$, $BF_{10} = 180.708$).

To compare the pattern of distortions in the perception of the length and width across different body parts we pooled the data from the two experiments. We fitted a Linear Mixed-Effects Model with body part and dimension as fixed effects, incorporating random intercepts and slopes to account for inter-subject variability. We confirmed that the residuals were normally distributed (Shapiro-Wilk test of normality: $p = .238$). **Figure 2.3** shows the error estimation for both dimensions and body parts. We found a significant effect of body part ($F(4,177) = 7.124$, $p < .001$), an interaction between body part and dimension ($F(4,177) = 5.291$, $p < .001$) and no main effect of dimension ($F(4,177) = .14$, $p = .906$). Post-hoc tests revealed that the length of the neck was more veridically perceived (less underestimated) than the length of the hand ($p < .001$), the foot ($p = .001$), and the lips ($p = .014$), whereas the perceived width of

the nose was significantly more distorted (underestimated) than that of all other body parts (nose vs. hand: $p = .008$, nose vs. foot: $p = .005$, nose vs. lips: $p < .001$, nose vs. neck: $p < .001$).

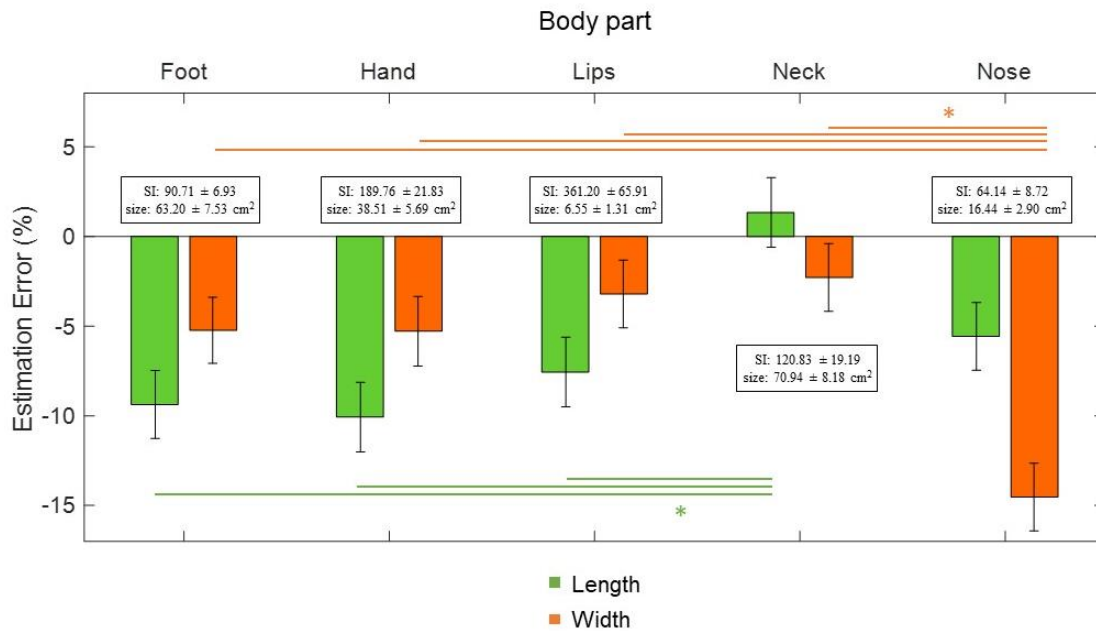


Figure 2.3 Body part estimation error ($100 * \text{perceived size} / \text{actual size}$) for 5 different body parts. Bars depict the mean estimation error (EE) and standard error of the mean for length (green) and width (orange). The inset above each body part denotes the actual Shape Index (SI: $100 * \text{body part width} / \text{body part length}$) and Size (body part length * body part width). Asterisks denote significance at $p < .05$, in post-hoc tests, Bonferroni corrected for multiple comparisons.

To further study and graphically describe how each representation relates to one another, we use multidimensional scaling. Starting from the Euclidean distances among the EEs referred to the body parts' length and width dimension, shape (width*length/100) and size (width*length), the multidimensional scaling can be projected to two dimensions (**Figure 2.4a**), and depicted as a dissimilarity matrix (**Figure 2.4b**). This analysis revealed that body parts cluster in three separable groups: a cluster with high similarity between the perceived size of the mouth, hand, foot and lips, which is differentiable from those representations of the neck and the foot. Specifically, hand, foot and lips representations are alike, as suggested by their closeness in **Figure 2.4a** and the dark blue cluster signaling high similarity in **Figure 2.4b**. Instead, both the representation of the neck and that of the nose are isolated and characterized by a distinct pattern of distortions.

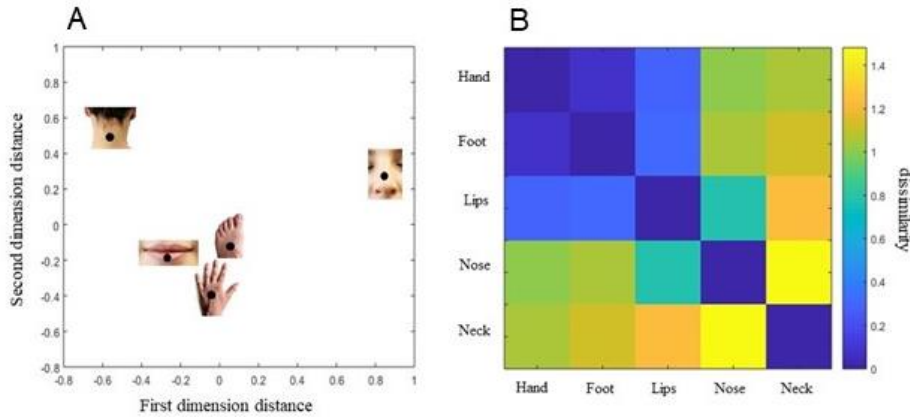


Figure 2.4 (a) Multidimensional scaling on the estimation errors (EE) for the length, the width, the shape (width*length/100) and the size (width*length) is projected onto two dimensions (b) dissimilarity matrix across body parts. Proximity in the 2D space and blue colors in the dissimilarity matrix indicate higher similarity.

The body parts tested in our study differ in their proportions: some body parts are larger in their horizontal than in their vertical dimensions e.g., the lips; while others have the opposite pattern i.e., they are larger in the vertical than in the horizontal dimension, e.g., the nose. They also differ in their tactile acuity. For instance, small distances across two points minimally separated are detected in the lips, while for the neck, much larger distances across two points are required to detect such a difference. We reasoned that those factors or a combination thereof could underlie the pattern of distortions observed across different body part. To test this hypothesis, we fitted four Linear Mixed-Effects Model testing for the effect of the actual size of the body part in their vertical and horizontal dimension, their respective tactile acuity, and their combined effect on each dependent variable (EE for length and width). Each model, along with the fixed intercept and slopes, incorporated random intercepts and slopes to account for inter-subject variability. We also included a null model. For all fitted models the residual distributions were checked through QQ-plots to ascertain the normality assumption. For the EE length, we found that tactile acuity explained a significant proportion of the variance (Likelihood ratio = 13.580, EE ($t(47)$) = 3.117, $p = .003$, with $\beta = .187$), while the size of the body part or its combined effect with tactile acuity did not improve the fitting (**Figure 2.5a**). This means that the lower is the tactile acuity, the more accurate is the length estimation. Regarding the EE on the width, the best model was the one considering the actual size of the body part (Likelihood ratio = 13.757, $p = .003$, $t(47) = 3.840$, $p < .001$, with $\beta = 1.479$). Introducing tactile acuity and combining it with the actual size of the body part did not further improve the fitting. Visual inspection of the scatterplot (**Figure 2.5b**) suggested that the EE related to the nose

width could be contributing to the pattern of results. The nose width - the body part with the smallest wide dimension investigated - was also unexpectedly highly underestimated, compared to the other body parts. We therefore fitted the Linear Mixed-Effects Models considering the four remaining body parts. When removing the nose from the model we observed that the effect of the actual size of the body part was no longer significant ($t(30) = .238$, $p = .813$, with $\beta = .123$) and the fitting did not improve (Likelihood ratio = .238, $p = .971$). The full set of results from the different models is reported in the **Supplementary materials**.

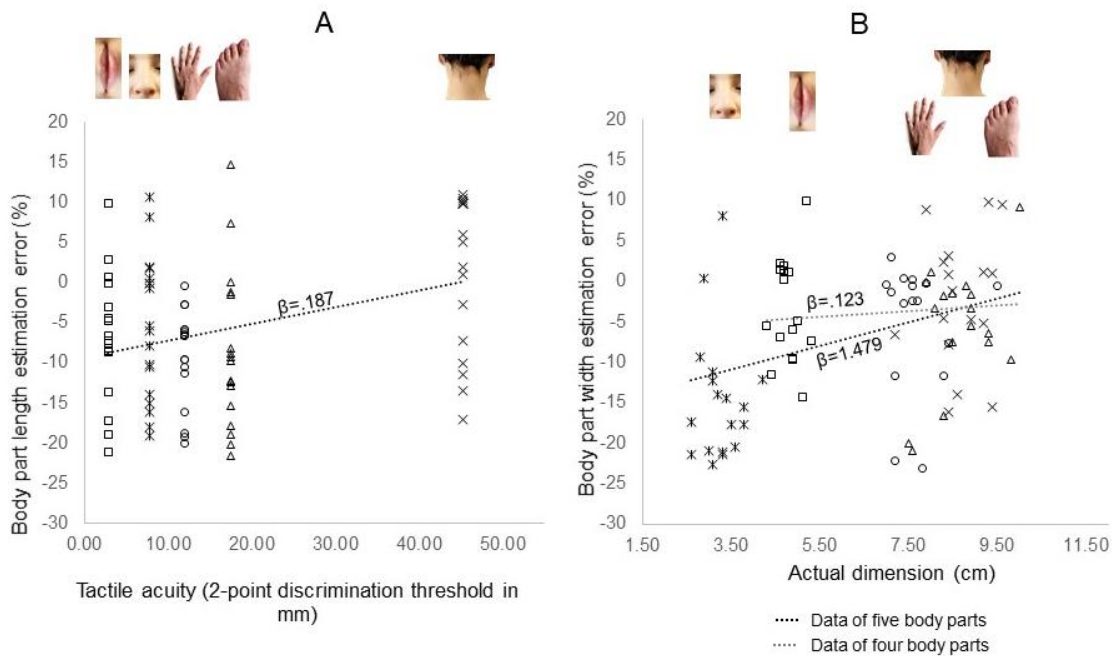


Figure 2.5 Best-fitting models predicting the EEs for length (a) and width (b) across five body parts. (a) The two-point discrimination threshold (expressed in mm) is plotted against the body part length EE for each subject and body part. Black dashed line depicts the slope relating the length EE to the tactile acuity of the five body parts; (b) the actual width is plotted against the width EE of each body part. Black dashed line depicts the slope relating actual size to the width EE for all body parts. Grey dashed line depicts the slope excluding the nose data.

Interim Discussion

Study 2 was set out to test whether distortions in the representations of one's own body parts arise from somatosensory or non-somatosensory, i.e., visual, factors. We found that the answer is not a simple “either, or”, but that both somatosensory and visual factors contribute to the misestimation of the dimensions of body parts.

In detail, we found that the perceived dimensions of the hand, of the foot, of the lips and partially of the nose are similarly underestimated, despite their different physical size and tactile acuity, supporting the hypothesis that a systematic metric bias affects mental representations. A particularly striking finding is that the dorsal portion of the neck was the only body part among those tested to be represented accurately in its dimensions. If our body representation is affected by an unspecific metric bias, such that body parts are underestimated in their dimensions, the neck should have been perceived similarly to other body parts, which was clearly not the case. Visual inputs are undoubtedly more relevant for building up and storing the representations of the hand, lips and foot, whereas it is unlikely that the representation of the dorsal portion of the neck has been built upon visual inputs. No significant variation across the perceived dimensions of the hand, foot and lips was observed, despite that their degree of visual exposure may also vary. Consequently, it can be argued that what drives the effect is an all-or-none cumulative exposure over time, which is virtually absent for the dorsal portion of the neck while comparatively high for the hand, foot and lips. Such striking difference possibly underlays the observed patterns of responses in terms of perceived dimensions.

As we measured the perceived dimensions of body parts along two orthogonal axes (medio-lateral dimension, or “width”, and rostral-caudal dimension, or “length”), we could further show that the effect of tactile acuity on perceived body part dimensions depends on whether the length or the width of the body part are judged. In fact, neither the tactile acuity alone nor its combined effect with the actual dimension were effectively explaining the variance of the width EEs. This, and results by previous work on leg representations (Stone, Keizer, & Dijkerman, 2018), speak against a purely somatosensory origin of the distortions because, following the reverse distortion hypothesis (Linkenauger et al., 2015), the representation of the body metric would need to compensate for the homunculus distortions in its longitudinal as well as transversal components.

Instead, our results also point to a visual influence on body representations: while the medio-lateral boundaries of the body parts considered in the present study were all clearly defined in visual terms, the proximo-distal boundaries were less clearly defined for the hand (tip and knuckle of the middle finger), foot (tip and knuckle of the toe) and neck (upper and higher boundary). This expands the results of Saulton and colleagues (2017), who focused on hand representations, to several other body parts.

Somewhat unexpectedly, we observed that the nose width was more underestimated than the width of all other body parts (while the estimation of the nose length was also similar to that of the lips, hand and foot). Given the small size of the nose width, it could be argued that an underestimation of a few millimeters is amplified resulting in a relatively high EE. However, if the size of the body part played a role, we should have obtained similar effects for body parts with small sizes such as the height of the lips or the length of the toe, which was not the case. Another possible explanation for the unexpected result

may be rooted in the intrinsic shape of the nose. Among all the distances considered, the nose width is probably the most difficult to be retrieved in 2D-space, as the LLJ task required. In fact, the nose can be represented as an irregular tetrahedron, with one of the vertices aligned with the nose tip. The task instructions implicitly required the participants to retrieve the 2D-size (in terms of basis and height) of one of the faces of the polygon, the one opposite to the nose tip. While the height of that face is easily projected onto the longitudinal edge of the tetrahedron, the basis cannot be projected onto an edge, possibly increasing the difficulty of its estimation.

It is interesting to note that our results regarding the perceived hand dimensions apparently diverge from those reported in the literature. A previous study reported an underestimation up to 40% of the distance between the tip of the middle finger and the knuckle (Longo, Mattioni & Ganea, 2015), using a Localisation Task. However, when using the LLJ task in the same group of participants such distance was underestimated by only 25%. The discrepancies in the size of the misestimation have been attributed to the fact that the LLJ task appears to rely less on a somatosensory representation and more on the visual body image which is more accurate (Longo, Mattioni, & Ganea, 2015; Longo & Haggard, 2012b). Furthermore, when participants were asked to refer to the distance between the middle fingertip and its basis rather than its knuckle, avoiding biases related to the mislocation of the finger knuckles, the underestimation decreased from 40% to about 30% (Saulton, Bühlhoff, & de la Rosa, 2017). We argue that our results, and in particular the size of the misestimation we obtained, are comparable to those that have been previously reported when using the LLJ Task. Similarly, in previous studies, the hand width (i.e., distance between the knuckles of the index and little fingers) was overestimated up to 80% using a Localisation Task (Longo & Haggard, 2010; Longo & Haggard, 2012b), but dropped to about 7-10% when assessed through the LLJ Task (Longo, Mattioni, & Ganea, 2015; Longo & Haggard, 2012b). Importantly, when participants were asked to estimate the width of their hand referring to the distance between the bases of the little and index fingers, it was perceived as slightly underestimated (around 4-5%, Saulton, Bühlhoff, & de la Rosa, 2017). This is a range comparable to the one we obtained in our study.

Taken together, our results support previous findings of systematic distortions of the dimensions of body parts. Both somatosensory components, i.e., tactile acuity and the overall size of a given body part, and visual components, i.e., the demarcation of visual landmarks, seem to contribute to these distortions. The pattern of size misestimation is similar for body parts that are visually accessible, but strikingly different for a body part which is not (the dorsal portion of the neck). This suggests that the two (and possibly other) sources of information are weighted to form a multisensory body representation depending on their respective availability. For instance, it is plausible that visual inputs are weighted more than the somatosensorial ones for the visually accessible body parts. Similarly, at least for the body

parts assessed in our experiments, the visual bias might be more relevant in building up the representation along the medio-lateral axis, compared to the proximo-distal one, as overall the medio-lateral boundaries are less visually defined in our body parts sample. As a matter of fact, we showed that the tactile acuity significantly predicts the misestimation of proximo-distal dimension of body parts whereas it does not have an effect on the medio-lateral estimation. Multisensory representations of the body are formed in parietal cortex (Corradi-Dell'Acqua, Tomasino, & Fink, 2009) and/or through interactions between unisensory processing centers: for example, it has been shown that visual information modulates somatosensory processing (Taylor-Clarke, Kennett, & Haggard, 2002) and conversely, that somatosensory information affects visual processing (Lunghi, Lo Verde, & Alais, 2017).

Study 4: Biases in body representation: are they body specific? ⁴

Introduction

In an ecological perspective, the selective misestimation of our body dimensions may not be functional for an efficient interaction with the environment. For instance, hand-object interaction is likely to be affected by the size misestimation of our hand (see Chapter 1). However, we have little (and contrasting) evidence about how objects are represented, compared to the hand. Previously, authors have administered a template matching task and a Localisation Task to study the perceived shape of the participant's hand and of some real objects (Saulton et al., 2015). Some of them (e.g. a CD-box) turned out to be misperceived in the template matching task, in which participants were required to compare the size of a previously observed object with that of a black silhouette. Responses regarding the hand, as well as other objects (e.g. a post-it pad and a rake), were instead accurate on average. In the Localisation Task, distortions were detected for all the object representations, but were larger for the hand representation. However, results of a recent study indicated that the biases affecting the hand map measured by the Localisation Task are amplified by a visual mislocation of the knuckles. When this visual error was controlled, no differences were observed between the hand and hand-shaped objects (Saulton et al., 2017).

Study 4 is an extensive investigation about the perceived dimensions of the hand and daily-life objects to evaluate whether the metric distortions previously reported for the body also extend to the representations of objects. We hypothesised that, if distortions described for the hand are body-specific, there would be a difference between the representation of the hand and those of objects. Instead, if the pattern of distortions is similar among the representations of the hand and different objects, our results would support the existence of an unspecific metric bias in mental representations. In addition, we asked whether those biases generalize to familiar as well as unfamiliar objects, to objects which are temporarily integrated as part of the body schema, and to objects which do not afford manipulation and interaction. In other words, we manipulated familiarity, sense of ownership and affordances of the objects, to assess whether any of these factors modulate their representations.

To this aim, a total of 152 participants were recruited in six experiments and administered with the previously described Line Length Judgment (LLJ) task, depicted in Figure 2.2.

In the first part of the study (Experiment 1, 2 and 3, resumed in **Figure 2.6**) we aimed at comparing the hand representation with the representations of objects of varying shapes (mobile phone, coffee mug and fake hand), and to test the effect of familiarity on their representations. By means of a fourth experiment, we investigated the effect of the ownership illusion toward a fake hand on its

⁴ The following sections (introduction, method, analysis and discussion relative to Study 4) have been largely extracted and adapted from Peviani, Magnani, Melloni & Bottini (in preparation).

perceived dimensions. To preview our results, we found that the pattern of distortions characterising the hand representation extends to daily-life objects.

In a second set of studies (Experiments 5 and 6, depicted in **Figure 2.6**) we aimed at testing whether this result (i.e., similar misestimation of the dimensions of the hand vs an object) generalizes to objects that do not afford interaction and manipulation. Previous studies have indicated that our perception of the objects in the environment is influenced by our ability to act on them, and thus that perception is action-specific (Witt, 2011). The action-specific perception account developed from Gibson's (1979) ecological approach posits that perception is shaped by affordances, which represent the possibility for action. Within the action-specific perception frame, we perceived the environment based on our abilities. For instance, the perceived size of a softball relates to the player's hitting success (Gray, 2013; Witt & Proffitt, 2005), the perceived size of objects that can be grasped differs from those that cannot be grasped because they are too wide (Linkenauger et al., 2011).

Since in visual perception our hand is thought to function as a ruler that scales the world (Linkenauger et al., 2014, 2011), it could be hypothesised that the mental representation of a graspable and manipulable object is scaled by the mental representation of our hand. To evaluate this prediction, we compared the metric representations of objects which elicit an interaction (mobile phone and computer mouse) with those of objects which are supposed to inhibit an interaction (cactus and disgusting soap).

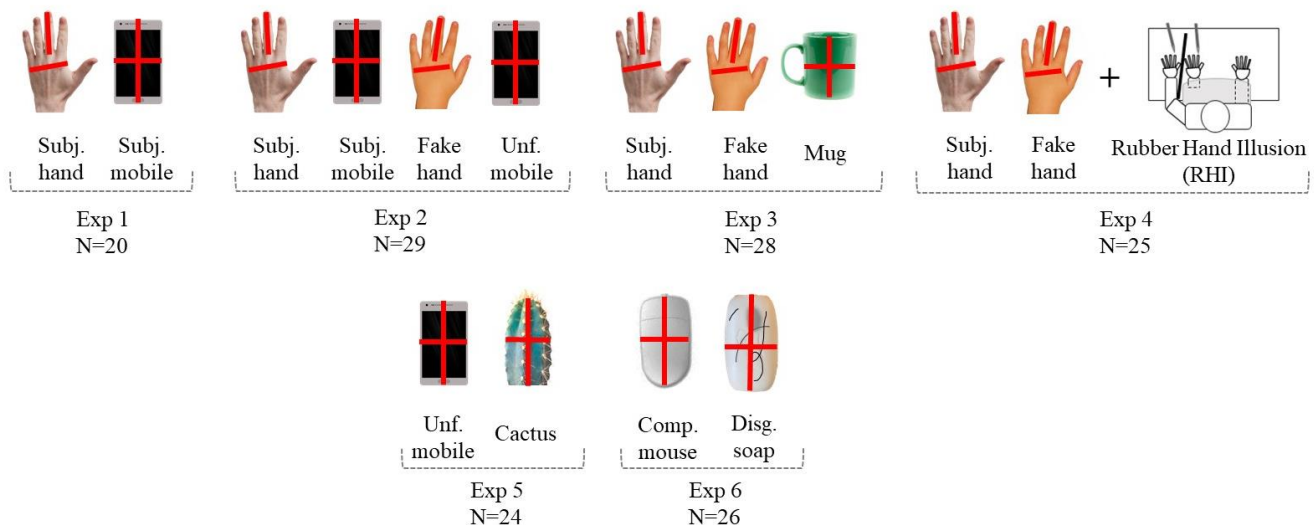


Figure 2.6 Experiments, sample sizes and targets addressed by the study are. For each target, two orthogonal dimensions were the object of participants' estimations.

Method

Experiment 1: Hand, owned Mobile phone

We investigated the mental representation of two targets: the participant hand and a highly familiar object, the participant's own mobile phone. We considered as vertical dimensions the length of the middle finger and the height of the mobile phone; and as horizontal dimensions the width of the hand dorsum, at the level of the knuckles, or the width of the mobile phone. We presented 120 trials per block (4 blocks in total) spanning lines that covered the range from -30% to -1% (shorter) and from 1% to 30% (longer) of the actual target's dimension, in step of 1%. Twenty healthy right-handed participants (16 females) aged 22 to 45 (mean age 27.10 ± 5.64) were enrolled in the experiment. The average hand dimensions were 8.50 ± 0.57 , 7.60 ± 0.72 cm; the average mobile phone dimensions were 13.66 ± 0.95 , 6.75 ± 0.51 cm. First and second values indicate vertical and horizontal dimensions respectively.

Experiment 1: Analysis

Firstly, the occurrence of inaccurate responses was plotted against the percentage of the line shortening (-1% to -30%) or lengthening (1% to +30%) compared to the actual dimensions of each target. We observed a clear asymmetry of the inaccurate responses distribution showed in the **Supplementary materials**.

Raw dichotomous responses ("shorter", "longer") were grouped into six line-distortion ranges: i) -30 to -21%, ii) -20 to -11%, iii) -10 to -1%, iv) 1 to 10%, v) 11 to 20 % and vi) 21 to 30%, assigned to labels -2, -1, 0, 1, 2 and 3. For each distortion range, the sum of "longer" responses was computed and used to fit a psychometric function to determine the Point of Subjective Equality (PSE). The PSE corresponds to the line-distortion range subjectively perceived as the same as the target i.e., the range at which participants choose randomly between shorter or longer lines compared to a given target dimension. When the $PSE = 0$, the representation of that target dimension equals the real one. A $PSE > 0$ indicates that the target dimension is overestimated i.e., considered longer than its real dimension, while a $PSE < 0$ indicates that the target dimension is underestimated i.e., considered shorter than its real dimension. We fitted a Cumulative Normal Psychometric function to estimate the threshold and slope while constraining the intercept (from 0 to 0.5 in steps of 0.1) and fixing the lapse rate (0.05). The estimated thresholds represent the PSEs. The functions were fitted using Palamedes toolbox (Prins & Kingdom, 2018) for MATLAB (The MathWorks, version R2017b). One subject was excluded from subsequent analyses due to poor fitting (Goodness of Fit $p < .01$) in more than the 50% of the experimental conditions.

Subsequently, for each subject, target and dimension, the PSE (ranging from -2 to 3) was transformed back to its original scale (-30 to +30%). Those values represent the estimation error (EE) i.e., underestimation (negative sign) or overestimation (positive sign) of a target and dimension. As an example, if the PSE = -1.129, the corresponding EE would be -11.29%, which, if referred to the estimation of a target 8.20cm wide, would result in a perceived size of 7.27cm and, thus an absolute underestimation of 0.93cm. Extreme outliers EE values defined as higher than the third quartile plus three times the third interquartile, or lower than the first quartile minus three times the first interquartile were removed. This excluded one further subject from subsequent analyses. Data were normally distributed as evaluated by means of the Shapiro-Wilk Normality Test (all p s > .05).

Finally, we conducted one-sample t-tests on EE distributions against zero, correcting for multiple comparisons within each target, and a 2x2 repeated-measures analysis of variance (rmANOVA) in SPSS (IBM Corp. Released 2010) to study the effect of Target (hand, mobile) and Dimension (horizontal, vertical) on the EE. In addition, we report Bayes factors - BF_{10} - (Rouder et al., 2009) which represent the likelihood of the presence of the effect (H1) to the likelihood of the absence of such effect (H0), given the data. BF_{10} values larger than 1 represent evidence for the alternative hypothesis (H1). Bayesian analyses were performed in JASP (JASP Team, 2018).

Experiment 1: Results and Discussion

The one-sample t-tests, after Bonferroni correction, showed only significant underestimation of the vertical dimension of the hand and mobile phone. Descriptive statistics (means, standard deviations and t statistics) are reported in **Table 2.1**. The rmANOVA revealed that the vertical dimension is significantly underestimated compared to the horizontal dimension (significant main effect of Dimension: $F(1,17) = 12.049$, $p=.003$, $BF_{10} = 33.299$), independently of the target considered (non-significant main effect of Target: $F(1,17) = .821$, $p=.553$, $BF_{10} = .379$; non-significant interaction: $F(1,17) = 1.873$, $p=.189$, $BF_{10} = .602$). See **Figure 2.7**.

In line with previous reports (Longo & Haggard, 2010, 2012b; Longo et al., 2015), we observed that the hand's vertical dimension was underrepresented compared to its horizontal dimension. This pattern of distortions is however not specific to the subject's hand as it generalised to the representation of a very familiar object i.e., the subject's mobile phone. As our mobile phone holds a special status among objects, since we see and interact with it frequently (i.e., we are extremely familiar with it), it is possible that the observed distortions in their representation are inherited from those of the hand representation. To directly investigate this possibility, in the next study we manipulated the degree of familiarity to the mobile phone.

Experiment 2: Hand and owned Mobile phone, Fake Hand and unfamiliar Mobile phone

The second experiment had three aims. First, we sought to replicate the results of the first experiment in an independent sample of subjects. Second, we aimed to determine whether familiarity with an object plays a role in how it is represented. In other words, we aimed to test whether the similarity between the representations of the participant's hand and mobile phone observed in experiment 1 was a "special case" due to the frequent interaction with the mobile phone. To this end, subjects judged the size of their own mobile phone, and an unfamiliar mobile phone, and those judgements were contrasted with the ones obtained for the participant's own hand. Finally, we investigated whether the metric distortions observed for the own hand extend to an unfamiliar, hand-shaped object, namely a fake hand.

As new targets, we used a plastic-made fake hand sized 9.50cm (middle finger length) x 9.60cm (palm width) and a smartphone Samsung A5 sized 14 x 7.1cm. None of the participants owned the same model of mobile phone. The experiment consisted of 8 blocks: 2 blocks per target, one per dimension i.e., vertical and horizontal. Based on the pattern of distortions observed in experiment 1, where inaccuracy was skewed towards smaller line segments (**Supplementary materials**), we presented lines whose length spanned -30% to +10% of the actual measures. Each block contained 80 lines, 2 per each unitary distortion, from -30% to -1% (shorter) and from 1% to 10% (longer) of the actual target's dimension. Twenty-nine healthy right-handed participants (25 females) aged 20 to 32 (mean age 23.34 ± 2.59) were enrolled. Data from one subject was removed as extreme outlier, detected through box-and-whiskers plots on the EEs. The average vertical and horizontal dimensions of the participants' hand were 8.48 ± 0.46 and 8.16 ± 0.48 cm; whereas the average vertical and horizontal dimensions of the mobile phone were 13.89 ± 1.02 and 6.87 ± 0.67 cm.

Experiment 2: Results and Discussion

All EE distributions were normally distributed as revealed by Shapiro-Wilk Normality tests (all p s > .05). We conducted one-sample t-tests to study the EEs and a 4x2 rmANOVA to study the effects of Target (hand, owned mobile, fake hand, unfamiliar mobile) and Dimension (vertical, horizontal) on the EEs. Each dimension was significantly underestimated, as reported in **Table 2.1**.

The rmANOVA showed significant main effects of Target ($F(3,25) = 3.364$, $p=.023$, $BF_{10} = 2708$) and Dimension ($F(1,27) = 12.947$, $p<.001$, $BF_{10} = 2475e+9$), which significantly interacted ($F(3,25) = 3.360$, $p<.001$, Greenhouse-Geisser corrected, $BF_{10} = 4697$). Bonferroni corrected post-hoc comparisons revealed that the vertical dimension was more underestimated than the horizontal dimension for all targets except for the fake hand (comparison between vertical and horizontal dimensions for participant's hand: $p=.037$; participant's mobile: $p<.001$; unfamiliar mobile: $p<.001$ and fake hand: $p=.926$). Furthermore,

post-hoc comparisons detected a smaller underestimation of the vertical dimension of the fake hand compared to that of the participant's mobile ($p < .001$), and unfamiliar mobile phone ($p < .001$); as well as a trend compared to the participant's hands ($p = .052$). See **Figure 2.7**.

These results replicate the findings of experiment 1, in which the dimensions of the participant's hand and mobile phone were misestimated. The same pattern of distortions was observed also for an object with which participants had never interacted before i.e., unfamiliar mobile phone. These findings support the hypothesis that metric distortions ascribed to the hand generalise to those of objects, regardless of the degree of familiarity with them. In other words, visually encoding and recalling the dimensions of an unfamiliar mobile phone resulted in similarly distorted representations compared to recalling the dimensions of one's own mobile phone. Importantly, participants were asked to observe only unfamiliar objects (i.e., mobile phone and fake hand) prior to the task, and not the familiar ones (i.e., own mobile phone and hand), indicating that neither familiarity nor previous observation of the objects plays a role in their misrepresentation.

Surprisingly, the representation of the fake hand revealed a different pattern of distortions, with the vertical and horizontal dimensions similarly underestimated. These results contrast to previous reports by Saulton et al., (2016), who reported a similar misestimation of participants' hand and fake hand in a size estimation task, with the vertical dimension underrepresented compared to the horizontal one. It is possible that dissimilarities in the experimental design and task used between studies explain that difference. Specifically, we identified two factors that might have driven the difference. First, Saulton and colleagues explicitly asked participants to memorise the distance between two landmarks of a target (e.g. index and little finger knuckles) observed for 40 seconds, and to provide an estimation of the target's dimensions ten seconds after the observation on a paper-and-pencil task. This process does not necessarily require the internalisation of a mental representation of the target as a whole. Instead, we asked participants to observe the target without further instruction. Our purpose was indeed to trigger the internalisation of a mental representation of the target as a whole, which was retrieved during the LLJ task. It is plausible that memorising and retrieving a distance resulted in a different outcome compared to internalising and retrieving the target's mental representation to make a distance judgment. Second, in their study, participants estimated the remembered vertical or horizontal dimension of the target, in relation to the origin of the axes of a two-dimensional coordinate system displayed in an answer sheet. Instead, in our task, we decided not to provide a coordinate system, which was internally defined as opposed to externally presented.

We speculate that our experimental paradigm might be more sensitive to detect fine differences in the represented size of different objects, perhaps more difficult to detect using Saulton's task, in which participants are facilitated during the encoding and retrieving of the object's dimensions. We believe that

investigating how changing task instructions and response modality drives to different outcomes is an important venue for future research, since it could shed the light on the cognitive mechanisms underlying object's size estimation and representation.

This study demonstrated that familiar as well as unfamiliar objects are similarly distorted. Do these distortions apply to other objects? To answer this question in the next experiment we used another target, i.e., a mug, which is more neutral (less linked to one's own identity), still manipulable yet less frequently manipulated than a mobile phone.

Experiment 3: Hand, Fake Hand, Mug

The Experiment 3 was aimed to i) test whether the similarity between the representation of the hand and the mobile phone extend to a different object, a coffee mug; ii) to replicate the results of experiment 2, in which we observed a difference between the perceived dimensions of the participant's hand and of a fake hand. We thus explored the mental representation of the participants' hand, of a mug and of a fake hand. The mug was cylindrical, 9cm wide (mug's diameter) and 10cm high. Its height was considered as the vertical dimension. Each block contained 80 trials, 2 per each unitary line distortion spanning from -30% to 10% of the actual target's dimension. Twenty-eight healthy right-handed participants (24 females) aged 19 to 45 (mean age 25.11 ± 8.90) were enrolled for this experiment. The average vertical and horizontal dimensions of the participant's hand were 8.44 ± 0.48 and 8.13 ± 0.59 cm. Data from four participants were excluded from further analysis, one due to poor fitting in one condition, and three others due to outlier responses in one or more conditions.

Experiment 3: Results and Discussion

Data were normally distributed as evaluated by the Shapiro-Wilk Normality Test (all p s > .05). We conducted one-sample t-tests on the EEs and a 3x2 rmANOVA with factors Target (hand, fake hand and mug), and Dimension (vertical, horizontal). Each target dimension was significantly underestimated, except for the fake hand vertical dimension (see **Table 2.1**). The rmANOVA revealed a significant main effect of Target ($F(2,22)=4.904$, $p=.012$, $BF_{10}=11.244$) which also interacted with Dimension ($F(1,23)=3.264$, $p=.047$, $BF_{10}=2.421$). Bonferroni corrected post-hoc comparisons revealed that the vertical dimension of both the participant's hand and the mug were more underestimated than the fake hand ($p=.023$ and $p=.018$ respectively). We also found a lower underestimation of the vertical dimension compared to the horizontal dimension for the fake hand only ($p=.032$). See **Figure 2.7**.

These results further corroborate our previous findings by showing systematic distortions of the metric representation of the hand, but also of objects, regardless of the degree of interaction and

familiarity with those objects. This finding questions the specificity of the distortions characterising the hand metric representation, at least when measured by a visual-based task.

The objects studied so far i.e., participant's mobile phone, unfamiliar mobile phone and mug, are highly manipulable and the body, specifically the hand, is used to interact with them. It could thus be argued that misestimation for objects is inherited from the pattern of distortion related to the hand, and does not represent an independent phenomenon. In visual perception, for instance, it has been proposed that the environment is scaled on the basis of the perceived size of one's own dominant hand (Linkenauger et al., 2014, 2011). Evidence for this conjecture comes from a study by Linkenauger and colleagues (2011). They investigated the impact of the perceived size of the participant hand on judgments of graspable and non-graspable (too large to be grasped) objects. Using virtual reality to modify the visually perceived size of the participant's hand, they found that object's perceived size scales with the perceived size of the hand e.g., when the hand was perceived as bigger, the object was judged as smaller. This effect applied to graspable objects only. In this context, the fake hand may be seen as a hybrid target. An object which, while resembling a body part, - is still an object - a body part surrogate. As such, it is unlikely to elicit a manipulation, as it is perceived as external and detached from one's body schema (Apps & Tsakiris, 2014; Botvinick & Cohen, 1998). The fake hand, is thus a special object as it varies from the others previously tested in at least two aspects: the sense of ownership and the degree of interaction. In the next set of studies, we thus aimed to investigate the role of the sense of ownership and embodiment toward the fake hand in shaping its metric representation (Experiment 4), and whether the degree of manipulability influence the metric distortions observed for objects (Experiments 5 and 6).

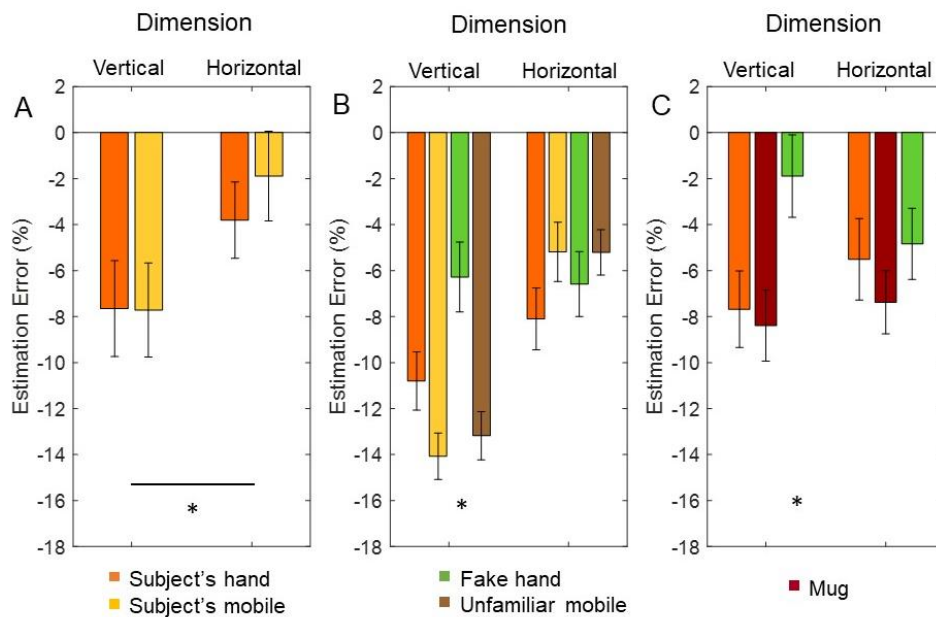
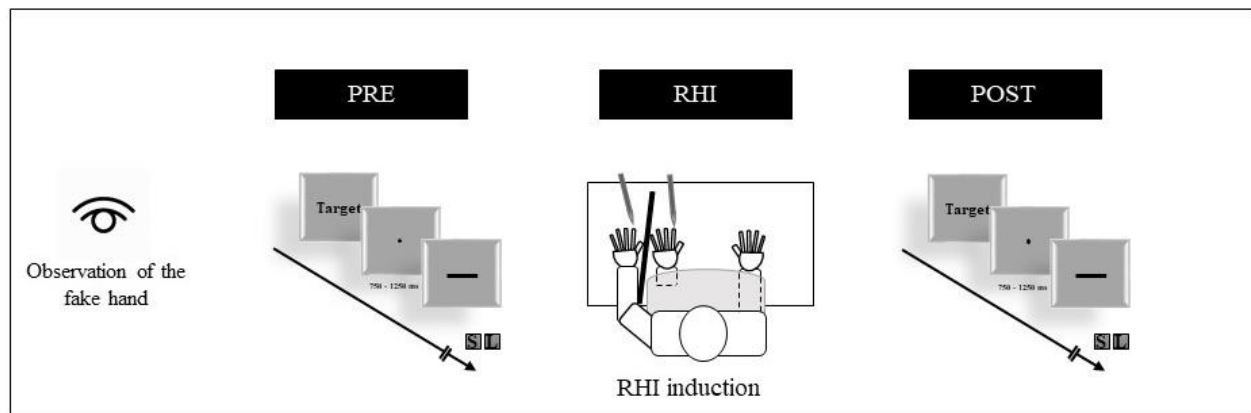


Figure 2.7 Mean EEs and their standard errors are plotted for Experiment 1, 2 and 3. Experiment 1 (a) compared the participant's hand and mobile phone metric representations. A significant main effect of Dimension was detected, as signaled by the asterisk. Experiment 2 (b) replicated the previous comparison and introduced an unfamiliar mobile phone as well as a fake hand. Experiment 3 (c) compared the representations of the participant's hand with that of a coffee mug and of a fake hand. The vertical dimension of the fake hand was underestimated less compared to that of the other objects considered in Experiment 2 and 3, as signaled by the asterisks.

Experiment 4: Fake Hand and Hand before and after the Rubber Hand Illusion

In Experiment 4 we took advantage of the Rubber Hand Illusion (RHI) paradigm (Botvinick & Cohen, 1998) to induce the illusion of ownership toward the fake hand and to assess possible changes in its metric mental representation as a consequence of the illusion.

We evaluated the metric representation of two targets: the participant's hand and a fake hand, before (pre) and after (post) inducing the RHI illusion (synchronous condition). As a control, we also evaluated the metric representation of each target without inducing the RHI illusion (asynchronous condition). Each participant thus underwent four experimental runs, divided in two consecutive days, resulting from the crossing of targets (hand and fake hand), RHI induction (synchronous or asynchronous), as depicted in **Figure 2.8**. The order of the experimental runs (target and RHI) was counterbalanced across participants. Each LLJ task run included 2 blocks (one for target vertical dimension estimation, one for target horizontal dimension estimation), containing 80 trials each, 2 per each unitary distortion ranging from -30% to -1% (shorter) and from 1% to 10% (longer) of the actual target's dimension. Participants were asked to observe the fake hand for 60 seconds before each of the two pre-LLJ tasks.



x4 RUNS in 2 days

		PRE - LLJ Task Target:	RHI Condition:	POST - LLJ Task Target:
counterbalanced across participants	RUN 1	Participant's Hand	Synchronous	Participant's Hand
	RUN 2	Participant's Hand	Asynchronous	Participant's Hand
	RUN 3	Fake Hand	Synchronous	Fake Hand
	RUN 4	Fake Hand	Asynchronous	Fake Hand

Figure 2.8 Experimental design of Experiment 4. Each participant underwent four experimental runs, resulting from the combination of two conditions with two levels each (LLJ target: participant's hand vs fake hand; RHI induction: synchronous vs asynchronous), in two consecutive days. Each experimental run consisted of: i) the administration of the LLJ task (PRE-RHI); ii) the RHI induction; iii) the administration of the LLJ task (POST-RHI). When the fake hand was the target, participants were asked to observe the fake hand for 60 seconds before each of the two pre-LLJ tasks.

During the RHI runs, we aimed to induce ownership of a fake hand to the participant's left hand. To that end, participants sat with their left and right hands comfortably resting on a table. Their right hand was aligned to their shoulder line while their left hand was placed to the left of the participants' shoulder line. A fake left hand, same as in previous experiments, was located 17.5cm from the real left hand and aligned to the participants' left shoulder line. To occlude visibility of the real left hand during tactile stimulation, the participant's hand and the fake hand were separated by an opaque vertical board. Tactile stimulation was delivered by means of two paintbrushes on the left index finger of the participant and on the index finger of the fake hand. During synchronous tactile stimulation, the investigator stroked vertically and simultaneously ($\sim 1\text{Hz}$) the index finger of the real and fake hand. During the asynchronous stimulation, the investigator stroked the index finger of the real and fake hands sequentially. Each RHI run comprised two synchronous and two asynchronous tactile stimulations, each lasting 90 seconds. After

each tactile stimulation, the strength of the illusion was determined through proprioceptive drift and ratings of the subjective illusion with an adapted version of the Illusion Rating Questionnaire (Botvinick & Cohen, 1998). Participants rated 9 statements on a Likert scale from -3 to +3. To record the proprioceptive drift, namely the change in the perceived position of the participants' hand after tactile stimulation, we followed established procedures (Marotta, Tinazzi, Cavedini, Zampini, & Fiorio, 2016; Peviani, Magnani, Ciricugno, Vecchi, & Bottini, 2018; Wold, Limanowski, Walter, & Blankenburg, 2014). Before and after tactile stimulation, the opaque vertical panel was replaced by a board (50cm x 40cm), horizontally placed 10cm above the participants' hands while they had their eyes closed. The horizontal board was equipped with a tape with numbers randomly selected from 0 to 40 at the same level of the participants' hands. The participants were asked to speak out the corresponding number of their left index finger perceived position, three times before and one time after each stimulation. For each judgment, the tape was replaced with a new one bearing a different number sequence. The proprioceptive drift was computed as the difference between the proprioceptive judgments before and after each tactile stimulation (Abdulkarim & Ehrsson, 2018).

Twenty-five healthy right-handed participants (17 females) aged 20 to 35 (mean age 23.00 ± 2.94) were enrolled for this experiment. The average hand dimensions were 8.52 ± 0.72 , 7.74 ± 0.57 cm.

Experiment 4: Analysis

With our experimental design we aimed at testing whether the experimental manipulation, i.e., the RHI, produced significant changes in how the hand is represented. Therefore, we decided to include in our analyses only participants for which the experimental manipulation was effective, i.e., participants who experienced the RHI. To determine which participants experienced the RHI, we considered the proprioceptive drift (PD) and the subjective illusion score (SIS) for questions 2 (q2) and 3 (q3) in the synchronous condition. We considered these two questions as they are sensitive to the ownership illusion and explicitly referring to the feeling of ownership toward the rubber hand (Botvinick & Cohen, 1998; Ocklenburg, R  ther, Peterburs, Pinnow, & G  nt  rk  n, 2011); q2: "It seemed as though the touch I felt was caused by the paintbrush touching the rubber hand" and q3: "I felt as if the rubber hand were my hand". The PD and SIS were not correlated (session 1: Spearman's $\rho = .046$, $p = .830$ and Spearman's $\rho = .225$, $p = .291$ for PD and SISq2, and PD and SISq3, respectively; session two: Spearman's $\rho = -.192$, $p = .368$ and Spearman's $\rho = .185$, $p = .386$ for PD and SISq2, and PD and SISq3, respectively), likely because they reflect partially independent phenomena (Peviani et al., 2018; Riemer, Bublatzky, Trojan, & Alpers, 2015; Rohde, Di Luca, & Ernst, 2011). Since we were mostly interested in the effects of the conscious feeling of ownership on the hand metric representation, we prioritised the subjective

rating as a criterion for selecting participants. Specifically, we selected participants whose rating on q2 and q3 were consistently high (>0) across the two synchronous stimulations conditions. Fifteen participants were selected based on this criterion. It is worth mentioning that high scores at Question 1 are also reported by participants who experienced the illusion (Botvinick & Cohen, 1998; Ocklenburg, R  ther, Peterburs, Pinnow, & G  nt  rk  n, 2011). Question 1 investigates the strength of the visuo-tactile binding (q1: “It seemed as if I felt the touch of the paintbrush in the location where I saw the rubber hand touched”), which has been shown to represent a different mechanism compared to the ownership illusion (Longo et al., 2008; Peviani et al., 2018). For this reason, we specifically considered q2 and q3 in our selection criterion. Nevertheless, all the participants selected basing on this criterion reported high (>0) scores at question 1 in both the synchronous conditions. Also, results are robust to the selection criterion, as comparable results were obtained on the entire sample. In order to study the effect of the illusion of ownership toward a fake hand on its mental representation, we ran a $2 \times 2 \times 2$ rmANOVA on the illusion group to study the effects of Target (hand, fake hand), RHI stimulation (synchronous, asynchronous), and Dimension (length, width) on the difference between the maps assessed prior and posterior to the RHI induction, computed as $\Delta(\text{EE post} - \text{EE pre})$ for each target, dimension and condition. Positive values indicate an increase of the EE value (meaning decreased underestimation) from pre to post, whereas negative values indicate a decrease of the EE value (meaning increased underestimation) from pre to post.

Experiment 4: Results and Discussion

We found a significant interaction between RHI stimulation and Dimension ($F(1,14)=5.492$, $p=.034$, $\text{BF} = .349$). From the pre to the post RHI, the EE for the vertical dimension are higher in the synchronous RHI trials (reduced underestimation) and smaller in the asynchronous RHI trials (increased underestimation) regardless of the Target. No other effects were found (Target: $F(1,14)=.011$, $p=.917$, $\text{BF}_{10} = .083$; RHI stimulation: $F(1,14)=.577$, $p=.460$, $\text{BF}_{10}= .206$; Dimension: $F(1,14)=.017$, $p=.897$, $\text{BF}_{10}= .142$; Target*RHI stimulation: $F(1,14)=.059$, $p=.812$, $\text{BF}_{10}= .040$; Target*Dimension: $F(1,14)=.919$, $p=.354$, $\text{BF}_{10}= .038$; three-way interaction: $F(1,14)=.243$, $p=.630$, $\text{BF}_{10}= .011$). Results are depicted in **Figure 2.9a**.

Additionally, we evaluated the stability of the metric representations across the four repetitions of the LLJ tasks by investigating the PRE conditions before any induction of the rubber hand illusion. We found that distortions of both the subject’s hand and the fake hand were stable across measurements (**Figure 2.9b**). No significant effects emerged from the rmANOVA on the fake hand EE (Dimension: $F(1,24)=1.465$, $p=.238$, $\text{BF}_{10}= 4.512$; Order: $F(3,24)=.798$, $p=.450$ Greenhouse-Geisser (GG) corrected, $\text{BF}_{10}= .049$; interaction: $F(3,24)=.475$, $p=.675$, GG corrected, $\text{BF}_{10}= .026$). Regarding the hand

representation, the rmANOVA revealed a significant main effect of Dimension ($F(1,24)=7.313$, $p=.001$, $BF_{10}= 89551.862$) but no significant effect of Order ($F(3,24)=.574$, $p=.579$, GG corrected, $BF_{10}= .094$) nor significant interaction ($F(3,24)=.398$, $p=.754$, GG corrected, $BF_{10}= .043$). The main effect of Dimension is in line with previous results, showing a higher underestimation of the hand vertical dimension compared to its horizontal dimension.

Altogether, the results of this study replicate our previous finding demonstrating differences in the metric representations of one's own hand and a fake hand. The differences across targets appear unrelated to the sense of ownership as the induction of the ownership illusion towards the fake hand did not affect the results. Thus, our data suggest that the pattern of distortion characterising the fake hand likely derives from intrinsic properties of the fake hand itself (e.g. its rigidity, its size). Further, our results speak to the stability of the metric representations. The representation of one's own hand did not significantly change over the course of four testing sessions, despite subjects not being naïve anymore to the task. This result further supports the unconscious nature, and the stability, of the misjudgment in our body dimensions. Moreover, a brief exposure to an unfamiliar target (fake hand) was enough to build a stable metric representation of it, which did not change over consecutive exposures.

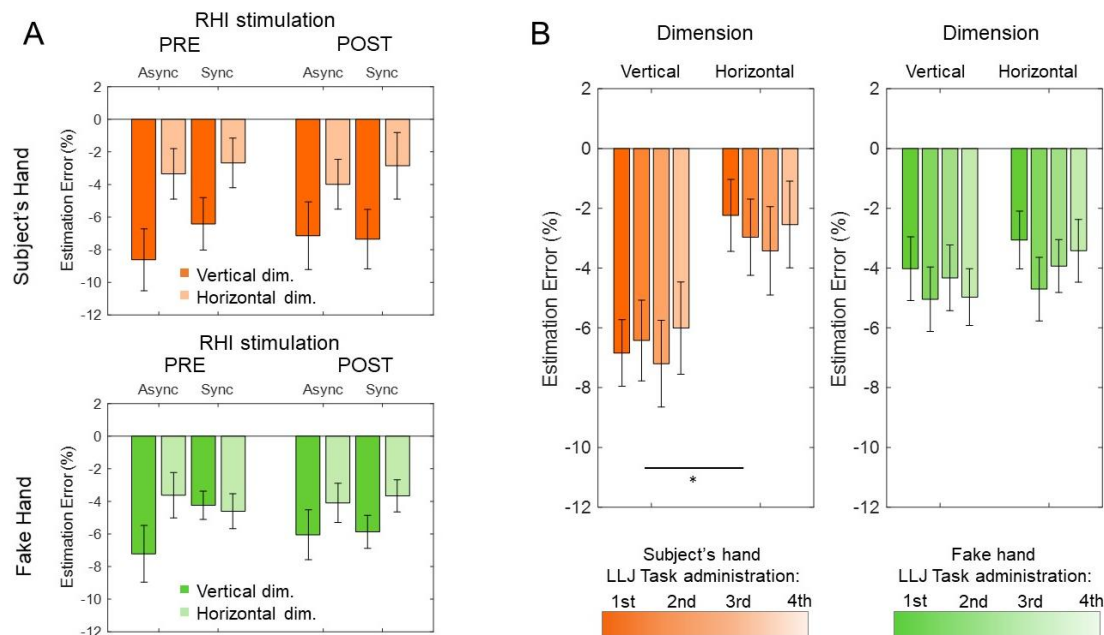


Figure 2.9 (a) Rubber Hand Illusion (RHI) did not affect the perceived dimensions of the participant's hand (upper panel) and fake hand (lower panel). Average estimation errors and standard errors of the mean per target dimension and RHI session are represented, considering the subsample selected based on the illusion rating ($N = 15$). (b) Stability of metric representations for the subject's hand (left panel) and fake hand (right panel). Average estimation errors and standard errors of the mean per target dimension and repetition are depicted. The pattern of distortions for both targets was maintained over repetitive exposures. A significant effect of dimension was only found for the hand, denoted by an asterisk. The difference between the two targets (participant's hand and fake hand), was not significantly reduced by the illusion of ownership toward the fake hand.

Experiment 5 and 6: the role of object affordances

Experiment 5 and 6 explored the role that manipulability plays in the distortions of the mental representations of objects. In Experiment 5 we compared the metric representations of a frequently manipulated object i.e., a mobile phone, with an object that does not elicit manipulation i.e., a small cactus with spines. The same unfamiliar mobile phone as in experiment 2 was used along with a cactus sized 10.4 x 4.8cm. The experiment consisted of 4 blocks, each containing 80 trials, 2 per unitary line distortion ranging from -30% (shorter) to 10% (longer) of the target dimension. Twenty-four healthy right-handed participants (17 females) aged 18 to 45 (mean age 24.65 ± 7.13) took part in the experiment. In Experiment 6, we investigated two highly familiar objects of roughly similar shapes but eliciting different degrees of manipulability i.e., a computer mouse and a soap smeared with hairs and dust eliciting disgust and therefore avoidance. The dimensions of the computer mouse were 11.00 x 6.00cm and of the soap 8.00 x 5.00cm. The experiment consisted of 4 blocks, each containing 80 trials, 2 per unitary distortion ranging from -30% (shorter) to 10% (longer) of the target dimension. Twenty-six (14 females) healthy right-handed participants aged 20 to 44 (mean age 23.86 ± 4.84) took part in the study.

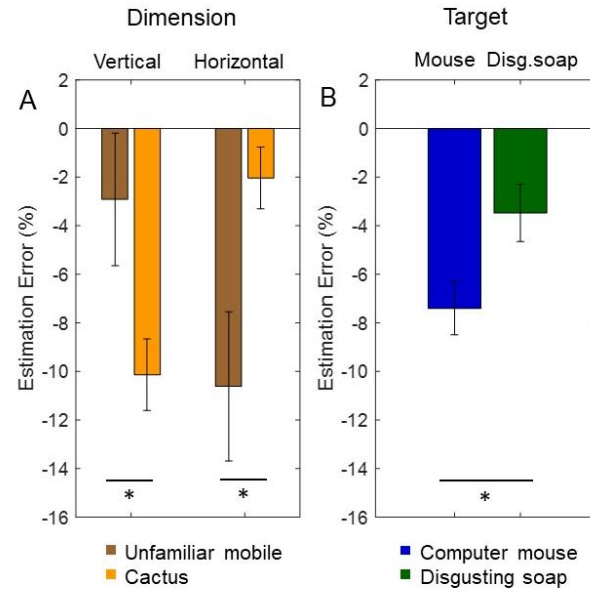
Experiment 5 and 6: Results and Discussion

In Experiment 5, data from 9 participants were removed (7 due to poor fitting and 2 due to extreme EE values in one or more conditions). All distributions were normally distributed as confirmed by the Shapiro-Wilk Normality Test (all p s > .05).

One-sample t -tests against zero, after Bonferroni correction, detected a significant underestimation of the cactus' horizontal dimension, as well as of the mobile phone's vertical dimension (see **Table 2.1**). The 2x2 rmANOVA studying the effects of Target (mobile, cactus) and Dimension (vertical, horizontal) on the EEs, revealed a significant interaction between Target and Dimension ($F(1,14)=13.710$, $p=.002$, $BF_{10}=22.486$) and non-significant main effects (Target: $F(1,14)=.122$, $p=.732$, $BF_{10}=4.916$; Dimension: $F(1,14)=.009$, $p=.926$, $BF_{10}=4.921$). The post-hoc comparisons, after Bonferroni correction, showed a higher underestimation of the vertical dimension compared to the horizontal dimension for the mobile phone only ($p<.001$). Moreover, the vertical dimension of the mobile phone was more underestimated ($p=.013$), whereas for the cactus the horizontal dimension was more underestimated ($p=.018$).



































In Experiment 6, one participant was excluded from the analysis due to extreme EE values. Bonferroni corrected one-sample t -tests revealed that all the dimensions were significantly underestimated except for the horizontal dimension of the disgusting soap (mouse vertical dimension EE: $-8.097\% \pm 8.311$, $t(24)=-4.871$, $p<.001$; mouse horizontal dimension EE: $-6.721\% \pm 4.916$, $t(24)=-6.836$,

$p < .001$; disgusting soap vertical dimension EE: $-5.073\% \pm 7.603$, $t(24) = -3.336$, $p = .003$; disgusting soap horizontal dimension EE: $-1.878\% \pm 6.811$, $t(24) = -1.379$, $p = .181$). See **Table 2.1**. The 2x2 rmANOVA investigating the effects of Target (mouse, disgusting soap) and Dimension (vertical, horizontal), revealed



a higher underestimation of the mouse's dimensions (significant main effect of Target: $F(1,24) = 11.930$, $p = .002$, $BF = 24.176$) independently of the dimension considered (non-significant interaction: $F(1,24) = 1.108$, $p = .303$, $BF = 1.115$). The main effect of Dimension was not significant as well ($F(1,24) = 2.650$, $p = .117$, $BF = .735$). See **Figure 2.10**. Altogether, experiments 5 and 6 revealed systematic metric distortions across four different objects, whereby the metric representations of manipulable objects (mobile phone and computer mouse) differ to those prompting avoidance either due to harm or disgust (a cactus and a dirty soap). These results suggest that the size representations of objects are affected by factors that modulate graspability and interaction with an object such as inducing potential harm or disgust.

Figure 2.10 Mean EEs and their standard errors are plotted for Experiments 5 (a) and 6 (b). In Experiment 5, a significant difference between the targets has been detected for both dimensions, as signaled by the asterisks. Experiment 6 showed that the disgusting soap is less underestimated, regardless of the dimension considered, than the computer mouse. Bars represent estimated marginal means relative to the main effect of Target.

Exp	Target and condition				Dim.	Mean	SD	t	df	Sig	Estimation Error
1	Subject's hand				V	-0.766	0.860	-3.671	16	0.002	
					H	-0.380	0.684	-2.292	16	0.036	
	Subject's mobile				V	-0.772	0.843	-3.774	16	0.002	
					H	-0.189	0.803	-0.972	16	0.346	
2	Subject's hand				V	-1.080	0.672	-8.501	27	<.001	
					H	-0.810	0.707	-6.069	27	<.001	
	Subject's mobile				V	-1.407	0.535	-13.917	27	<.001	
					H	-0.519	0.684	-4.014	27	<.001	
	Fake hand				V	-0.628	0.803	-4.135	27	<.001	
					H	-0.659	0.748	-4.662	27	<.001	
	Unfamiliar mobile				V	-1.318	0.555	-12.577	27	<.001	
					H	-0.521	0.521	-5.288	27	<.001	
3	Subject's hand				V	-0.768	0.813	-4.627	23	<.001	
					H	-0.551	0.867	-3.113	23	0.005	
	Mug				V	-0.839	0.761	-5.397	23	<.001	
					H	-0.738	0.673	-5.372	23	<.001	
	Fake hand				V	-0.189	0.876	-1.055	23	0.302	
					H	-0.484	0.760	-3.12	23	0.005	
4	Subject's hand	Pre-RHI	Synch.		V	-0.667	0.597	-5.474	23	<.001	
					H	-0.265	0.643	-2.017	23	0.056	
			Async		V	-0.558	0.533	-5.127	23	<.001	
					H	-0.203	0.593	-1.673	23	0.108	
		Post-RHI	Synch.		V	-0.536	0.714	-3.679	23	0.001	
					H	-0.338	0.708	-2.341	23	0.028	
			Async		V	-0.527	0.564	-4.578	23	<.001	
					H	-0.229	0.769	-1.457	23	0.159	
	Fake hand	Pre-RHI	Synch.		V	-0.465	0.605	-3.767	23	0.001	
					H	-0.276	0.519	-2.609	23	0.016	
			Async		V	-0.379	0.417	-4.459	23	<.001	
					H	-0.513	0.502	-5.008	23	<.001	
		Post-RHI	Synch.		V	-0.355	0.563	-3.089	23	0.005	
					H	-0.341	0.514	-3.249	23	0.004	
		Async			V	-0.516	0.419	-6.041	23	<.001	
					H	-0.384	0.474	-3.969	23	0.001	





5	Cactus	V	-0.292	1.059	-1.068	14	0.304	
		H	-1.062	1.188	-3.462	14	0.004	
	Unfamiliar mobile	V	-1.014	0.568	-6.911	14	<.001	
		H	-0.204	0.490	-1.615	14	0.129	
6	Computer mouse	V	-0.810	0.831	-4.871	24	<.001	
		H	-0.672	0.492	-6.836	24	<.001	
	Disgusting soap	V	-0.507	0.760	-3.336	24	0.003	
		H	-0.188	0.681	-1.379	24	0.181	

Table 2.1 For each experiment, target and dimension (V = vertical, H = horizontal) Mean and Standard deviation of the EE are reported together with a graphical representation of the distributions. Test statistics refer to one-sample *t*-tests against zero. Bonferroni correction has been applied within each Target.

Analysis on the pooled data

As a last step, we aimed at directly comparing the perceived dimensions of the different objects tested across the six studies. To this end, we pooled all the EE data and analysed them by means of a Linear Mixed-Effects Model in SPSS, with target and dimension as fixed effects, including random intercepts and slopes to account for inter-subject variability. Note that, concerning the fourth experiment, we included in the analysis only the data of the first sessions. We found significant effects of Target ($F(7,710) = 4.294$, $p < .001$) and Dimension ($F(1,710) = 15.895$, $p < .001$), as well as a significant interaction ($F(7,710) = 7.845$, $p < .001$). Bonferroni corrected post-hoc comparisons confirmed significant differences in the estimation of the vertical dimension between the cactus and familiar (subject's $p = .005$) and unfamiliar mobile phone ($p = .002$), as well as between the disgusting soap and familiar (subject's $p = .004$) and unfamiliar mobile phone (unfamiliar: $p = .001$). Further, the fake hand differed both from the mobile phones (unfamiliar: $p < .001$; subject's $p < .001$) and the hand ($p = .007$). No differences were observed between the hand and the mobile phones and the mouse (all $p = 1.000$). Considering the estimation of the horizontal dimension, the cactus differed from mobile phones (unfamiliar: $p = .006$; subject's $p = .006$), the hand ($p = .021$) and the disgusting soap ($p = .001$). See **Figure 2.11a**.

Additionally, we used a multidimensional scaling approach to evaluate the pattern of similarities across targets. Given a matrix of interpoint distances, multidimensional scaling allows to summarize the distances (or dissimilarities) among different instances and to represent them in an *N*-dimensional space. Concretely, we applied multidimensional scaling in MATLAB (The MathWorks, version R2017b) on the Euclidean distances computed among the EEs referring to the vertical and horizontal dimensions of the 8 targets, to obtain a two-dimensional plane (**Figure 2.11b**). While we did not actually reduce the number of dimensions considered, we used such approach to clearly depict the similarity and relationships among the target's representations. In the 2D plane, the physical distance between two targets depicts their

distance in the representational space. Interestingly, the hand representation occupies a central position in the plane, close to the mug, the computer mouse and the mobile phones, which are spatially clustered together. This configuration reflects the similarity between the representation of the hand with that of objects which elicit manipulation. On the contrary, the disgusting soap, the fake hand and the cactus turned out to be isolated from the “hand cluster”, as a result of their different and peculiar representation.

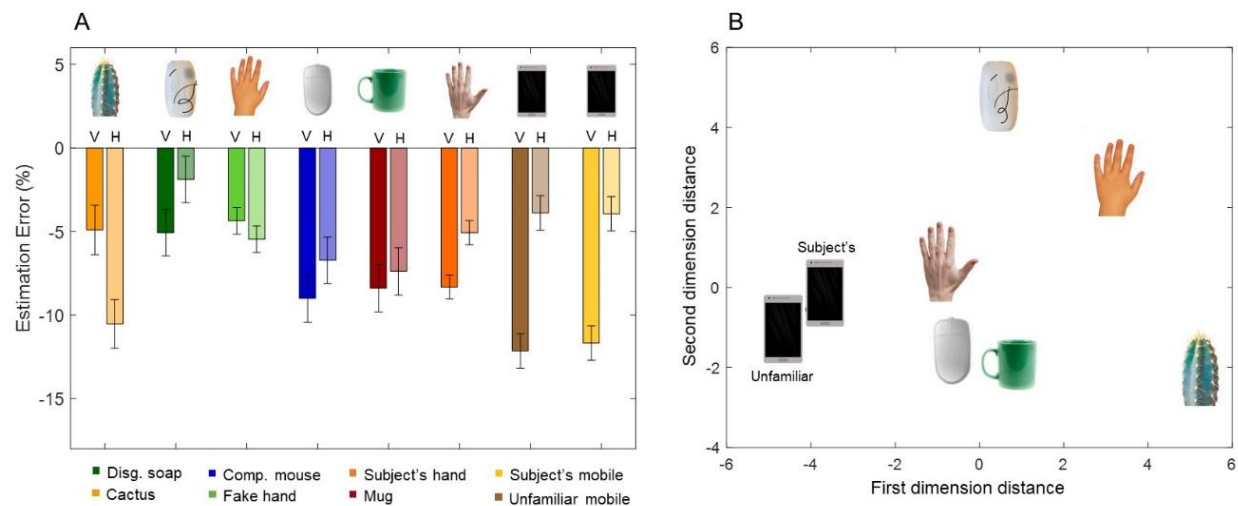


Figure 2.11 (a) Estimation Errors for the vertical (V) and horizontal (H) dimensions of the eight targets investigated. (b) Multidimensional scaling on the Estimation Errors. Representational distance is depicted as physical distance in a two-dimensional plane.

Interim Discussion

Our results replicate previous findings with regard to the biases in the metric representation of the hand. We further found that the pattern of distortions is not specific to the hand but extends to objects. We showed that participants similarly underestimated the dimensions of a mobile phone, a coffee mug and a computer mouse. By comparing the perceived dimensions of the participant's mobile phone with those of an unfamiliar mobile phone, we found that familiarity with an object does not play a significant role on its metric representations. This indicates that the representation of an unfamiliar object, which is built and stored over the course of a few seconds of observation, is as biased as the detailed, long-standing representation of one's own mobile phone. While familiarity with a specific object does not underlie the pattern of distortions, an interesting and open question is whether stable representations that are formed through frequent interactions and manipulation with an object are used as priors for the estimation of unfamiliar objects, or whether representations of unfamiliar objects are created *de novo* upon exposure. Relatedly, we also found strong evidence for the stability of the metric biases, both over time, as similar distortions were observed over multiple test sessions of the participant's hand and of a fake hand. Together, this suggests that, once the mental representation of a target is built up and stored, even when it is based on a few seconds of observation, further modifications are unlikely.

We observed similar misestimations for the hand, the mobile phone, the mouse and the mug; and the results of the multidimensional scaling indicate that their representations were grouped within a cluster. What is common to all those objects is that they are often the object of our actions; we frequently interact and manipulate them. It has been put forward that perception is action-specific, meaning that the environment is perceived and therefore represented depending on our ability to act upon it (Witt, 2011). Under this perspective, the perceived size of objects eliciting grasping and manipulation would differ from that of objects whose features inhibit action-oriented behavior. Our results are compatible with the action-specific perception account (Witt, 2011), as we found that objects that are potentially harmful (cactus) or disgusting (dirty soap), thereby inhibiting manipulation, were perceived differently in their dimensions compared to manipulable objects (a mobile phone and a computer mouse, respectively). Our results also fit well with previous data suggesting that in visual perception our dominant hand might function as a ruler to perceive the dimensions of graspable - but not of too-big-to-be-grasped - objects (Linkenauger, Witt & Proffitt, 2011). Thus, biases characterising the hand representation might be inherited by objects that afford manipulation and interaction.

Another aspect that might affect the size estimation of objects relates to emotions. Emotions might mediate interactions with objects via prompting interaction or avoiding them but also through their known effects on memory (e.g., Bradley, Greenwald, Petry & Lang, 1992; Sharot & Phelps, 2004;

Kesinger, 2004). Specifically, emotions, such as disgust, are known to lead to better encoding and more accurate recall, e.g., greater recall for disgusting pictures compared to neutral pictures (Chapman et al., 2013). Thus, inducing the feeling of disgust in one of our targets might have also led to a more accurate memory of its physical dimensions, and thereby to lower distortions. These two effects (i.e., affordance of manipulation and emotional content), which are not mutually exclusive, could also explain the results of Experiment 4, in which we compared the representations of the hand and the fake hand. The fake hand is an interesting object as it shares a similar appearance to the real hand, yet we found that the fake hand was less underestimated than the real hand. The fake hand is unlikely to elicit manipulation, since we do not use it. It can also induce a sense of disgust, as it was often informally reported during our studies. Teasing apart the role that manipulability and different emotions e.g., disgust, fear, joy might play in the metric representation of objects is an important avenue for future research.

Inducing a feeling of ownership over the fake hand through the Rubber Hand Illusion (Botvinovk and Cohen, 1998) did not affect its metric representation, indicating that factors other than the hand-like shape and the feeling of ownership modulate the pattern of distortions of a hand-like object. For instance, intrinsic properties of the fake hand, such as its texture, rigidity and size, as well as the emotions that it possibly elicits, may influence its size estimation.

To conclude, the present study showed that the metric biases which affect the representation of the hand extend to the representation of real objects that are more likely to afford manipulation and interaction. Previous research asked how accurate hand movements are possible given the systematic biases affecting hand perception (Peviani & Bottini, 2018) or given those affecting the perception of objects (Lee et al., 2008; Coats et al., 2008). Our results suggest that both the effector and the object of the action are not accurately perceived, providing a new perspective on the hand-object interaction problem and how this might be addressed in future work. For instance, it can be argued that, if we misperceive the dimensions of our hand, misperceiving the dimensions of objects we are likely to interact with would facilitate hand-object interaction. This might be functional in our daily interaction with the environment.

Considering that all the objects investigated were not accurately perceived in their dimensions, we argue that there are general perceptual distortions happening at the visual or representational level. Yet, our data also support the existence of a specific pattern of distortions, which was detected for the hand and extended to objects which were more likely to trigger manipulation, but not to objects that conceivably inhibited manipulation. Our results therefore highlight the importance of considering and addressing the interaction between body representation and perception of the surrounding environment, as well as the specific and unspecific biases related to each of them; in addition to the role that other factors, such as emotions, might play in the fidelity of the representation of each object.

Study 5: Exploring the direct electrophysiological correlates of hand and object size estimation: an sEEG study ⁵

Introduction

As anticipated, Study 5 was set out to investigate the neural correlates of the hand and object metric representations in humans. Despite the rich behavioural evidence attesting the similarity between the perceived dimensions of the hand and of manipulable objects, it cannot be excluded that different neurocognitive mechanisms underlie the size estimation of one's own hand compared to an object. We therefore chose to compare the brain activity triggered by the size estimation of one's own unseen hand and a manipulable object, i.e., the mobile phone.

We recruited six patients undergoing stereo-EEG (sEEG) recordings for a careful definition of the epileptogenic zone for surgical purposes and administered them with a computerised task assessing the hand metric representation along with the mental representation of control objects. Specifically, we administered patients with the LLJ task (**Figure 2.2**) and analysed the electrophysiological responses elicited by the task under the two conditions.

We focused our sEEG analysis on high- γ (70–150 Hz) changes, which represent a reliable electrophysiological index of average neuronal population firing, thus a specific correlate of local behavior (Miller et al., 2007; Ray & Maunsell, 2011; Suffczynski et al., 2014).

Since distortions of body representations have been previously attributed to the somatotopic cerebral representation (Linkenauer et al., 2015; Longo, 2015c; Longo & Haggard, 2010; Sadibolova et al., 2019), we ran additional analysis considering the activity in a lower frequency range, the β range (12.5 to 25 Hz) over the sensorimotor cortices. Indeed, changes in this frequency range over those areas have been considered a marker of cortical activation, as detected during actual or imagined movement (Crone, 1998; Pfurtscheller, Graimann, Huggins, Levine, & Schuh, 2003). We adopted two different analysis approaches (**Figure 2.13c**) in order to address our research question. First, we adopted a data-driven approach to test for differences across conditions. Second, we ran the analyses considering a specific Region of Interest (ROI), namely the sensorimotor cortex (pre- and postcentral gyri).

⁵ The following sections (introduction, method, analysis and discussion relative to Study 5) have been largely extracted and adapted from Peviani, Mariani, Tassi, Lo Russo, Melloni & Bottini (in preparation)

Method

Patients

All 6 participants (all females) were undergoing sEEG monitoring aimed at defining the epileptogenic zone for surgical purposes at Niguarda Epilepsy Unit in Milan, Italy. Demographic and clinical information are summarised in **Table 2.2**. All patients were right-handed and underwent a complete neuropsychological evaluation, which detected only domain-specific impairments compatible with their diagnosis, and confirmed a normal level of intellectual functioning assessed through the Raven Coloured Progressive Matrices (Basso, Capitani, & Laiacina, 1987). Importantly, significant MR anomalies were not reported for any patient.

Patients gave their informed consent to participate to the study. The study was approved by the local Ethics Committee and adhered to the ethical standards of the Declaration of Helsinki.

Patient #	Age	Epileptogenic zone	Side of implantation	Raven CPM
1	44	Temporal pole	Left	35/36
2	25	Operculo-Insular	Right	34/36
3	18	Latero-occipital	Right	29/36
4	43	Basal temporal	Left	34/36
5	18	Posterior insula	Right	33/36
6	41	Anterior temporal	Bilateral	29/36

Table 2.2 Patients' demographic and clinical details.

Task and procedure

Originally, the task comprised four experimental conditions, requiring the participants to estimate the horizontal and vertical dimensions of four different targets, namely their own hand and mobile phone, a fake hand and an unfamiliar mobile phone. No visual exposure to the former two was granted before the experiment. For the purpose of the current discussion, we will be focusing the analysis on these two former conditions: comparing the line dimensions to their own hand and mobile phone. In so doing, we aimed at studying mental representations that are not influenced by recent visual information.

As in Study 1, participants were asked to determine whether vertically and horizontally oriented lines were shorter or longer compared to the specific target serving as a reference. The procedure was the same as described earlier, except that each block contained 50 lines, one for each unitary distortion ranging from -30% to -1% (shorter) and from 1% to 20% (longer) of the actual target's dimension. Patients performed the task in their hospital room, seated in front of a desk at about 55cm from the

computer screen. Their hands were concealed by a white opaque panel (40 x 40 cm) while they performed the task.

Behavioural results

Behavioral data were processed similarly to what was described earlier in this chapter. Responses in the LLJ task were grouped in five ranges: i) -30 to -21%, ii) -20 to -11%, iii) -10 to -1%, iv) 1 to 10%, and v) 11 to 20% and labels -2, -1, 0, 1, 2 were assigned to each range respectively. For each range, we computed the sum of “longer” responses, and used those values to fit a psychometric function to estimate the Point of Subjective Equality (PSE) separately per participant, body part and dimension. Psychometric functions were fitted using the Palamedes Toolbox (Prins & Kingdom, 2018) in MATLAB (The MathWorks, version R2017b). We used the cumulative normal function to obtain PSE per each patient. Subsequently, for each subject, body part and dimension, the PSE (ranging from -2 to 2) was transformed back into its original scale (-30 to +20%), which represents the Estimation Error (EE), meant as the percentage of underestimation (negative sign) or overestimation (positive sign) of a certain body part and dimension. **Figure 2.12a** represents the EEs for each target and dimension. Since the trials regarding the length and width judgements were pooled together for the sEEG analysis, we decided to compute the Estimation Error relative to the Shape Index (SI), which combines the perceived length and width of the target returning an estimation of its perceived proportions. The SI is computed as (perceived width / perceived length)*100, and its EE is obtained by computing the ratio between the perceived SI and the actual one. **Figure 2.12b** represents the Shape Index EEs for each target. We aimed at ascertaining that the behavioural responses of the patients were coherent with the behavioural responses of healthy controls. To this purpose, we pooled the behavioural data collected in the first two experiments of Study 1, in which healthy participants estimated the dimensions of their own hand and mobile phone in a LLJ task. The control sample (N=48, 41 females) had mean age 25.22 ± 3.31 . As expected, the hand and mobile phone were similarly represented in terms of shape index (hand SI EE: 10.45 ± 1.11 vs mobile SI EE: 10.81 ± 1.03 ; $t(47) = -1.452$, $p = .153$). Similarly, at a group level, patients did not show any significant difference between the hand and mobile representations in terms of shape index (hand SI EE: 12.01 ± 1.02 vs mobile SI EE: 10.98 ± 0.74 ; $t(5) = 1.776$, $p = .135$).

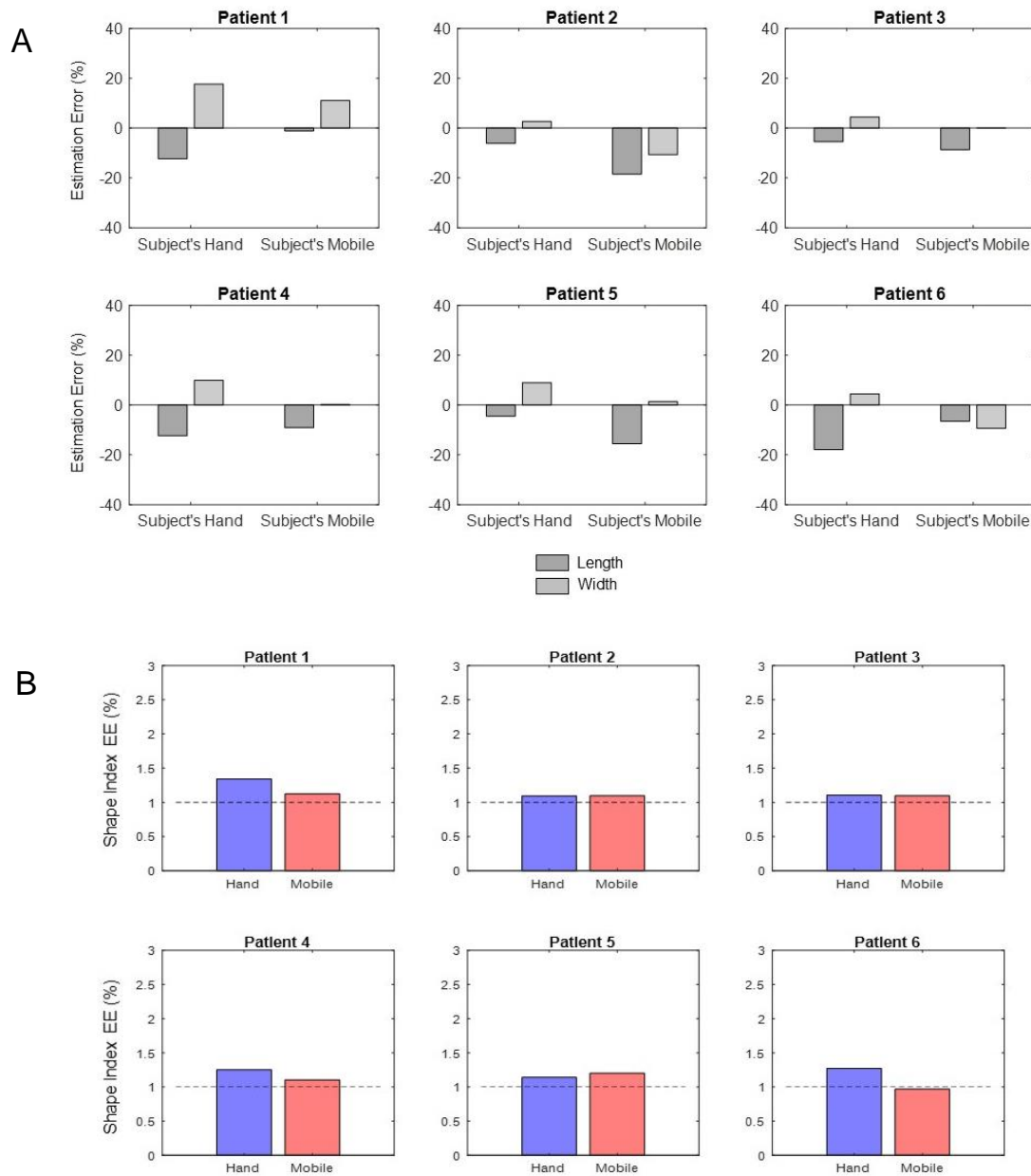


Figure 2.12 (a) The Estimation Errors (EE) for each target (Hand and Mobile) and dimension (length and width) are plotted for each patient. (b) The Shape Index EEs for each target are plotted for each patient.

sEEG coverage and acquisition

Patients underwent stereotactic procedure of intracerebral electrode implantation (Cossu et al., 2005; Munari et al., 1994; Talairach & Bancaud, 1973) aimed at the epileptogenic zone prior to the surgical treatment. For each patient, platinum iridium, semiflexible multilead intracerebral electrodes (diameter, 0.8 mm; 5–18 contacts 1.5 mm in length and 2 mm apart [Dixi Medical, Besançon, France]) were implanted. sEEG signals were sampled at 1 kHz with a Neurofax EEG-1100 system (Nihon Kohden, Tokyo, Japan), with HPF at 0.016 Hz and LPF at 300 Hz. Data were digitised with 16-bit resolution. Weighted average of two contacts recorded from the white matter was used as the reference signal. The overall coverage across patients is represented in **Figure 2.13b**.

Cortical reconstruction

For each patient, the reconstruction of the cortical surface was generated through FreeSurfer (Dale, Fischl, & Sereno, 1999). Channel positions were estimated using S EEG assistant (Narizzano et al., 2017), an extension of 3DSlicer (Kikinis, Pieper, & Vosburgh, 2014). In detail, the post-implant MRI and the Markups Fiducial list (planned entry and target points with respect to the cortical surface for each electrode) were used to estimate channel positions relative to the patient's geometrical space, and to determine their most probable cerebral location within a volumetric brain atlas (Destrieux).

After alignment to ACPC coordinates, the pre-implantation and post-implantation MRIs (1.5-tesla ACS-NT unit; Philips Medical Systems, Brest, The Netherlands) customised according to electro-clinical information (Cardinale et al., 2013) were coregistered and normalised in MNI space using SPM (Friston, Jezzard, & Turner, 1994). The transformation matrices used for MRI alignment to ACPC and normalisation were applied to align channel positions in ACPC and normalise them in MNI space. The anatomical pipeline is summarised in **Figure 2.13a**.

sEEG analysis

The analysis pipeline is summarised in **Figure 2.13c**. Firstly, we manually excluded channels and trials showing non-physiological artifacts or epileptic activity. The notch filter at was applied at 50, 100 and 150 Hz to remove line noise and its second and third harmonics. Furthermore, we applied a low-pass filter at 160 Hz and a high-pass filter at 3 Hz. To reject common-mode noise, all channels were re-referenced to a common average reference. Channels located in white matter were excluded from the subsequent preprocessing steps and analyses. In **Figure 2.13b**, selected channels are colored in red. Then, the average β and high- γ power for each channel over time was extracted by band-passing the signal for the frequency

bands of interest: 12.5 to 25 Hz and 70 to 150 Hz for β and high- γ , respectively, and then applying a Hilbert transform.

For each channel, the signal was segmented into epochs of 2500 ms duration, from 1000 ms before stimulus onset (line presented on the screen) to 1500 ms afterwards. For each trial and channel, the power was normalised in the dB scale relative to the mean baseline power (500 to 100 ms before stimulus onset). Each epoch was labelled as belonging to one out of four conditions of interest: participant's hand length, participant's hand width, participant's mobile length, participant's mobile width.

Trials included in the hand length and hand width blocks were pooled together, as well as trials included in the mobile length and mobile width blocks. Indeed, we decided to pool together the length and width trials because we wanted to increase the statistical power by doubling the trials included in the hand and mobile conditions.

Firstly, we used a two-step data-driven approach to select channels of interest for each patient. We aimed at selecting channels in which a significant change in power after the stimulus onset was detected, independently of the condition, and ran the comparison between conditions only on those responsive channels. Note that, since we used two orthogonal tests on the data (baseline vs task to select responsive channels, and condition 1 vs condition 2 to compare after-stimulus responses), we minimised the likelihood of falling into a circular analysis bias (Kriegeskorte, Simmons, Bellgowan, & Baker, 2010). In detail, for each patient and frequency range, we computed the average Baseline (-500 to -100 ms) and Task (0 to 600 ms) power over time and trials (**Figures 2.14a and 2.14c**). Then, for each channel we pooled the Hand and Mobile trials together and we performed permutation statistics to compare their Task power with their Baseline power. More specifically, we compared the observed difference between Task and Baseline with the distribution of differences expected under the null hypothesis (H_0), which states that there is no power change between Baseline and Task. The H_0 distribution was obtained by applying the analysis on 1000 permutations of the data: at each permutation, randomly assigning the “Task” and “Baseline” labels to the actual values and computing the difference between their averages (**Figures 2.14b and 2.14d**). The deviance of the observed Task-Baseline difference from the H_0 distribution was expressed in z-scores along with their relative p-values. After having applied FDR correction over channels, we selected channels with a p-value $<.05$, representing a significant change in power from the Baseline to the Task. As a second step, we ran permutation statistics to compare the average high- γ and β power between the two conditions in the selected channels. In detail, we computed the average Task (0 to 600 ms) power for each condition and calculated their difference. Similarly to what was described above, we compared the observed Hand-Mobile difference to the distribution of differences expected under the null hypothesis, which in this case states that there is no difference between the Hand and Mobile conditions. The H_0 distribution was obtained by applying the analysis on 1000 permutations of the data: at

each permutation, randomly assigning the “Hand” and “Mobile” labels to the actual values and computing the difference between their averages. The deviance of the observed Hand-Mobile difference from the H_0 distribution was expressed in z-scores along with their relative p-values, on which FDR correction over channels was applied.

Next, we adopted a different approach aimed at testing the specific role of sensorimotor cortices in shaping the hand mental representation. To this aim, we performed an a-priori selection of the channels located in the ROI (pre- and postcentral gyri) and, for each patient and frequency band, we ran the permutation statistics with FDR correction to test for a difference between conditions within those channels, following the procedure described above. Concretely, we selected 6 channels located in the precentral gyrus for patient 1, 11 channels in the precentral and 12 in the postcentral gyrus for patient 2, 1 channel in the precentral and 3 in the postcentral gyrus for patient 4 and 6 channels in the precentral and 4 in the postcentral gyrus for patient 5, for a total of 24 channels located in the precentral gyrus and 19 channels located in the postcentral gyrus.

Data analysis was performed using Fieldtrip (Oostenveld, Fries, Maris, & Schoffelen, 2011) and custom MATLAB (The MathWorks, version R2017b) code.

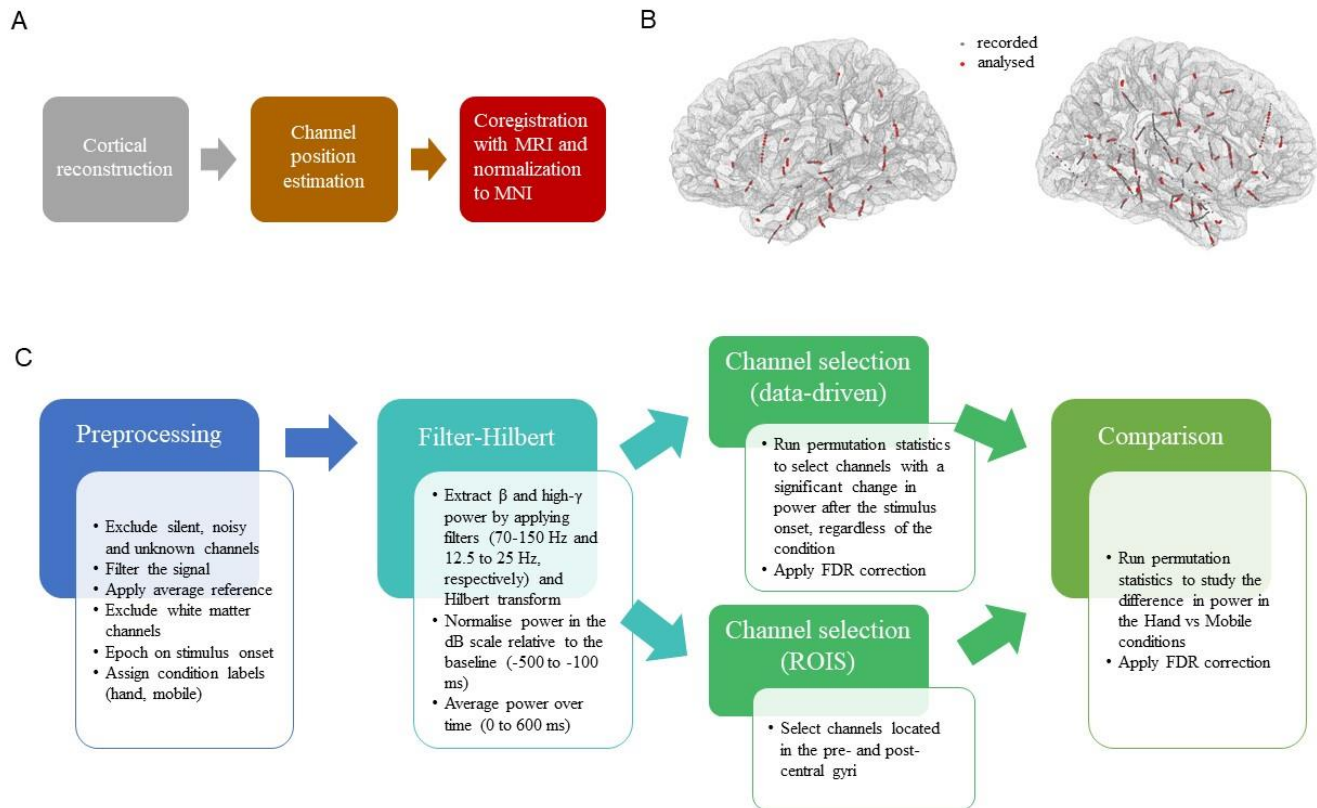


Figure 2.13 (a) Summary of anatomical pipeline. (b) The overall coverage is represented in MNI space, with gray dots representing recorded channels and red dots representing channels selected at the preprocessing step. (c) The sEEG analysis pipeline is summarised.

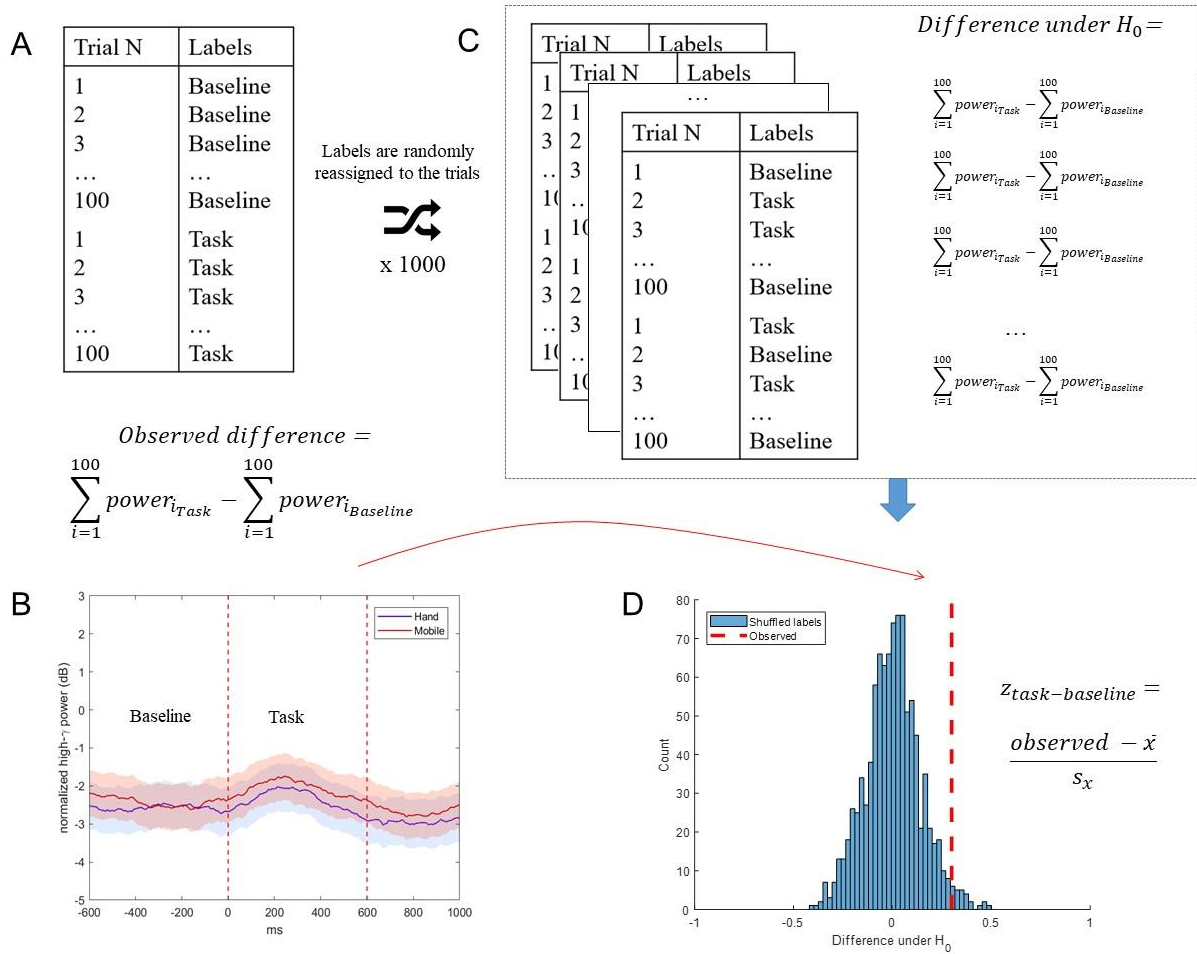


Figure 2.14 (a) For each channel, the observed difference between Task and Baseline power (averaged over trials and over time (b) is computed, regardless of the condition, and compared to the H_0 distribution of the task-baseline differences obtained by permuting ($\times 1000$) the random assignment of the task-baseline labels (b). The distance between the observed difference and the mean difference under H_0 is expressed in z-value and transformed in p-value (d). A similar procedure was used to compare the average high- γ power across conditions.

Results

The analysis on the β and high- γ after-stimulus response showed that the neural activity triggered by the LLJ task is similar when patients were required to estimate the dimensions of their own hand and of a familiar object, their own mobile phone. In other words, we did not find evidence of a different β nor high- γ response when patients retrieved the mental representation of their own hand or their own mobile phone. As for high- γ power, we only observed higher mean high- γ power was recorded in the Mobile

phone condition, compared to the Hand condition, in the Fusiform gyrus (channel E'7: $z=-3.183$, $p=.025$, FDR corrected), in patient 4 (**Figure 2.15**); no other test survived corrections for multiple comparisons. Statistical tests' results, along with corrected and uncorrected p-values, are reported in the **Supplementary materials**.

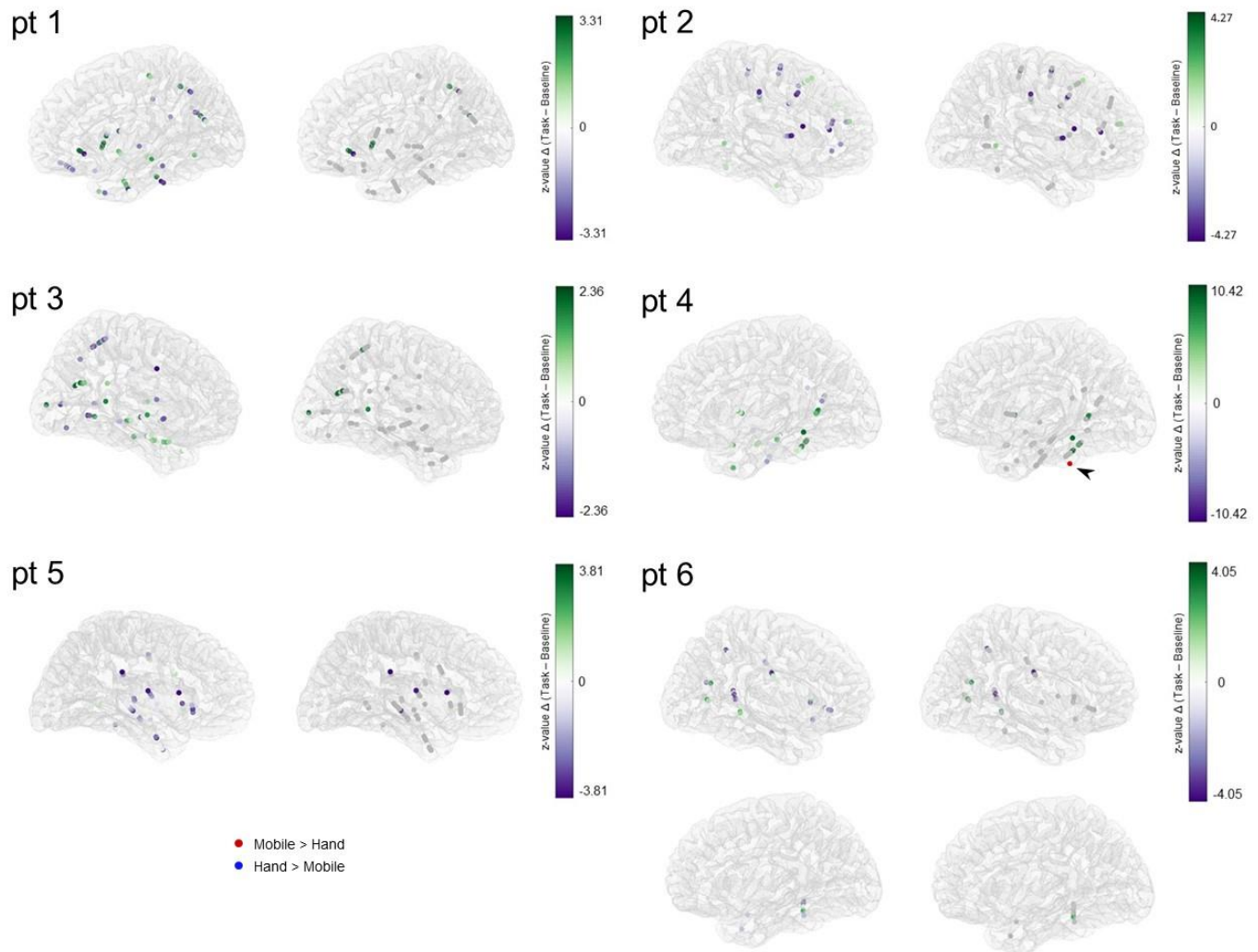


Figure 2.15 Results of the contrast Task vs Baseline and Hand vs Mobile on the high- γ power. For each patient, the figure on the left depicts all the analysed channels, where green dots represent an increase in the high- γ power after the stimulus onset, whereas purple dots represent a decrease in high- γ power after the stimulus onset. The figure on the right represent channels in which the change in high- γ power was statistically significant ($p < .05$, FDR corrected). Grey dots indicate non-responsive channels, i.e., channels in which the neural response did not significantly change from the Baseline to the Task. A significant difference across conditions (Hand vs Mobile) was detected in one channel located in the Fusiform gyrus (patient 4). The channels are plotted in MNI space.

Interestingly, our analysis detected a significant increase in high- γ power from before to after the stimulus onset in occipito-temporal, temporal (**Figure 2.16a**), occipital, parietal (**Figure 2.16b**) and frontal (**Figure 2.16c**) areas, similarly across conditions, and quite consistently across patients (**Figure 2.15**). Importantly, a positive change in high- γ power is usually considered a specific correlate of local behavior (Miller et al., 2007; Ray & Maunsell, 2011; Suffczynski et al., 2014), and therefore, in this case, it might reflect the activation of a broad network in the task, which is triggered regardless of the condition.

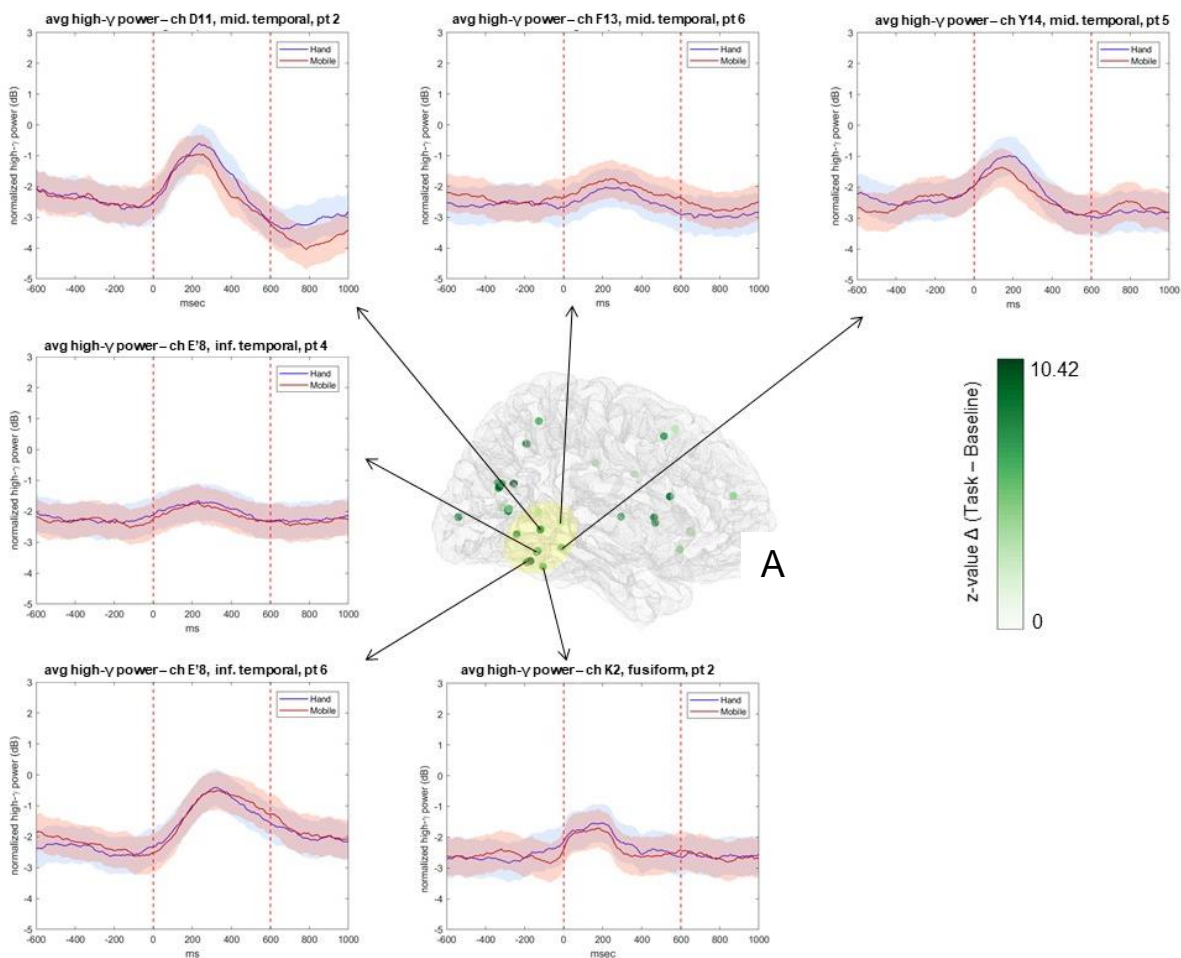


Figure 2.16a Channels from all the patients in which a significant ($p < .05$, FDR corrected) increase of high- γ power after the stimulus onset was detected are plotted in MNI space. Channels which were originally located in the left hemisphere have been flipped and plotted in the right hemisphere. Representative plots depicting the average power over time are displayed for some of the channels located in occipito-temporal and temporal regions.

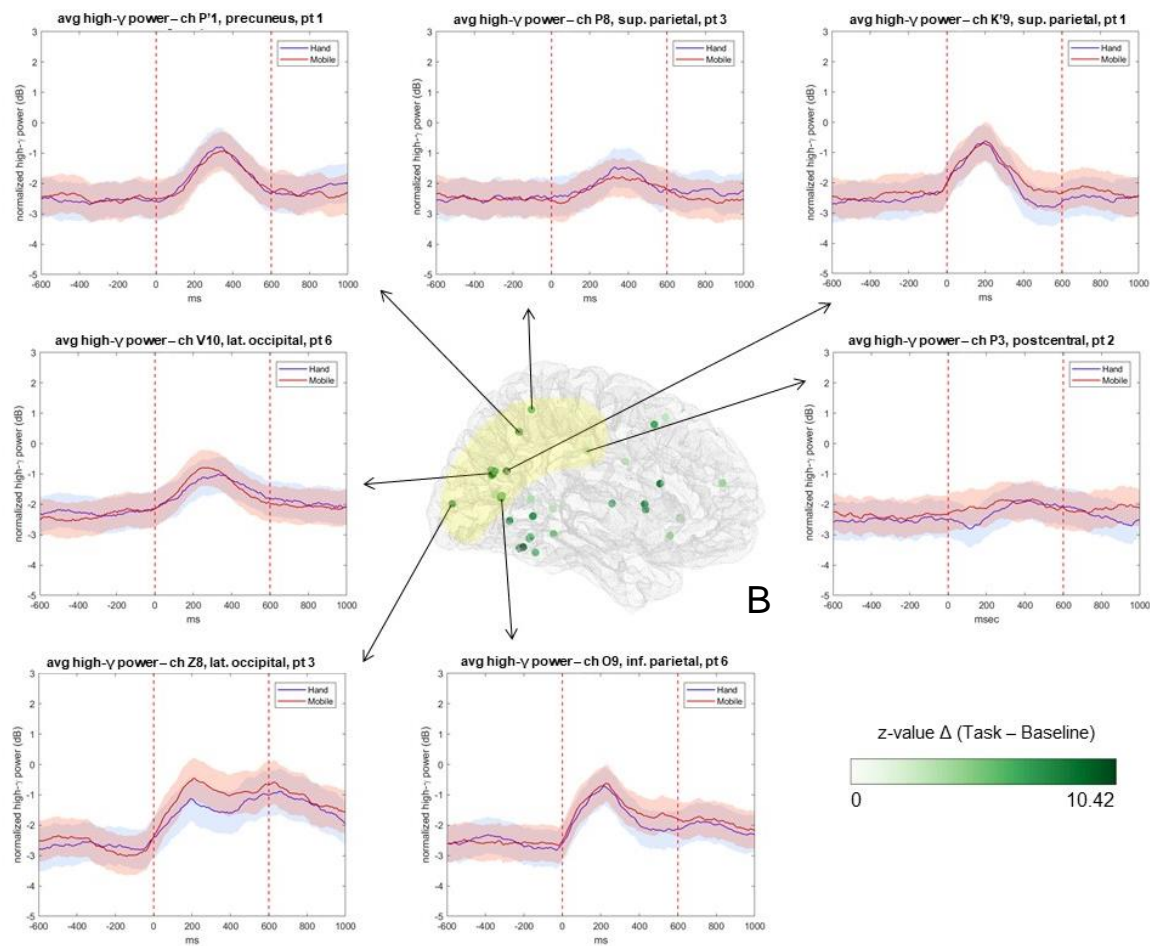


Figure 2.16b Channels from all the patients in which a significant ($p < .05$, FDR corrected) increase of high- γ power after the stimulus onset was detected are plotted in MNI space. Channels which were originally located in the left hemisphere have been flipped and plotted in the right hemisphere. Representative plots depicting the average power over time are displayed for some of the channels located in occipito-parietal and parietal regions.

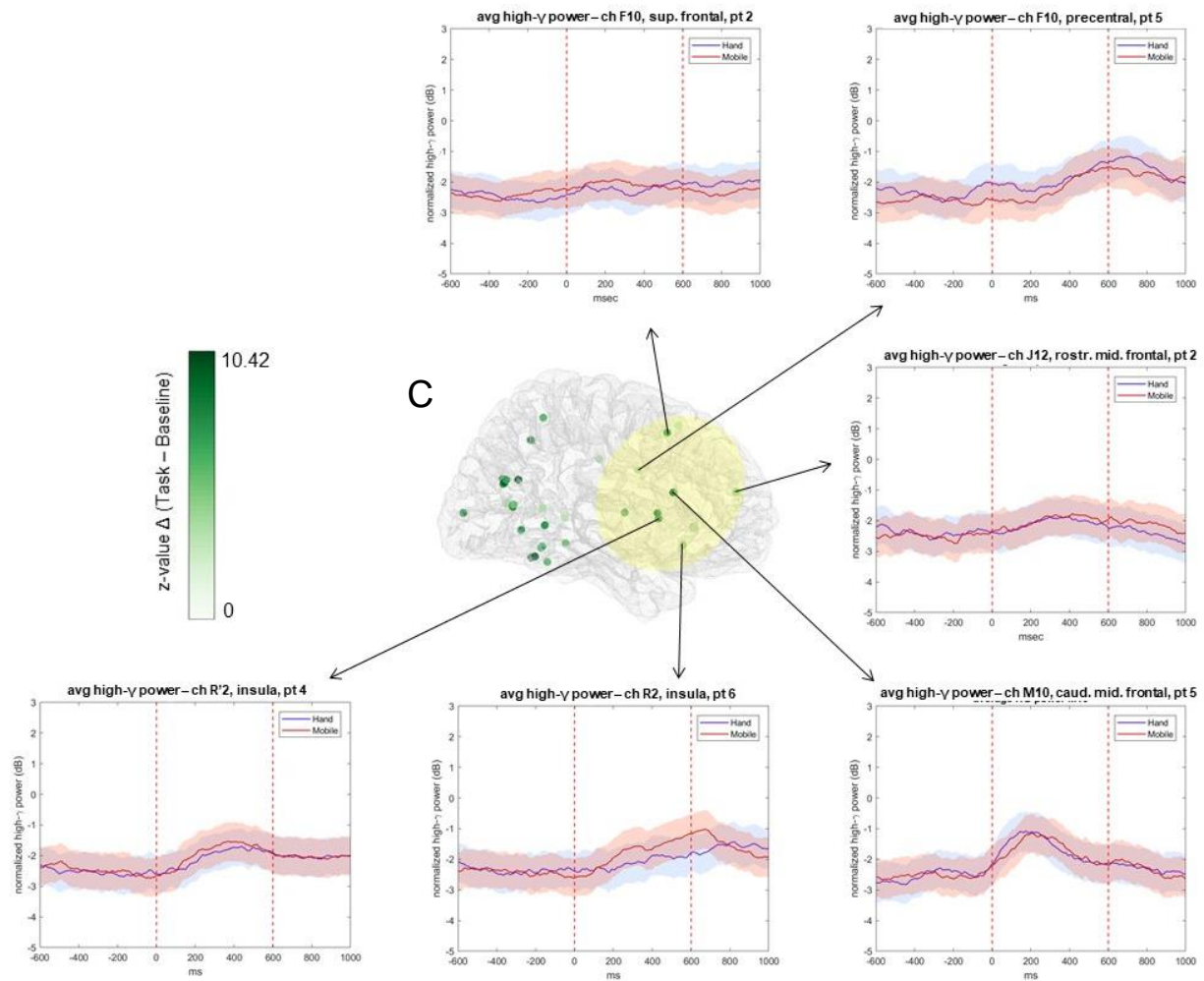


Figure 2.16c Channels from all the patients in which a significant ($p < .05$, FDR corrected) increase of high- γ power after the stimulus onset was detected are plotted in MNI space. Channels which were originally located in the left hemisphere have been flipped and plotted in the right hemisphere. Representative plots depicting the average power over time are displayed for some of the channels located in frontal regions.

Finally, the analysis which focused on the ROI detected a significantly higher β power during the Hand estimation compared to the Mobile in three channels located in the precentral gyrus, in patient 1 (channel S'3: $z = 2.426$, $p = .046$; channel S'4: $z = 2.466$, $p = .046$; channel S'5: $z = 2.389$, $p = .046$; **Figure 2.17**). A similar effect was detected for patient 2 but did not survive FDR correction (channel M6: $z = 2.292$, $p = .029$ (uncorrected), $p = .399$ (FDR corrected), **Figure 2.17**). No other significant difference was detected (**Supplementary materials**).

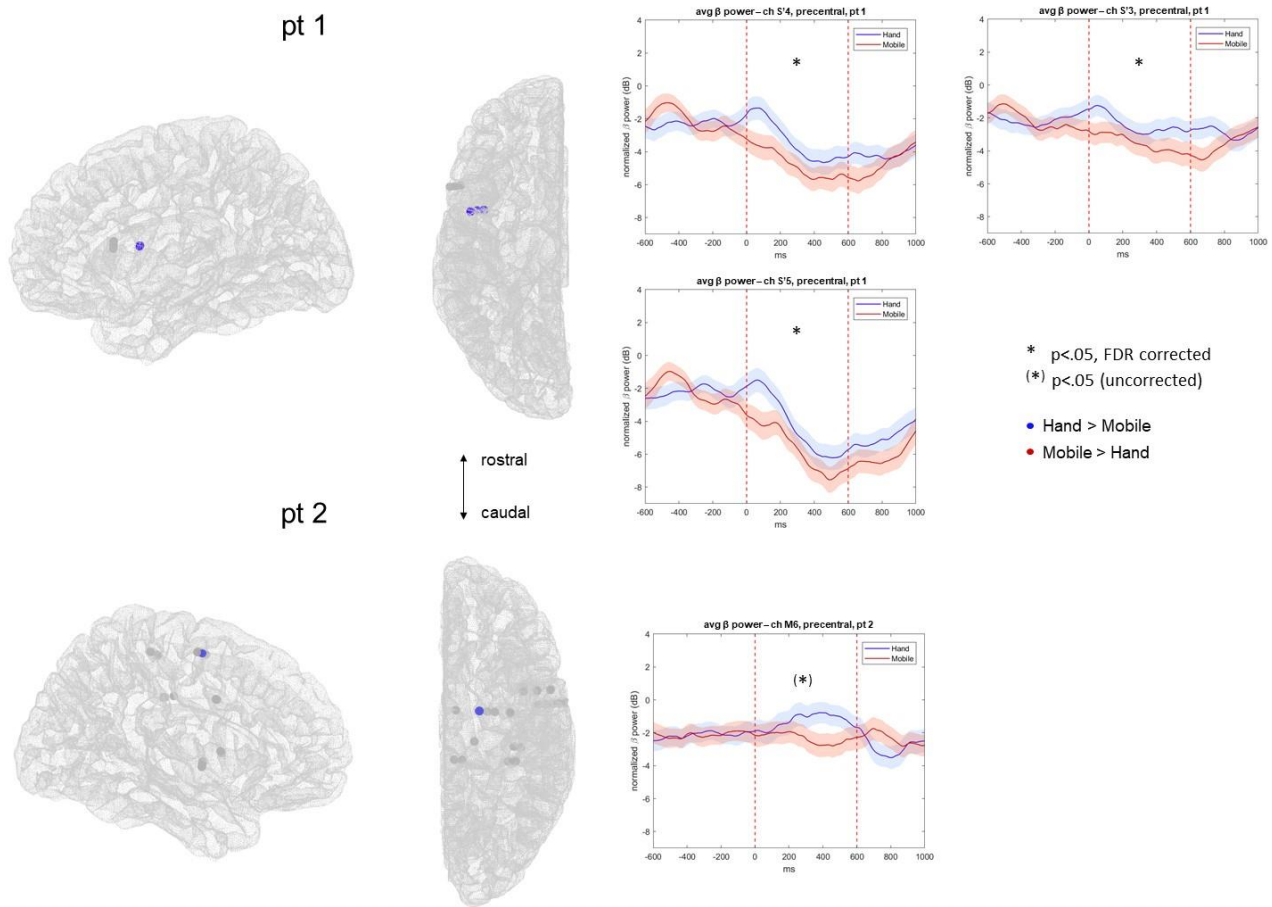


Figure 2.17 Results of the contrast Hand vs Mobile conducted on channels located in pre- and postcentral gyri (ROI). A significant difference in β power was detected in three channels located in the premotor cortex in patient 1 and one channel in the premotor cortex in patient 2, despite the latter was not significant after FDR correction for multiple comparisons.

Interim discussion

By adopting an exploratory, fully data-driven approach, we showed that the Line Length Judgment Task triggers the activation of a broad neural network, which mainly involves occipito-temporal, inferior temporal, posterior parietal and frontal areas. Crucially, the same network was activated when participants were required to perform the line length judgments referring to the dimensions of their own hand and mobile phone (**Figure 2.16a, b and c**). In other words, we did not find evidence for a body-specific area

or network underlying the estimation of body part size, compared to the estimation of a manipulable object.

The behavioural results reported in Study 4, showing the similarity between the perceived dimensions of one's own hand and mobile phone, are mirrored by similar neural activations during the size estimation of these two targets. Our data therefore are in line with the hypothesis that the representation of the mobile phone is scaled on the representation of the hand.

In detail, we documented the activation of a broad network during the LLJ task, independently of which target was being estimated. Interestingly, such pattern of activations well overlaps with brain areas activated during visual imagery tasks. A recent meta-analysis (Winlove et al., 2018) conducted on 40 fMRI experiments addressing visual imagery identified activations in the superior parietal lobule, premotor area, middle and inferior frontal gyri, occipital cortex and occipito-temporal cortex (**Figure 2.18**). Parietal and frontal areas are likely to be responsible for the top-down selection and control of the mental image (Ishai, Ungerleider, & Haxby, 2000; Mechelli, Price, Friston, & Ishai, 2004). Instead, occipital and occipito-temporal areas are thought to be responsible for the activation and maintenance of the visual aspects of an image. Our results seem to suggest that patients mainly used a visual imagery strategy, possibly consisting in retrieving the mental image of the target (i.e., hand or mobile) and comparing it with the lines displayed on the screen.

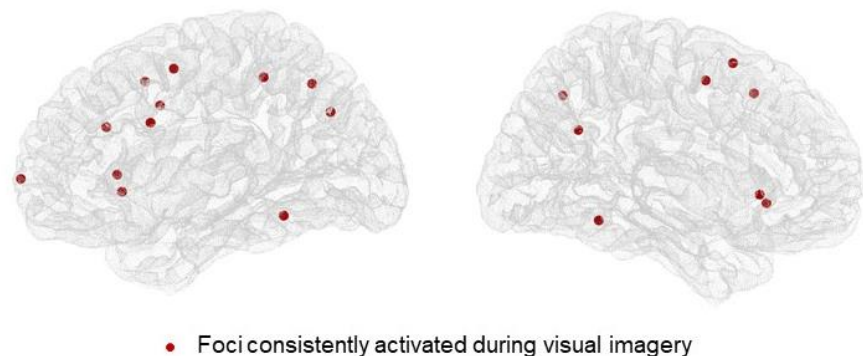


***Figure 2.18** Foci systematically activated during visual imagery, as a result of a meta-analysis on 40 fMRI studies involving the contrast visual imagery task > baseline condition. Adapted from Winlove et al., 2018*

Previous work suggested that the biases affecting the size estimation of the hand might originate from the highly distorted cortical representation in sensorimotor areas (Longo, 2015; Linkenauger et al., 2015). Therefore, additional analyses were run to investigate the activity over sensorimotor cortices

during size estimation of the hand in the Line Length Judgment Task. When the analysis focused on the sensorimotor cortex, we found a significantly higher β response during the Hand estimation compared to the Mobile in the precentral gyrus. Such effect was clearly detected in three channels of patient 1, and one channel of patient 2, although the latter did not survive correction for multiple comparisons (**Figure 2.12**).

This result must be interpreted with caution, since it was not consistently detected across patients. Furthermore, in the two patients for which the Hand-Mobile difference in β power was detected, the results are not totally overlapping. More specifically, in patient 1 a decreased β power was also detected after the stimulus onset in the same channels, regardless of the condition, whereas no overall change in β power was detected in patient 2 in the same channel. The event-related decrease of β power, or β event-related desynchronisation (ERD), has been interpreted as an electrophysiological correlate of an increased cortical excitability or an activated cortical area (Pfurtscheller, 2000). During motor imagery involving one hemi body, β ERD over the contralateral sensorimotor cortex, along with an increased β -power (event-related synchronisation, ERS) over the ipsilateral sensorimotor cortex have been detected in healthy participants. While the contralateral ERD possibly reflects the involvement of the motor cortex in imagined movement, authors interpreted the ipsilateral ERS as correlate of deactivated or actively inhibited motor area neurons (Neuper & Pfurtscheller, 1997). In our study, patients were asked to estimate the dimensions of their left hand and to respond by pressing a button with the right hand. It could be speculated that in patient 1 the overall left β desynchronisation reflects the motor preparation and response of the contralateral hand, whereas the higher left β power in the Hand vs Mobile condition reflects the synchronisation over the sensorimotor cortex underlying motor imagery referred to the ipsilateral hand. Partially aligned with such speculation, in patient 2 we did not find a desynchronisation related to movement, since the channel is located in the right hemisphere, ipsilateral to the hand which was in charge of pressing the button. However, if related to motor imagery, the higher β response might indicate that motor imagery involved the right hemi body, which should not have been the case, given the task instructions; though, we cannot exclude that patient 2 estimated the dimensions of her right hand, instead of her left one as instructed.

Besides this speculation, it is interesting to consider how and why motor imagery might have been triggered. Motor imagery is often involved in body representation tasks. For instance, in Hand Laterality Judgment tasks (Parsons, 1987) participants are required to judge the laterality of a picture of a human hand. It has been proposed that participants use implicit motor imagery in order to mentally rotate their left or right hand and match it with the hand displayed in the picture. Both behavioural and neurocognitive evidence support such hypothesis (Lange, Hagoort, & Toni, 2005; Parsons, 1987, 1994; Rumiat, Tomasino, Vorano, Umiltà, & De Luca, 2001). Similarly, it could be argued that some participants adopt a motor imagery strategy in the LLJ task, for example by imagining positioning their

hand next to or above the line displayed on the screen in order to perform a visual comparison. Contrarily to the Hand Laterality Judgment task, in the LLJ task the line orientation was kept constant within each block, reducing the motor imagery to its proprioceptive component (i.e., imagining the hand in a certain posture and spatial position). In other words, the strategy might involve imagining fixed hand posture and position over trials, rather than imagining changing hand posture or position on each trial, as in the Hand Laterality Judgment task. Acknowledging the lack of a systematic investigation of the strategies used in the LLJ task, which would be interesting to study in the future, the proprioceptive imagery strategy is in line with many spontaneous reports by our participants.

Although the way we interpreted our results relatively to changes in β activity in the precentral cortex is intriguing, no firm conclusion can be drawn from our data alone. First, and perhaps most obviously, it would be crucial to test the consistency of this result by increasing the sample size. Second, further investigation is needed to test whether the neural correlate of proprioceptive imagery is overlapping with that of motor imagery. Indeed, while several studies have investigated the behavioural and neurocognitive counterparts of the ability to imagine movement (Hardwick, Caspers, Eickhoff, & Swinnen, 2018; Jeannerod, 2001), few have specifically addressed the ability to imagine a body part in a posture or spatial position different from its actual ones (e.g. Ganea & Longo, 2017). Finally, it would be important to relate the neural findings to behaviour, by implicitly and explicitly investigating the strategies adopted in the LLJ task.

While our data show that performing the Line Length Judgment Task under the Hand and Mobile conditions triggered a similar neural activation over overlapping brain regions, likely to involve the visual imagery network, we cannot disentangle the activity underlying the retrieval of the mental representation of the target from the activity reflecting other processing related to the task (e.g. visual processing of the stimulus, decision making, preparation of the motor response). Future studies are needed to test whether (and to which extent) the visual imagery network is involved in the estimation of body parts' size, by isolating its activation through the inclusion of control tasks in the design (e.g. judging the orientation of a line, without recurring to a mental representation). Furthermore, it might be interesting to investigate how the activity of the visual imagery network is modulated by different conditions (e.g. judging the size body parts characterised by different degrees of tactile acuity and visual accessibility, see Study 3). Finally, it would be interesting to compare the neural responses triggered by the size estimation of objects that afford or inhibit the interaction and manipulation, and test the relationship between the behavioral responses and the possible involvement of areas described as the neurofunctional correlates of affordances (Sakreida et al., 2016).

To summarise, our exploratory analysis indicates that a broad neural network is activated when participants estimate the dimensions of their hand or of their mobile phone in an LLJ task, suggesting that

similar neural mechanisms underlie the estimation of the hand and of a manipulable, highly familiar object. Interestingly, this network comprises regions that are triggered in visual imagery tasks (Winlove et al., 2018), suggesting that visual representations of the targets are triggered to estimate their size in the Line Length Judgment Task, therefore that the metric biases affecting those representations are mainly visual-based. We also reported a difference in β power between Hand and Mobile conditions over the precentral gyrus, pointing at a possible specific role of the sensorimotor cortices in the representation of the metric properties of the body. While further investigations are needed to better document such an effect and therefore refine our interpretation, we believe that the present study provides important evidence regarding the nature of the metric biases observed in previous studies (Longo & Haggard, 2010; Longo, 2015a; Saulton et al., 2017) as well as in our own research (Study 2 and 3), when the dimensions of one's own hand or an object are retrieved.

Factors modulating metric biases in body and objects representations: general discussion

Study 3 studied the perceived dimensions of five body parts, affording different degrees of tactile acuity and visual accessibility, namely the hand, the foot, the dorsal portion of the neck, the nose and the lips. We found that both visual and somatosensory factors are likely to contribute to the metric body representation, which is likely to be originated by the weighted contribution of different sources of information, depending on their availability in a particular moment. Study 4 compared the perceived dimensions of the hand with those of several objects in order to investigate whether the metric biases are body-specific, or extend to objects, and, if this is the case, which factors modulate their representation. We concluded that biases characterising the hand representation measured through the LLJ task are not body-specific, instead they generalise to objects, especially when objects elicit manipulation. This is supported by similar behavioural and electrophysiological patterns of response. This result, in line with the action-specific perception account (Witt, 2011), indicate that affordances may play a role in metric representations, since objects which are unlikely to elicit manipulation and interaction (i.e., a cactus and a disgusting soap) turned out to be differently perceived compared to objects that afford these actions (i.e., a mobile phone and a computer mouse). Taken together, our data indicate that both the effector and the object of the action are similarly misperceived in their dimensions, providing a new perspective on the hand-object interaction problem and how this might be addressed in future work.

Conclusions

Metric biases in body and object representations

Although the body has a critical role in many aspects of our behavior, it is still largely unknown how our brain integrates available sensory inputs and stored knowledge about the body in order to represent our body parts in terms of their different features, such as their spatial position, dimensions, motor and tactile properties. The present thesis aimed at exploring the mental representation of the body with a focus on the metric biases characterising it, which have been described in previous research (e.g.: Longo & Haggard, 2010; Longo, 2015a; Linkenauger et al., 2015).

In the first chapter of the thesis, we addressed the relationship between movement and metric biases characterising the hand representation. We showed that the motor system makes use of a biased metric representation (Study 1) but partially overcomes these biases, possibly by integrating current somatosensory inflow and motor outflow in the forward models, which refine movement trajectories (Study 2).

Within the framework of body representation, our results provide evidence against the theoretical differentiation between the body schema and the body model. The body schema has been traditionally defined as the sensorimotor representation of the body that guide actions (de Vignemont, 2010; Dijkerman & de Haan, 2007; Gallagher, 2005; Paillard, 1999; Rossetti, Rode, & Boisson, 1995). The fact that simple movements are based on the biased metric representation of the hand, previously defined as body model (Longo & Haggard, 2010; Longo, 2015a), leads to the conclusion that the body metric representation can be conceptualised as a component of the body schema. As a matter of fact, a broader definition of body schema refers to “a highly plastic representation of the body parts, in terms of posture, shape, and size, that can be used to execute or imagine executing movements” (Medina & Coslett, 2010).

Furthermore, our results are extremely salient in the context of motor control research, especially when movements rely on proprioception (i.e., when visual feedback is not available). Our data indeed demonstrate that motor plans rely on biased body representations. These biases should be accounted for in models of motor control (Desmurget & Grafton, 2000), and might be relevant to the explanation of error patterns in proprioceptive and visuo-proprioceptive matching tasks (Kuling et al., 2016). In parallel, we showed that sensorimotor integration in the forward models is partially overcoming body representation misperception, highlighting the relevance of considering the body as integrated in the environment.

The second chapter (Study 3, 4 and 5) enters the debate regarding the specificity of the metric biases affecting body representations, by testing whether these biases extend to the surrounding environment, and which sensorial information and higher-order factors modulate them.

Study 3 showed that the pattern of size misestimation is similar among body parts which are visually accessible (hand, foot, lips and partially nose), despite their different physical size and tactile acuity, but strikingly different for a body part which is not (the dorsal portion of the neck). Furthermore, we found evidence supporting the existence of different mechanisms underlying the estimation of the length and of the width of the body parts considered. While the length Estimation Error (EE) is predicted by the tactile acuity, the width EE is not, pointing at the different weight of somatosensory and visual information in estimating distances between the horizontal boundaries versus the vertical ones. Our results thus suggest that visual and somatosensory information both contribute to generating a mental representation of body dimensions. We argue that visual, somatosensory, and possibly other sources of information are weighted differently based on their availability for a given body part and spatial dimension.

Study 4 and 5 showed that biases affecting body representations are not body-specific, instead they extend to objects in the surrounding environment. Specifically, we observed similar misestimations for the hand, the mobile phone, the mouse and the mug; whose representations cluster together in the multidimensional scaling matrix. Electrophysiological data further supported the finding that the representations of the hand and a mobile phone are underpinned by similar neurofunctional mechanisms. What is common to all those objects is that they are often the targets of our actions. It has been put forward that perception is action-specific, meaning that the environment is perceived and therefore represented depending on our ability to act upon it (Witt, 2011). Our results are compatible with the action-specific perception account, especially since we also found that objects perceived as potentially harmful (cactus) or disgusting (dirty soap), thereby inhibiting manipulation, were perceived differently from manipulable objects. As a plausible explanation, we thus argue that biases characterizing the hand representation are inherited by objects that afford manipulation and interaction. While previous research tried to solve the mismatch between accurate hand movements and biases in hand representation (Study 1 and 2 of this thesis) or biases in object perception (Lee et al., 2008; Coats et al., 2008), we demonstrated that both the effector and the object of the action are not accurately perceived. We argue that this might be functional in our daily interaction with the environment: misperceiving the dimensions of our hand as well as of objects we are likely to interact with would facilitate hand-object interaction.

Altogether, our research prompts to shift the focus of the investigation from the body as an isolated system, to the body integrated and active into the environment. Research on biases in body representation too often considered the body as the object of our perception, disregarding its role as an effector of our actions. By providing insights on the role of body representation in motor planning and execution, this thesis eventually offers an original perspective that integrates body perception and action, and contribute to bridging the gap between body representation and motor control models. Along these

lines, we showed that body representation is strongly related to how we represent the surrounding environment, especially when objects in the environment afford manual interaction. Here, we addressed body-environment interaction from an ecological point of view, by facing (and providing possible solutions to) the mismatch between biases in body representation and our need to efficiently interact with the environment. We argue that sensorimotor integration by internal models of motor control, as well as the generalisation of metric biases to objects that we are more likely to interact with, are possible mechanisms to improve our functional interaction with the surrounding environment.

Supplementary materials

Supplementary materials - Study 2

Descriptive statistics

The mean (M) or median (Mdn) estimation ratios (ER), along with their standard deviations (SD) or interquartile ranges (IQR) are reported for each dimension considered, separately for each condition (visuo-proprioceptive matching task, VP; Proprioceptive matching task, P and rest, R) and time (pre and post). To be noted that when the $ER = 1$, the dimension is accurately estimated, whereas $ER > 1$ or $ER < 1$ reflects overestimation or underestimation, respectively. Each ER distribution has been compared against zero by means of one-sample t-tests or Wilcoxon Signed Rank Test against 1, whose results are reported in the last two columns.

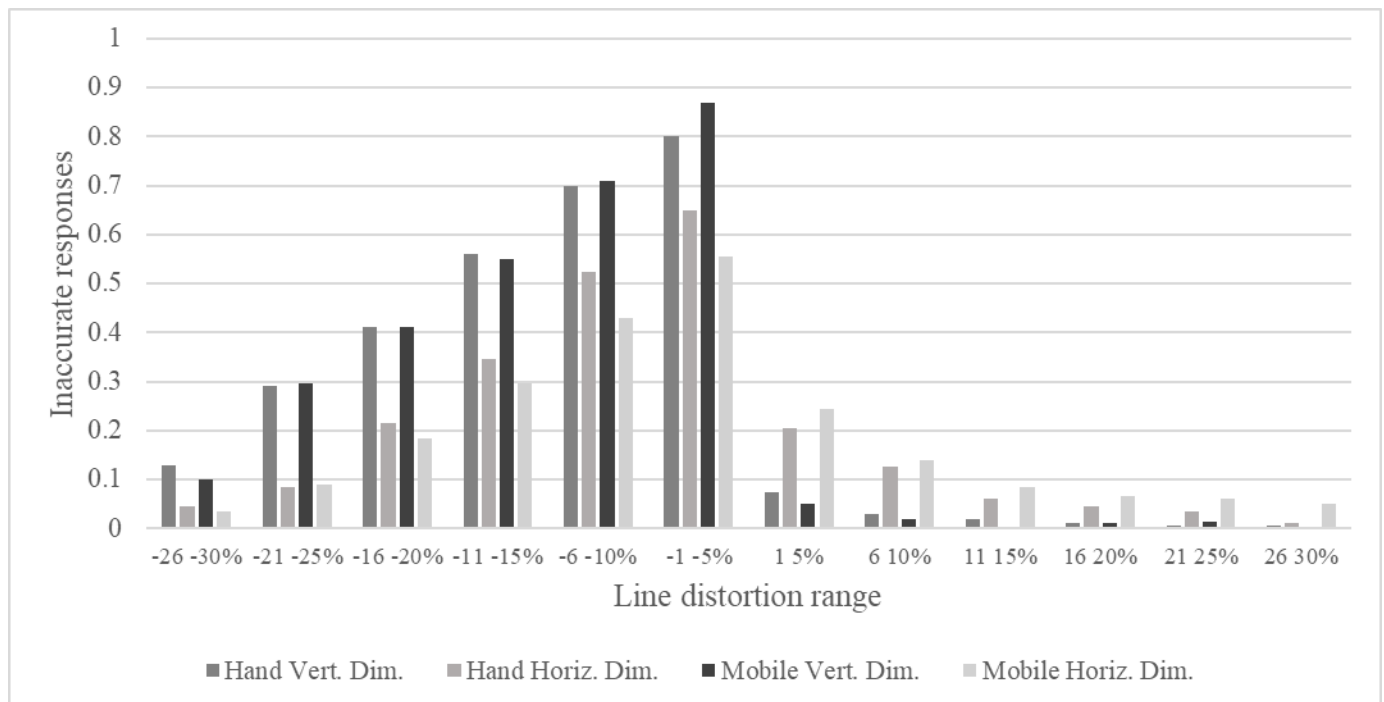
Dimension	Condition, Time	Estimation Ratio Central tendency measure		Test statistic (df)		p
Thumb length	VP, pre	M \pm SD	0.677 \pm 0.139	t (21)	-10.874	<.001
	VP, post		0.684 \pm 0.152		-9.758	<.001
	P, pre		0.650 \pm .112		-14.707	<.001
	P, post		0.679 \pm 0.133		-11.302	<.001
	R, pre		0.688 \pm 0.126		-11.591	<.001
	R, post		0.693 \pm 0.136		-10.599	<.001
Index finger length	VP, pre	Mdn \pm IQR	0.587 \pm 0.196	Z (21)	-4.107	<.001
	VP, post		0.647 \pm 0.165		-4.107	<.001
	P, pre		0.593 \pm 0.098		-4.107	<.001
	P, post		0.627 \pm 0.135		-4.107	<.001
	R, pre		0.549 \pm 0.177		-4.107	<.001
	R, post		0.565 \pm 0.182		-4.107	<.001
Middle finger length	VP, pre	Mdn \pm IQR	0.508 \pm 0.134	Z (21)	-4.107	<.001
	VP, post		0.588 \pm 0.129		-4.107	<.001
	P, pre		0.550 \pm 0.086		-4.107	<.001
	P, post		0.587 \pm 0.141		-4.107	<.001
	R, pre		0.524 \pm 0.201		-4.107	<.001
	R, post		0.524 \pm 0.217		-4.107	<.001
Ring finger length	VP, pre	M \pm SD	0.508 \pm 0.110	t (21)	-20.955	<.001
	VP, post		0.539 \pm 0.092		-23.415	<.001
	P, pre		0.514 \pm 0.091		-24.902	<.001
	P, post		0.523 \pm 0.110		-20.266	<.001
	R, pre		0.526 \pm 0.119		-18.633	<.001
	R, post		0.529 \pm 0.112		-19.766	<.001
Little finger length	VP, pre	Mdn \pm IQR	0.499 \pm 0.186	Z (21)	-4.107	<.001
	VP, post		0.573 \pm 0.069		-4.107	<.001
	P, pre		0.544 \pm 0.246		-4.107	<.001
	P, post		0.536 \pm 0.112		-4.107	<.001
	R, pre		0.516 \pm 0.204		-4.107	<.001
	R, post		0.583 \pm 0.136		-4.107	<.001
Mean finger length	VP, pre	Mdn \pm IQR	0.525 \pm 0.151	Z (21)	-4.107	<.001
	VP, post		0.599 \pm 0.109		-4.107	<.001
	P, pre		0.571 \pm 0.105		-4.107	<.001
	P, post		0.607 \pm 0.141		-4.107	<.001
	R, pre		0.553 \pm 0.179		-4.107	<.001
	R, post					

	R, post		0.568 ± 0.162		-4.107	<.001
Hand width	VP, pre	$M \pm SD$	1.332 ± 0.219	t (21)	7.090	<.001
	VP, post		1.257 ± 0.220		7.307	<.001
	P, pre		1.267 ± 0.212		5.775	<.001
	P, post		1.266 ± 0.204		6.098	<.001
	R, pre		1.283 ± 0.185		7.148	<.001
	R, post		1.263 ± 0.288		5.303	<.001
Shape index	VP, pre	$M \pm SD$	2.537 ± 0.619	t (21)	11.636	<.001
	VP, post		2.262 ± 0.536		11.052	<.001
	P, pre		2.352 ± 0.587		10.795	<.001
	P, post		2.224 ± 0.617		9.304	<.001
	R, pre		2.386 ± 0.622		10.456	<.001
	R, post		2.368 ± 0.899		7.130	<.001

Supplementary materials - Study 3

Distribution of response accuracy

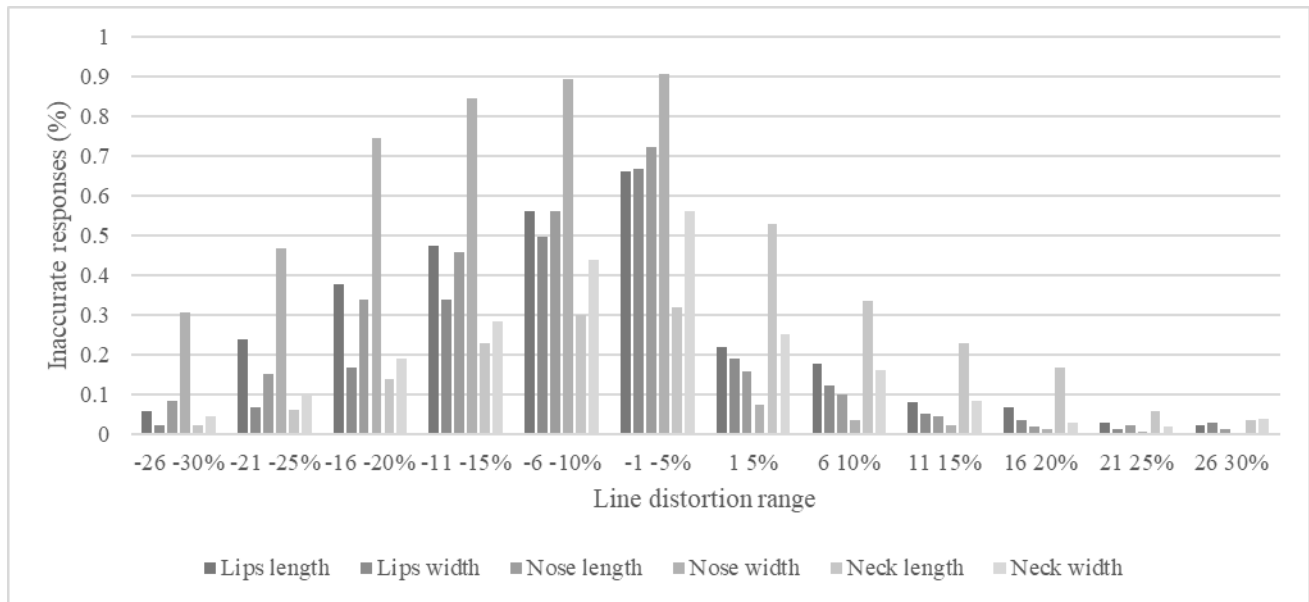
Asymmetry in the response accuracy has been observed in a pilot experiment investigating the perceived horizontal and vertical dimension of participants' own hand and mobile phone. Twenty participants (17 females) were enrolled in the study. Each participant underwent two blocks (one for the length and one for the width) of 120 trials each, with lines that covered a distortion range from -30% to -1% (shorter) and from 1% to 30% (longer) of the actual hand dimension. To be noted that the inaccurate responses referred to shorter lines were always reflecting an underestimation of the hand dimension, whereas the inaccurate response referred to longer lines were always representing an overestimation of the hand dimension.



Supplementary materials - Study 3

Distribution of response accuracy

Response accuracy for each line distortion range is depicted for the second experiment of the third study, assessing the mental representation of the nose, the lips and the rostral portion of the neck. The asymmetry observed in the pilot data regarding the hand is evident in the data referred to other body parts.



Supplementary materials - Study 3

Results of the Linear Mixed-Effects Models

The results for each Linear Mixed-Effects Model aimed at exploring the effects of the tactile acuity, the actual dimension and their interaction on the EEs are reported for each dimensions (Dim.). Regarding the width, the first set of models considered all the data, whereas in the second set of models the data referring to the nose representation are excluded.

Dim.	Data-set	Model	Fixed effects	Random intercepts and slopes	Log-likelihood	Likelihood ratio test statistics (against null model)
Length	All the data	0 (null)		Subjects	-111.140	/
		1	Actual length	Subjects, Actual length	-109.942	2.397, p=.494
		2	Tactile acuity	Subjects, Tactile acuity	-104.350	13.580, p=.003
		3	Tactile acuity*Actual length	Subjects, Tactile acuity*Actual length	-102.755	16.769, p=.158
Width	All the data	0 (null)		Subjects	-107.303	/
		1	Actual width	Subjects, Actual width	-100.424	13.757, p=.003
		2	Tactile acuity	Subjects, Tactile acuity	-104.856	4.914, p=.178
		3	Tactile acuity*Actual length	Subjects, Tactile acuity*Actual length	-97.848	18.909, p=.091
Width	Nose excluded	0 (null)		Subjects	-73.615	/
		1	Actual width	Subjects, Actual width	-73.496	.238, p=.971
		2	Tactile acuity	Subjects, Tactile acuity	-73.204	.821, p=.844
		3	Tactile acuity*Actual length	Subjects, Tactile acuity*Actual length	-71.877	3.476, p=.991

Supplementary materials - Study 5

Comparison between task and baseline activity

Patient 1 - comparison between Task and Baseline						
	z-score	p-value	adjusted p-value	z-score	p-value	adjusted p-value
	β			High- γ		
O'1	-3.481	0.001	0.003	-1.280	0.176	0.399
O'2	-0.316	0.379	0.384	-1.017	0.238	0.399
O'7	-1.851	0.072	0.101	-1.428	0.144	0.395
O'8	-1.736	0.088	0.121	-0.894	0.268	0.399
O'9	0.139	0.395	0.395	-2.009	0.053	0.274
O'10	0.702	0.312	0.337	-0.638	0.325	0.399
O'11	-0.537	0.345	0.361	-2.185	0.037	0.228
O'14	-0.468	0.357	0.366	-1.303	0.171	0.399
B'11	-2.986	0.005	0.010	-1.819	0.076	0.316
O'12	-0.794	0.291	0.326	-0.336	0.377	0.399
O'13	-0.857	0.276	0.317	-1.282	0.175	0.399
B'13	-1.445	0.140	0.179	-1.721	0.091	0.338
B'14	-2.018	0.052	0.076	0.176	0.393	0.399
C'1	-2.687	0.011	0.021	0.499	0.352	0.399
C'2	-0.919	0.261	0.312	0.698	0.313	0.399
C'3	-0.549	0.343	0.361	0.725	0.307	0.399
C'4	-2.164	0.038	0.060	0.334	0.377	0.399
C'5	-2.057	0.048	0.072	1.436	0.142	0.395
F'1	-0.871	0.273	0.317	-0.220	0.389	0.399
F'5	-3.270	0.002	0.005	1.223	0.189	0.399
C'14	-4.581	<.001	<.001	-1.591	0.112	0.354
R'1	-3.406	0.001	0.003	1.426	0.144	0.395
R'2	-2.600	0.014	0.025	5.338	<.001	<.001
R'3	-4.123	<.001	<.001	7.984	<.001	<.001
R'6	-7.086	<.001	<.001	2.804	0.008	0.073
R'7	-9.593	<.001	<.001	-0.962	0.251	0.399
R'8	-6.083	<.001	<.001	-0.539	0.345	0.399
R'9	-5.409	<.001	<.001	0.357	0.374	0.399
U'1	-4.430	<.001	<.001	1.267	0.179	0.399
U'2	-2.985	0.005	0.010	0.809	0.287	0.399
U'4	2.303	0.028	0.048	0.589	0.335	0.399
U'6	2.186	0.037	0.059	0.407	0.367	0.399
U'7	0.462	0.358	0.366	-0.418	0.366	0.399
Y'1	-3.688	<.001	0.001	-1.300	0.171	0.399
Y'18	-5.708	<.001	<.001	-1.108	0.216	0.399
T'2	-2.242	0.032	0.053	0.112	0.396	0.399
T'3	-2.754	0.009	0.018	-0.122	0.396	0.399
T'7	-1.575	0.115	0.153	-0.742	0.303	0.399
E'1	-4.288	<.001	<.001	0.395	0.369	0.399
E'2	-3.837	<.001	0.001	0.645	0.324	0.399
E'3	-4.023	<.001	<.001	0.067	0.398	0.399
E'4	-3.992	<.001	<.001	0.251	0.387	0.399
E'5	-2.785	0.008	0.017	-0.815	0.286	0.399
E'6	-3.270	0.002	0.005	2.099	0.044	0.256
E'9	-2.014	0.052	0.076	-0.072	0.398	0.399
E'10	-3.068	0.004	0.008	-2.407	0.022	0.158
E'12	-3.171	0.003	0.006	-1.839	0.073	0.316
E'13	-3.878	<.001	0.001	-0.938	0.257	0.399
E'14	-4.215	<.001	<.001	-2.306	0.028	0.186
K'1	-1.607	0.110	0.148	-0.688	0.315	0.399
K'5	-1.056	0.229	0.280	-2.744	0.009	0.078

K'6	-2.238	0.033	0.053	-1.762	0.085	0.327
K'9	-7.291	<.001	<.001	6.544	<.001	<.001
K'10	-4.432	<.001	<.001	1.806	0.078	0.316
K'12	-4.411	<.001	<.001	0.042	0.399	0.399
K'13	-4.765	<.001	<.001	-2.063	0.047	0.260
K'14	-4.667	<.001	<.001	-1.236	0.186	0.399
K'15	-5.994	<.001	<.001	0.472	0.357	0.399
K'16	-5.288	<.001	<.001	0.579	0.337	0.399
K'17	-8.525	<.001	<.001	-0.384	0.371	0.399
D'1	-3.084	0.003	0.008	1.897	0.066	0.307
D'2	-2.159	0.039	0.060	1.117	0.214	0.399
D'4	-1.539	0.122	0.160	0.384	0.371	0.399
D'5	-0.893	0.268	0.315	1.091	0.220	0.399
D'6	-0.740	0.303	0.336	1.105	0.217	0.399
D'9	-0.558	0.341	0.361	0.794	0.291	0.399
N'1	-3.919	<.001	0.001	1.070	0.225	0.399
N'2	-3.600	0.001	0.002	1.462	0.137	0.395
N'3	-4.380	<.001	<.001	0.702	0.312	0.399
W'2	-3.033	0.004	0.009	0.406	0.367	0.399
W'3	-1.239	0.185	0.233	-1.625	0.106	0.354
P'1	-2.431	0.021	0.037	6.334	<.001	<.001
P'2	-2.313	0.028	0.048	3.444	0.001	0.016
P'8	-4.159	<.001	<.001	0.678	0.317	0.399
P'10	-2.645	0.012	0.022	-0.376	0.372	0.399
P'11	-2.109	0.043	0.066	-3.034	0.004	0.041
P'12	-3.251	0.002	0.005	-1.651	0.102	0.352
P'13	-4.506	<.001	<.001	-0.580	0.337	0.399
I'1	-0.725	0.307	0.336	0.778	0.295	0.399
X'2	-1.026	0.236	0.285	3.107	0.003	0.037
X'3	-1.910	0.064	0.092	1.913	0.064	0.307
X'4	-4.671	<.001	<.001	3.549	0.001	0.014
X'8	-1.500	0.129	0.167	-3.314	0.002	0.022
I'8	-1.131	0.210	0.261	-0.370	0.372	0.399
I'9	-0.798	0.290	0.326	-0.693	0.314	0.399
I'10	-2.252	0.032	0.053	-1.582	0.114	0.354
S'2	-2.790	0.008	0.017	-1.669	0.099	0.352
S'3	-2.685	0.011	0.021	2.547	0.016	0.121
S'4	-5.983	<.001	<.001	0.109	0.397	0.399
S'5	-7.642	<.001	<.001	-0.379	0.371	0.399
W'6	-4.314	<.001	<.001	-0.467	0.358	0.399
W'8	-1.785	0.081	0.113	-0.074	0.398	0.399
W'10	-3.810	<.001	0.001	-0.353	0.375	0.399

Patient 2 - comparison between Task and Baseline						
	z-score	p-value	adjusted p-value	z-score	p-value	adjusted p-value
	β			High- γ		
G15	0.168	0.393	0.399	-1.216	0.190	0.316
M1	0.964	0.251	0.399	-1.887	0.067	0.156
M4	1.770	0.083	0.294	-1.348	0.161	0.285
M5	3.113	0.003	0.041	-0.845	0.279	0.396
M6	1.352	0.160	0.399	-2.849	0.007	0.040
B1	0.403	0.368	0.399	1.261	0.180	0.312
B2	-0.177	0.393	0.399	1.986	0.056	0.149
B3	0.207	0.391	0.399	1.241	0.185	0.313
B4	-1.132	0.210	0.399	0.327	0.378	0.398
E1	-2.000	0.054	0.222	-4.097	<.001	0.002
J1	-1.405	0.149	0.399	-2.053	0.049	0.135

J8	1.747	0.087	0.294	-0.450	0.361	0.398
J9	-1.139	0.208	0.399	-2.510	0.017	0.070
J10	-0.607	0.332	0.399	-2.292	0.029	0.098
J11	-0.363	0.374	0.399	-0.900	0.266	0.384
J12	0.383	0.371	0.399	3.115	0.003	0.030
D3	-2.220	0.034	0.147	0.653	0.322	0.398
D4	-2.239	0.033	0.147	0.388	0.370	0.398
D5	-0.511	0.350	0.399	-0.052	0.398	0.398
D6	-0.888	0.269	0.399	-0.499	0.352	0.398
D11	0.785	0.293	0.399	4.917	<.001	<.001
M8	0.342	0.376	0.399	-1.630	0.106	0.217
F1	0.739	0.304	0.399	-1.909	0.065	0.156
F5	-3.322	0.002	0.025	4.340	<.001	0.001
F6	-1.073	0.224	0.399	-0.412	0.366	0.398
F7	0.572	0.339	0.399	2.446	0.020	0.078
F10	0.193	0.392	0.399	2.831	0.007	0.040
E3	-2.674	0.011	0.073	-2.575	0.014	0.065
E4	-1.266	0.179	0.399	-2.118	0.042	0.124
E9	-1.868	0.070	0.272	1.059	0.228	0.348
E10	-1.218	0.190	0.399	0.728	0.306	0.398
E11	-0.731	0.305	0.399	0.059	0.398	0.398
E12	-0.038	0.399	0.399	-0.553	0.342	0.398
H2	0.029	0.399	0.399	-2.788	0.008	0.040
H3	-0.359	0.374	0.399	-1.089	0.220	0.344
H10	2.889	0.006	0.048	-0.603	0.333	0.398
H12	3.021	0.004	0.042	-3.484	0.001	0.010
H14	2.845	0.007	0.049	-2.375	0.024	0.088
N1	1.761	0.085	0.294	-1.024	0.236	0.354
N2	0.487	0.354	0.399	-1.550	0.120	0.233
N5	2.375	0.024	0.132	-0.987	0.245	0.361
N6	-0.159	0.394	0.399	-2.124	0.042	0.124
N7	1.168	0.202	0.399	-3.953	<.001	0.002
N8	0.706	0.311	0.399	0.215	0.390	0.398
N9	1.322	0.166	0.399	-0.602	0.333	0.398
X1	-2.313	0.028	0.134	-2.113	0.043	0.124
K1	-5.060	<.001	<.001	0.459	0.359	0.398
K2	-6.866	<.001	<.001	4.051	<.001	0.002
K4	-7.606	<.001	<.001	-1.920	0.063	0.156
K5	-3.391	0.001	0.025	1.882	0.068	0.156
P3	1.098	0.218	0.399	3.065	0.004	0.032
P8	0.154	0.394	0.399	-2.955	0.005	0.040
P9	-0.804	0.289	0.399	-2.564	0.015	0.065
P10	-0.694	0.314	0.399	-1.449	0.140	0.259
P11	-0.907	0.264	0.399	-1.159	0.204	0.331
P13	0.334	0.377	0.399	-1.585	0.114	0.227
P14	0.997	0.243	0.399	-2.296	0.029	0.098
P15	0.661	0.321	0.399	-2.809	0.008	0.040
S2	0.942	0.256	0.399	-1.357	0.159	0.285
X15	3.011	0.004	0.042	-1.858	0.071	0.158
S5	-0.586	0.336	0.399	-2.141	0.040	0.124
S6	-0.602	0.333	0.399	-1.650	0.102	0.215
S7	-1.049	0.230	0.399	-1.945	0.060	0.156
S8	-0.536	0.346	0.399	-1.783	0.081	0.176
S9	-0.404	0.368	0.399	-2.901	0.006	0.040
S10	-0.107	0.397	0.399	-2.884	0.006	0.040
R2	0.312	0.380	0.399	0.324	0.379	0.398
R3	1.410	0.148	0.399	-0.573	0.339	0.398
R9	1.467	0.136	0.399	-4.266	<.001	0.001
Y1	-1.686	0.096	0.313	-0.780	0.294	0.398

Y2	-1.221	0.189	0.399	-0.296	0.382	0.398
Y3	0.807	0.288	0.399	0.670	0.319	0.398
Y4	0.660	0.321	0.399	-0.242	0.387	0.398
Y5	0.183	0.392	0.399	-1.131	0.210	0.335
Y6	-0.821	0.285	0.399	-1.536	0.123	0.233
Y12	-2.919	0.006	0.048	0.088	0.397	0.398
Y13	-2.610	0.013	0.079	0.225	0.389	0.398
Y14	-2.335	0.026	0.134	0.403	0.368	0.398

Patient 3 - comparison between Task and Baseline						
	z-score	p-value	adjusted p-value	z-score	p-value	adjusted p-value
	β			High- γ		
Q1	-0.349	0.375	0.398	-0.732	0.305	0.398
Q17	1.977	0.057	0.161	-2.362	0.025	0.197
T3	3.487	0.001	0.006	-0.169	0.393	0.398
T4	0.810	0.287	0.398	-1.245	0.184	0.398
A1	-0.381	0.371	0.398	-0.835	0.282	0.398
A2	0.322	0.379	0.398	-0.687	0.315	0.398
V8	-7.323	<.001	<.001	4.107	<.001	0.001
V9	-5.576	<.001	<.001	8.307	<.001	<.001
V10	-7.739	<.001	<.001	-0.252	0.386	0.398
V11	-6.209	<.001	<.001	4.485	<.001	<.001
V12	-4.390	<.001	<.001	1.717	0.091	0.324
V13	-4.285	<.001	<.001	1.151	0.206	0.398
U1	-1.031	0.234	0.369	0.883	0.270	0.398
U2	-0.169	0.393	0.398	0.300	0.381	0.398
U3	1.431	0.143	0.318	-1.446	0.140	0.371
U4	3.246	0.002	0.013	-1.648	0.103	0.324
K8	-1.244	0.184	0.347	-1.293	0.173	0.398
C1	-2.520	0.017	0.082	-0.679	0.317	0.398
C3	-1.040	0.232	0.369	2.037	0.050	0.247
C4	-0.261	0.386	0.398	1.812	0.077	0.301
C5	-1.617	0.108	0.257	1.625	0.107	0.324
C6	-0.181	0.392	0.398	0.502	0.352	0.398
C11	2.401	0.022	0.092	0.715	0.309	0.398
C12	1.736	0.088	0.233	-1.947	0.060	0.277
C13	2.000	0.054	0.160	-0.256	0.386	0.398
C14	2.039	0.050	0.154	-0.328	0.378	0.398
C15	0.729	0.306	0.398	-0.274	0.384	0.398
C16	1.392	0.151	0.320	1.825	0.076	0.301
E1	1.133	0.210	0.353	-2.187	0.037	0.244
E2	1.230	0.187	0.347	-1.514	0.127	0.361
E4	-3.494	0.001	0.006	2.339	0.026	0.197
E14	-2.069	0.047	0.151	-0.763	0.298	0.398
E15	-0.413	0.366	0.398	-0.935	0.258	0.398
F4	-1.508	0.128	0.296	-1.202	0.194	0.398
F5	2.911	0.006	0.031	-1.139	0.209	0.398
F12	-2.222	0.034	0.132	2.998	0.004	0.047
B3	-1.167	0.202	0.347	0.494	0.353	0.398
B4	1.659	0.101	0.249	1.257	0.181	0.398
B5	-3.215	0.002	0.013	1.201	0.194	0.398
B11	0.524	0.348	0.398	1.401	0.150	0.382
B13	-0.228	0.389	0.398	1.489	0.132	0.361
B14	-1.184	0.198	0.347	0.976	0.248	0.398
D1	-2.184	0.037	0.136	2.076	0.046	0.245
D10	0.278	0.384	0.398	-1.216	0.190	0.398
D11	1.780	0.082	0.224	0.123	0.396	0.398

D12	0.522	0.348	0.398	0.075	0.398	0.398
D13	0.731	0.305	0.398	0.664	0.320	0.398
W2	-1.319	0.167	0.337	-0.955	0.253	0.398
W3	-1.417	0.146	0.318	0.196	0.391	0.398
W4	-1.180	0.199	0.347	1.003	0.241	0.398
W10	-0.070	0.398	0.398	-1.253	0.182	0.398
I1	-0.452	0.360	0.398	0.165	0.394	0.398
I2	-0.690	0.315	0.398	0.239	0.388	0.398
Z1	-4.341	<.001	<.001	-1.607	0.110	0.324
Z8	-6.663	<.001	<.001	5.869	<.001	<.001
Z10	-7.820	<.001	<.001	4.466	<.001	<.001
Y2	0.740	0.303	0.398	0.977	0.248	0.398
O1	-0.691	0.314	0.398	-1.833	0.074	0.301
O3	-2.403	0.022	0.092	-1.697	0.095	0.324
O4	-1.313	0.168	0.337	-0.910	0.264	0.398
O5	-2.116	0.043	0.147	-0.627	0.328	0.398
Y17	0.578	0.337	0.398	-0.215	0.390	0.398
P1	-0.366	0.373	0.398	0.548	0.343	0.398
P2	-1.716	0.091	0.233	-0.525	0.348	0.398
P3	-0.846	0.279	0.398	-2.326	0.027	0.197
P4	1.032	0.234	0.369	-2.087	0.045	0.245
P7	-2.103	0.044	0.147	-2.150	0.040	0.244
P8	-2.495	0.018	0.082	3.974	<.001	0.002
P9	-0.388	0.370	0.398	-1.010	0.240	0.398
P10	1.169	0.201	0.347	-1.669	0.099	0.324
P11	0.375	0.372	0.398	-1.094	0.219	0.398
I7	-0.203	0.391	0.398	0.315	0.380	0.398
I8	-0.335	0.377	0.398	0.774	0.296	0.398
I9	0.093	0.397	0.398	-0.186	0.392	0.398

Patient 4 - comparison between Task and Baseline						
	z-score	p-value	adjusted p-value	z-score	p-value	adjusted p-value
	β			High- γ		
Y'1	-2.375	0.024	0.047	-0.934	0.258	0.380
Y'3	-0.379	0.371	0.397	-1.630	0.106	0.215
Y'17	-1.506	0.128	0.194	-1.868	0.070	0.206
B'1	-4.238	<.001	<.001	1.119	0.213	0.367
B'2	-4.151	<.001	<.001	1.059	0.228	0.375
B'3	-4.374	<.001	<.001	1.105	0.217	0.367
Y'12	0.647	0.323	0.397	0.107	0.397	0.398
C'1	0.096	0.397	0.397	1.435	0.142	0.280
C'2	-2.709	0.010	0.025	-0.272	0.384	0.398
C'3	-2.671	0.011	0.026	0.054	0.398	0.398
C'4	-1.753	0.086	0.141	0.056	0.398	0.398
C'5	-1.494	0.131	0.194	1.858	0.071	0.206
C'12	0.860	0.276	0.358	-0.988	0.245	0.376
C'13	0.564	0.340	0.397	-0.988	0.245	0.376
T'1	-0.423	0.365	0.397	2.069	0.047	0.159
T'2	-1.430	0.143	0.204	0.516	0.349	0.398
W'2	0.149	0.395	0.397	0.190	0.392	0.398
D'2	-2.898	0.006	0.017	0.393	0.369	0.398
D'3	-2.732	0.010	0.024	-0.268	0.385	0.398
D'4	-1.318	0.167	0.232	0.919	0.262	0.380
D'5	-2.091	0.045	0.080	0.515	0.349	0.398
D'6	-0.674	0.318	0.397	-1.666	0.100	0.215
D'7	-0.358	0.374	0.397	-1.630	0.106	0.215
D'11	-1.428	0.144	0.204	-0.697	0.313	0.398

D'12	-1.068	0.225	0.299	-2.182	0.037	0.132
E'1	-7.276	<.001	<.001	1.778	0.082	0.215
E'2	-5.270	<.001	<.001	10.423	<.001	<.001
E'3	-8.324	<.001	<.001	3.967	<.001	0.001
E'7	-3.915	<.001	0.001	6.170	<.001	<.001
E'8	-2.111	0.043	0.079	9.262	<.001	<.001
E'9	-0.242	0.387	0.397	1.699	0.094	0.215
E'10	-3.234	0.002	0.008	0.569	0.339	0.398
E'11	-2.528	0.016	0.034	0.077	0.398	0.398
E'12	-2.557	0.015	0.033	0.522	0.348	0.398
F'1	-2.944	0.005	0.016	-3.586	0.001	0.005
F'2	-3.155	0.003	0.010	-0.647	0.324	0.398
F'13	-1.677	0.098	0.153	4.974	<.001	<.001
I'1	-2.562	0.015	0.033	-0.230	0.389	0.398
I'6	0.097	0.397	0.397	1.987	0.055	0.178
R'2	-1.677	0.098	0.153	4.775	<.001	<.001
R'3	-4.317	<.001	<.001	1.352	0.160	0.305
R'4	-2.922	0.006	0.016	0.523	0.348	0.398
R'6	-5.177	<.001	<.001	-0.982	0.246	0.376
R'7	-4.155	<.001	<.001	1.633	0.105	0.215
R'9	-4.779	<.001	<.001	0.375	0.372	0.398
S'5	-2.979	0.005	0.015	2.620	0.013	0.071
S'6	-4.431	<.001	<.001	-0.803	0.289	0.398
S'7	-3.103	0.003	0.011	-1.644	0.103	0.215
S'8	-2.837	0.007	0.019	2.584	0.014	0.072
S'9	-5.050	<.001	<.001	7.396	<.001	<.001
Z'1	-4.179	<.001	<.001	1.108	0.216	0.367
Z'2	-0.495	0.353	0.397	-2.318	0.027	0.104
Z'3	-0.238	0.388	0.397	-1.714	0.092	0.215
Z'4	-1.899	0.066	0.111	-0.844	0.279	0.396
Z'5	-1.949	0.060	0.104	-2.467	0.019	0.083
Z'10	-3.990	<.001	0.001	2.539	0.016	0.075
Z'11	-2.472	0.019	0.038	3.248	0.002	0.012
Z'12	-2.322	0.027	0.051	3.373	0.001	0.009
Z'13	0.166	0.393	0.397	1.716	0.092	0.215
Z'16	-1.168	0.202	0.273	2.380	0.023	0.095

Patient 5 - comparison between Task and Baseline						
	z-score	p-value	adjusted p-value	z-score	p-value	adjusted p-value
	β			High- γ		
Y1	3.041	0.004	0.127	-1.750	0.086	0.188
Y12	-1.431	0.143	0.399	-0.510	0.350	0.385
Y13	-2.237	0.033	0.305	1.962	0.058	0.188
Y14	0.739	0.304	0.399	3.568	0.001	0.012
Y15	-0.202	0.391	0.399	1.777	0.082	0.188
T1	-1.119	0.213	0.399	-1.831	0.075	0.188
Q1	1.615	0.108	0.395	-1.935	0.061	0.188
Q2	0.038	0.399	0.399	-1.858	0.071	0.188
Q14	-1.000	0.242	0.399	-1.711	0.092	0.194
Q15	-1.775	0.083	0.358	-4.084	<.001	0.003
X2	0.703	0.312	0.399	1.006	0.241	0.348
X3	-0.854	0.277	0.399	-2.137	0.041	0.165
X4	-0.908	0.264	0.399	-1.763	0.084	0.188
X5	0.555	0.342	0.399	-2.320	0.027	0.117
X8	0.286	0.383	0.399	-1.276	0.177	0.287
U3	0.847	0.279	0.399	-0.978	0.247	0.349
U5	1.253	0.182	0.399	0.542	0.345	0.385

U8	3.461	0.001	0.065	0.511	0.350	0.385
A1	-0.425	0.364	0.399	-0.272	0.385	0.385
A2	0.160	0.394	0.399	-1.918	0.063	0.188
A3	0.246	0.387	0.399	0.268	0.385	0.385
A4	0.047	0.398	0.399	-0.356	0.375	0.385
A10	1.190	0.197	0.399	2.001	0.054	0.188
A11	-0.034	0.399	0.399	0.287	0.383	0.385
A12	1.208	0.192	0.399	-2.604	0.013	0.080
A13	1.656	0.101	0.395	-1.774	0.083	0.188
M1	-0.534	0.346	0.399	1.390	0.152	0.259
M10	1.939	0.061	0.305	6.008	<.001	<.001
M11	2.420	0.021	0.278	2.481	0.018	0.092
M12	0.643	0.324	0.399	-0.318	0.379	0.385
M13	-2.516	0.017	0.274	1.747	0.087	0.188
M14	-2.124	0.042	0.305	-0.376	0.372	0.385
N2	0.836	0.281	0.399	-0.941	0.256	0.354
N3	-2.106	0.043	0.305	0.331	0.378	0.385
N11	1.173	0.201	0.399	2.926	0.006	0.045
N12	-1.861	0.071	0.328	-1.117	0.214	0.331
N13	0.015	0.399	0.399	-1.478	0.134	0.245
R2	0.160	0.394	0.399	3.411	0.001	0.015
R3	-0.468	0.357	0.399	-0.694	0.314	0.385
R4	-1.608	0.110	0.395	-2.099	0.044	0.169
R8	-0.163	0.394	0.399	-3.556	0.001	0.012
S4	-0.535	0.346	0.399	-0.817	0.286	0.379
S7	0.258	0.386	0.399	-1.467	0.136	0.245
S8	-1.326	0.166	0.399	-1.750	0.086	0.188
S9	-1.958	0.059	0.305	-2.938	0.005	0.045
W1	2.894	0.006	0.131	-1.373	0.155	0.259
W2	2.068	0.047	0.305	-1.622	0.107	0.211
W4	0.235	0.388	0.399	-0.288	0.383	0.385
W5	-0.620	0.329	0.399	-0.347	0.376	0.385
W6	-0.113	0.396	0.399	-2.696	0.011	0.073
W7	-0.964	0.251	0.399	-1.630	0.106	0.211
W8	0.815	0.286	0.399	-1.246	0.183	0.291
W9	1.967	0.058	0.305	-0.487	0.354	0.385
W10	1.305	0.170	0.399	-0.379	0.371	0.385
IN1	-1.138	0.209	0.399	-1.074	0.224	0.339
IN2	-0.328	0.378	0.399	-1.430	0.143	0.252
IN4	-1.970	0.057	0.305	-3.088	0.003	0.037
IN5	-1.338	0.163	0.399	-2.550	0.015	0.084
IN6	-1.537	0.122	0.399	-2.401	0.022	0.104
IN7	0.521	0.348	0.399	-1.005	0.241	0.348
IN8	-0.812	0.287	0.399	-1.523	0.125	0.239
IN9	-0.261	0.386	0.399	-1.917	0.064	0.188
IN10	-0.601	0.333	0.399	-0.484	0.355	0.385
IN11	-1.119	0.213	0.399	-0.827	0.283	0.379

Patient 6 - comparison between Task and Baseline						
	z-score	p-value	adjusted p-value	z-score	p-value	adjusted p-value
	β			High- γ		
Y2	-3.184	0.003	0.006	-0.390	0.370	0.399
Y3	-2.619	0.013	0.027	-0.690	0.314	0.399
Y4	-2.525	0.016	0.033	-1.024	0.236	0.399
Y5	-2.106	0.043	0.071	-0.788	0.292	0.399
Y12	-3.707	<.001	0.001	-1.427	0.144	0.386
Y13	-3.088	0.003	0.008	-3.810	<.001	0.003

Y14	-4.123	<.001	<.001	-2.767	0.009	0.049
CZ	0.709	0.310	0.353	-1.454	0.139	0.386
F1	1.702	0.094	0.133	-2.543	0.016	0.078
F2	-0.679	0.317	0.355	-0.675	0.318	0.399
F3	-0.563	0.340	0.372	-4.051	<.001	0.001
P3	-0.152	0.394	0.398	-2.973	0.005	0.032
P4	-0.176	0.393	0.398	-2.370	0.024	0.111
P5	-2.704	0.010	0.023	-0.238	0.388	0.399
Y15	-4.750	<.001	<.001	1.085	0.221	0.399
Y16	-4.479	<.001	<.001	0.673	0.318	0.399
P16	2.093	0.045	0.072	0.014	0.399	0.399
T1	-2.434	0.021	0.037	-0.996	0.243	0.399
S3	-0.048	0.398	0.398	0.400	0.368	0.399
X1	-3.167	0.003	0.007	-1.658	0.101	0.354
X2	-2.918	0.006	0.013	0.680	0.317	0.399
X3	-0.934	0.258	0.307	0.236	0.388	0.399
X4	-2.155	0.039	0.069	-0.390	0.370	0.399
X5	0.992	0.244	0.296	-1.182	0.198	0.399
X6	1.326	0.166	0.211	-1.180	0.199	0.399
X7	0.921	0.261	0.307	-0.884	0.270	0.399
X8	0.844	0.279	0.323	-1.003	0.241	0.399
F5	1.677	0.098	0.137	-3.484	0.001	0.008
F6	-0.087	0.397	0.398	-1.913	0.064	0.237
F13	-5.682	<.001	<.001	2.891	0.006	0.038
F14	-4.861	<.001	<.001	1.123	0.212	0.399
B1	-2.489	0.018	0.033	-0.741	0.303	0.399
O2	-1.999	0.054	0.085	0.634	0.326	0.399
O3	-3.484	0.001	0.002	0.769	0.297	0.399
W1	1.291	0.173	0.217	-0.216	0.390	0.399
W11	-1.991	0.055	0.085	0.440	0.362	0.399
E1	-0.492	0.354	0.374	-0.993	0.244	0.399
E2	-5.388	<.001	<.001	-3.151	0.003	0.021
E3	-8.606	<.001	<.001	-1.422	0.145	0.386
E4	-5.890	<.001	<.001	1.418	0.146	0.386
E5	-5.508	<.001	<.001	-0.361	0.374	0.399
R3	-0.500	0.352	0.374	-0.900	0.266	0.399
R4	-1.777	0.082	0.122	-1.923	0.063	0.237
R7	-2.121	0.042	0.071	1.550	0.120	0.370
R8	-4.880	<.001	<.001	1.126	0.212	0.399
R9	-4.090	<.001	<.001	-0.527	0.347	0.399
E7	-4.334	<.001	<.001	4.471	<.001	<.001
E8	-3.704	<.001	0.001	2.257	0.031	0.136
E9	-5.437	<.001	<.001	0.639	0.325	0.399
E10	-5.057	<.001	<.001	0.010	0.399	0.399
O9	-9.826	<.001	<.001	8.042	<.001	<.001
O10	-11.225	<.001	<.001	5.129	<.001	<.001
O11	-10.633	<.001	<.001	3.738	<.001	0.003
O12	-8.390	<.001	<.001	0.843	0.280	0.399
O13	-7.185	<.001	<.001	1.200	0.194	0.399
B'2	-2.664	0.011	0.025	-0.779	0.295	0.399
B'14	-2.502	0.017	0.033	-0.782	0.294	0.399
Z'4	-2.138	0.041	0.070	-0.475	0.356	0.399
Z'5	-0.557	0.342	0.372	0.909	0.264	0.399
Z'6	-1.879	0.068	0.103	-0.114	0.396	0.399
E'1	1.640	0.104	0.139	0.247	0.387	0.399
E'2	-1.729	0.089	0.130	-0.567	0.340	0.399
E'3	-1.652	0.102	0.139	-2.682	0.011	0.058
E'4	-5.394	<.001	<.001	-2.159	0.039	0.159
E'5	-6.353	<.001	<.001	1.562	0.118	0.370

E'6	-7.228	<.001	<.001	-0.281	0.383	0.399
E'7	-5.877	<.001	<.001	0.551	0.343	0.399
E'8	-5.024	<.001	<.001	4.168	<.001	0.001
E'11	-2.506	0.017	0.033	-0.806	0.288	0.399
PZ	-1.632	0.105	0.139	-0.302	0.381	0.399
V2	0.997	0.243	0.296	-1.633	0.105	0.354
V10	-9.319	<.001	<.001	9.172	<.001	<.001
Z'10	-2.501	0.017	0.033	0.388	0.370	0.399

Comparison across conditions on responsive channels

Comparison across conditions on responsive channels							
Channel	z-score	p-value	adjusted p-value	Channel	z-score	p-value	adjusted p-value
	β				High- γ		
Patient 1							
O'1	0.352	0.375	0.399	R'2	-0.177	0.393	0.393
B'11	0.429	0.364	0.399	R'3	-0.239	0.388	0.393
C'1	0.722	0.307	0.399	K'9	-1.103	0.217	0.393
F'5	-0.224	0.389	0.399	P'1	0.166	0.393	0.393
C'14	1.086	0.221	0.399	P'2	0.267	0.385	0.393
R'1	1.084	0.222	0.399	P'11	-0.590	0.335	0.393
R'2	1.568	0.117	0.399	X'2	-0.737	0.304	0.393
R'3	2.561	0.015	0.245	X'4	-2.197	0.036	0.321
R'6	0.505	0.351	0.399	X'8	-0.869	0.273	0.393
R'7	0.889	0.269	0.399				
R'8	1.425	0.145	0.399				
R'9	1.728	0.090	0.399				
U'1	0.322	0.379	0.399				
U'2	0.244	0.387	0.399				
U'4	-0.517	0.349	0.399				
Y'1	0.738	0.304	0.399				
Y'18	3.510	0.001	0.045				
T'3	1.421	0.145	0.399				
E'1	-1.346	0.161	0.399				
E'2	-0.410	0.367	0.399				
E'3	0.294	0.382	0.399				
E'4	0.025	0.399	0.399				
E'5	-1.663	0.100	0.399				
E'6	-0.869	0.274	0.399				
E'10	1.261	0.180	0.399				
E'12	0.954	0.253	0.399				
E'13	0.248	0.387	0.399				
E'14	0.539	0.345	0.399				
K'9	0.778	0.295	0.399				

K'10	0.004	0.399	0.399				
K'12	0.472	0.357	0.399				
K'13	0.307	0.381	0.399				
K'14	0.472	0.357	0.399				
K'15	1.079	0.223	0.399				
K'16	1.155	0.205	0.399				
K'17	1.605	0.110	0.399				
D'1	1.107	0.216	0.399				
N'1	0.114	0.396	0.399				
N'2	1.117	0.214	0.399				
N'3	1.383	0.153	0.399				
W'2	0.189	0.392	0.399				
P'1	1.528	0.124	0.399				
P'2	1.688	0.096	0.399				
P'8	-0.889	0.269	0.399				
P'10	0.724	0.307	0.399				
P'12	1.699	0.094	0.399				
P'13	2.182	0.037	0.332				
X'4	-0.755	0.300	0.399				
S'2	1.355	0.159	0.399				
S'3	2.486	0.018	0.245				
S'4	2.542	0.016	0.245				
S'5	2.378	0.024	0.255				
W'6	0.155	0.394	0.399				
W'10	0.258	0.386	0.399				

Patient 2

M5	1.363	0.157	0.397	M6	-1.524	0.125	0.399
F5	-0.118	0.396	0.397	E1	1.543	0.121	0.399
H10	0.106	0.397	0.397	J12	-0.315	0.380	0.399
H12	0.578	0.338	0.397	D11	0.817	0.286	0.399
H14	1.101	0.218	0.397	F5	1.244	0.184	0.399
K1	0.766	0.297	0.397	F10	-0.556	0.342	0.399
K2	-0.103	0.397	0.397	H2	-0.772	0.296	0.399
K4	0.955	0.253	0.397	H12	-0.656	0.322	0.399
K5	-0.410	0.367	0.397	N7	0.007	0.399	0.399
X15	1.219	0.190	0.397	K2	0.721	0.308	0.399
Y12	0.113	0.396	0.397	P3	-1.132	0.210	0.399
M5	1.363	0.157	0.397	P8	0.047	0.399	0.399
F5	-0.118	0.396	0.397	P15	-1.015	0.238	0.399
				S9	-0.019	0.399	0.399
				S10	0.595	0.334	0.399
				R9	-0.014	0.399	0.399
				M6	-1.524	0.125	0.399

				E1	1.543	0.121	0.399
Patient 3							
T3	0.582	0.337	0.389	V8	-0.149	0.395	0.395
V8	0.248	0.387	0.389	V9	0.278	0.384	0.395
V9	-1.781	0.082	0.389	V11	0.877	0.272	0.395
V10	-1.355	0.159	0.389	F12	0.307	0.381	0.395
V11	-1.465	0.136	0.389	Z8	-1.088	0.221	0.395
V12	-0.850	0.278	0.389	Z10	0.337	0.377	0.395
V13	-1.443	0.141	0.389	P8	0.706	0.311	0.395
U4	0.457	0.359	0.389				
E4	-2.444	0.020	0.282				
F5	-0.795	0.291	0.389				
B5	0.604	0.333	0.389				
Z1	-0.225	0.389	0.389				
Z8	0.598	0.334	0.389				
Z10	0.774	0.296	0.389				
Patient 4							
Y'1	1.211	0.192	0.399	E'2	-0.851	0.278	0.388
B'1	0.055	0.398	0.399	E'3	-2.401	0.022	0.112
B'2	0.083	0.398	0.399	E'7	-3.183	0.003	0.025
B'3	-0.012	0.399	0.399	E'8	-0.239	0.388	0.388
C'2	1.801	0.079	0.399	F'1	0.268	0.385	0.388
C'3	1.588	0.113	0.399	F'13	-0.243	0.387	0.388
D'2	1.731	0.089	0.399	R'2	-0.792	0.292	0.388
D'3	1.680	0.097	0.399	S'9	1.177	0.200	0.388
E'1	-0.766	0.298	0.399	Z'11	-1.154	0.205	0.388
E'2	0.733	0.305	0.399	Z'12	0.525	0.348	0.388
E'3	0.606	0.332	0.399				
E'7	-1.009	0.240	0.399				
E'10	-0.976	0.248	0.399				
E'11	-0.835	0.281	0.399				
E'12	0.017	0.399	0.399				
F'1	0.755	0.300	0.399				
F'2	-0.224	0.389	0.399				
I'1	0.135	0.395	0.399				
R'3	0.015	0.399	0.399				
R'4	0.596	0.334	0.399				
R'6	-1.020	0.237	0.399				
R'7	-0.661	0.321	0.399				
R'9	-0.509	0.350	0.399				
S'5	0.396	0.369	0.399				
S'6	-0.913	0.263	0.399				
S'7	0.769	0.297	0.399				

S'8	-1.066	0.226	0.399				
S'9	-0.203	0.391	0.399				
Z'1	0.015	0.399	0.399				
Z'10	0.715	0.309	0.399				
Z'11	1.934	0.062	0.399				
Patient 5							
				Y14	0.903	0.265	0.395
				Q15	1.986	0.056	0.395
				M10	0.135	0.395	0.395
				N11	0.818	0.285	0.395
				R2	-1.087	0.221	0.395
				R8	-1.043	0.232	0.395
				S9	-0.489	0.354	0.395
				IN4	0.450	0.361	0.395
Patient 6							
Y2	-1.215	0.191	0.398	Y13	-0.931	0.259	0.384
Y3	-0.773	0.296	0.398	Y14	-0.509	0.350	0.384
Y4	-1.213	0.191	0.398	F3	0.597	0.334	0.384
Y12	1.102	0.217	0.398	P3	-2.742	0.009	0.121
Y13	0.211	0.390	0.398	F5	-0.958	0.252	0.384
Y14	-0.784	0.293	0.398	F13	-1.446	0.140	0.384
P5	-0.166	0.393	0.398	E2	-2.143	0.040	0.261
Y15	-0.596	0.334	0.398	E7	-0.709	0.310	0.384
Y16	-0.430	0.364	0.398	O9	-1.174	0.200	0.384
T1	2.248	0.032	0.398	O10	0.960	0.252	0.384
X1	-1.291	0.173	0.398	O11	0.325	0.378	0.384
X2	-0.528	0.347	0.398	E'8	0.509	0.351	0.384
F13	-0.219	0.389	0.398	V10	-0.276	0.384	0.384
F14	0.785	0.293	0.398				
B1	-1.404	0.149	0.398				
O3	-0.251	0.387	0.398				
E2	0.078	0.398	0.398				
E3	-0.860	0.276	0.398				
E4	0.217	0.390	0.398				
E5	1.311	0.169	0.398				
R8	1.588	0.113	0.398				
R9	1.786	0.081	0.398				
E7	0.777	0.295	0.398				
E8	1.238	0.185	0.398				
E9	0.713	0.309	0.398				
E10	0.317	0.379	0.398				
O9	-0.573	0.338	0.398				
O10	0.442	0.362	0.398				

O11	-0.626	0.328	0.398				
O12	-0.848	0.278	0.398				
O13	0.453	0.360	0.398				
B'2	-1.429	0.144	0.398				
B'14	-1.528	0.124	0.398				
E'4	0.286	0.383	0.398				
E'5	0.091	0.397	0.398				
E'6	0.544	0.344	0.398				
E'7	1.547	0.121	0.398				
E'8	2.439	0.020	0.398				
E'11	-1.509	0.128	0.398				
V10	-1.711	0.092	0.398				
Z'10	-0.186	0.392	0.398				

Comparisons across conditions on channels located in the ROIs

Comparisons across conditions on channels located in the ROIs						
Channel	z-score	p-value	adjusted p-value	z-score	p-value	adjusted p-value
	β			High- γ		
Patient 1						
S'4	2.466	0.019	0.046	-1.777	0.082	0.278
S'3	2.426	0.021	0.046	0.348	0.376	0.376
R'7	0.931	0.259	0.259	-1.708	0.093	0.278
R'8	1.438	0.142	0.170	-1.036	0.233	0.350
R'9	1.795	0.080	0.120	-0.493	0.353	0.376
S'5	2.389	0.023	0.046	-1.402	0.149	0.299
Patient 2						
N1	-0.617	0.330	0.399	0.386	0.370	0.399
N2	-0.494	0.353	0.399	0.238	0.388	0.399
P3	-0.947	0.255	0.399	-1.091	0.220	0.399
N8	-0.238	0.388	0.399	0.902	0.265	0.399
N9	-1.023	0.236	0.399	0.917	0.262	0.399
P8	-0.212	0.390	0.399	0.033	0.399	0.399
P9	0.230	0.389	0.399	-1.495	0.131	0.399
S10	-0.295	0.382	0.399	0.626	0.328	0.399
S5	0.801	0.289	0.399	0.380	0.371	0.399
S6	-0.026	0.399	0.399	0.067	0.398	0.399
S7	0.022	0.399	0.399	-1.104	0.217	0.399
S8	-0.182	0.392	0.399	-1.127	0.211	0.399
S9	-0.267	0.385	0.399	-0.057	0.398	0.399
H10	0.114	0.396	0.399	0.401	0.368	0.399
H12	0.535	0.346	0.399	-0.624	0.328	0.399
H14	1.055	0.229	0.399	-1.091	0.220	0.399
M1	-1.762	0.084	0.399	-1.746	0.087	0.399
M4	1.272	0.178	0.399	0.090	0.397	0.399
M5	1.391	0.152	0.399	-1.818	0.076	0.399
M6	2.292	0.029	0.399	-1.489	0.132	0.399
M8	1.676	0.098	0.399	-0.223	0.389	0.399
R3	-0.033	0.399	0.399	-0.479	0.356	0.399
R10	0.412	0.367	0.399	0.009	0.399	0.399
Patient 4						
R'6	-0.973	0.248	0.352	0.340	0.377	0.377
R'7	-0.720	0.308	0.352	1.822	0.076	0.303
R'9	-0.501	0.352	0.352	1.254	0.182	0.363
Patient 5						
N13	-0.063	0.398	0.398	0.751	0.301	0.354
S7	0.591	0.335	0.398	1.052	0.229	0.354

S9	0.503	0.351	0.398	-0.391	0.370	0.370
S8	0.870	0.273	0.398	-2.181	0.037	0.354
S4	-0.891	0.268	0.398	0.672	0.318	0.354
N12	-0.729	0.306	0.398	1.268	0.178	0.354
M13	0.566	0.340	0.398	0.854	0.277	0.354
S3	-1.866	0.070	0.398	0.801	0.289	0.354
N11	-1.399	0.150	0.398	0.942	0.256	0.354
M14	-0.215	0.390	0.398	0.691	0.314	0.354

References

- Abdulkarim, Z., & Ehrsson, H. H. (2018). Recalibration of hand position sense during unconscious active and passive movement. *Experimental Brain Research*, 236(2), 551–561. <https://doi.org/10.1007/s00221-017-5137-7>
- Abràmoff, M. D., Magalhães, P. J., & Ram, S. J. (2004). Image processing with imageJ. *Biophotonics International*, 11(7), 36–41. <https://doi.org/10.1117/1.3589100>
- Apps, M. A. J., & Tsakiris, M. (2014). The free-energy self: A predictive coding account of self-recognition. *Neuroscience and Biobehavioral Reviews*, 41, 85–97. <https://doi.org/10.1016/j.neubiorev.2013.01.029>
- Barut, C., Sevinc, O., & Sumbuloglu, V. (2011). Evaluation of hand asymmetry in relation to hand preference. *Collegium Antropologicum*, 35(4), 1119–1124. Retrieved from <http://www.ncbi.nlm.nih.gov/pubmed/22397247>
- Basso, A., Capitani, E., & Laiacona, M. (1987). Raven's coloured progressive matrices: normative values on 305 adult normal controls. *Functional Neurology*, 11(2).
- Bedell, H. E., & Johnson, C. A. (1984). The perceived size of targets in the peripheral and central visual fields. *Ophthalmic and Physiological Optics*, 4(2), 123–131.
- Bookstein, F. L. (1997). *Morphometric tools for landmark data : geometry and biology*. Cambridge University Press.
- Botvinick, M., & Cohen, J. (1998). Rubber hands “feel” touch that eyes see. *Nature*, 391(6669), 756. <https://doi.org/10.1038/35784>
- Brownell, C. A., Nichols, S. R., Svetlova, M., Zerwas, S., & Ramani, G. (2010). The head bone's connected to the neck bone: When do toddlers represent their own body topography? *Child Development*, 81(3), 797–810. <https://doi.org/10.1111/j.1467-8624.2010.01434.x>
- Brownell, C. A., Zerwas, S., & Ramani, G. B. (2007). “So Big”: The Development of Body Self-Awareness in Toddlers. *Child Development*, 78(5), 1426–1440. <https://doi.org/10.1111/j.1467-8624.2007.01075.x>
- Cardinale, F., Cossu, M., Castana, L., Casaceli, G., Schiariti, M. P., Miserocchi, A., ... Lo Russo, G. (2013). Stereoelectroencephalography. *Neurosurgery*, 72(3), 353–366. <https://doi.org/10.1227/NEU.0b013e31827d1161>
- Cardinali, L., Brozzoli, C., & Farnè, A. (2009). Peripersonal space and body schema: Two labels for the same concept? *Brain Topography*, 21(3–4), 252–260. <https://doi.org/10.1007/s10548-009-0092-7>
- Chen, C. C., Essick, G. K., Kelly, D. G., Young, M. G., Nestor, J. M., & Masse, B. (1995). Gender-, side- and site-dependent variations in human perioral spatial resolution. *Archives of Oral Biology*, 40(6), 539–548. [https://doi.org/10.1016/0003-9969\(94\)00202-M](https://doi.org/10.1016/0003-9969(94)00202-M)
- Cocchini, G., Galligan, T., Mora, L., & Kuhn, G. (2018). The magic hand: Plasticity of mental hand representation. *Quarterly Journal of Experimental Psychology*, 71(11), 2314–2324. <https://doi.org/10.1177/1747021817741606>
- Cody, F. W. J., Garside, R. A. D., Lloyd, D., & Poliakoff, E. (2008). Tactile spatial acuity varies with site and axis in the human upper limb. *Neuroscience Letters*, 433(2), 103–108. <https://doi.org/10.1016/j.neulet.2007.12.054>
- Coelho, L. A., & Gonzalez, C. L. (2018). The visual and haptic contributions to hand perception. *Psychological Research*, 82(5), 866–875. <https://doi.org/10.1007/s00426-017-0870-x>
- Coelho, L. A., Schacher, J. P., Scammel, C., Doan, J. B., & Gonzalez, C. L. R. (2019). Long- but not short-term tool-use changes hand representation. *Experimental Brain Research*, 237(1), 137–146. <https://doi.org/10.1007/s00221-018-5408-y>
- Corradi-Dell'Acqua, C., Tomasino, B., & Fink, G. R. (2009). What is the position of an arm relative to the body? Neural correlates of body schema and body structural description. *J Neurosci*, 29(13), 4162–4171. <https://doi.org/10.1523/JNEUROSCI.4861-08.2009>

- Cossu, M., Cardinale, F., Castana, L., Citterio, A., Francione, S., Tassi, L., ... Lo Russo, G. (2005). Stereoelectroencephalography in the Presurgical Evaluation of Focal Epilepsy: A Retrospective Analysis of 215 Procedures. *Neurosurgery*, 57(4), 706–718. <https://doi.org/10.1093/neurosurgery/57.4.706>
- Costas, P. D., Heatley, G., & Seckel, B. R. (1994). Normal sensation of the human face and neck. *Plastic and Reconstructive Surgery*, 93(6), 1141–1145.
- Crone, N. (1998). Functional mapping of human sensorimotor cortex with electrocorticographic spectral analysis. I. Alpha and beta event-related desynchronization. *Brain*, 121(12), 2271–2299. <https://doi.org/10.1093/brain/121.12.2271>
- Dale, A. M., Fischl, B., & Sereno, M. I. (1999). Cortical Surface-Based Analysis: I. Segmentation and Surface Reconstruction. *NeuroImage*, 9(2), 179–194. <https://doi.org/10.1006/NIMG.1998.0395>
- de Vignemont, F. (2010). Body schema and body image-Pros and cons. *Neuropsychologia*, 48(3), 669–680. <https://doi.org/10.1016/j.neuropsychologia.2009.09.022>
- Desmurget, M., & Grafton, S. (2000). Forward modeling allows feedback control for fast reaching movements. *Trends in Cognitive Sciences*, 4(11), 423–431. [https://doi.org/S1364-6613\(00\)01537-0](https://doi.org/S1364-6613(00)01537-0) [pii]
- Dijkerman, H. C., & de Haan, E. H. F. (2007). Somatosensory processing subserving perception and action: Dissociations, interactions, and integration. *Behavioral and Brain Sciences*, 30(02), 224. <https://doi.org/10.1017/S0140525X07001641>
- Friston, K. J., Jezzard, P., & Turner, R. (1994). Analysis of functional MRI time-series. *Human Brain Mapping*, 1(2), 153–171. <https://doi.org/10.1002/hbm.460010207>
- Ganea, N., & Longo, M. R. (2017). Projecting the self outside the body: Body representations underlying proprioceptive imagery. *Cognition*, 162, 41–47. <https://doi.org/10.1016/J.COGNITION.2017.01.021>
- Ganel, T., & Goodale, M. A. (2003). Visual control of action but not perception requires analytical processing of object shape. *Nature*, 426(6967), 664.
- Ganel, T., Chajut, E., & Algom, D. (2008). Visual coding for action violates fundamental psychophysical principles. *Current Biology*, 18(14), R599–R601.
- Gentilucci, M., Benuzzi, F., Gangitano, M., & Grimaldi, S. (2001). Grasp With Hand and Mouth: A Kinematic Study on Healthy Subjects. *Journal of Neurophysiology*, 86(4), 1685–1699. <https://doi.org/10.1152/jn.2001.86.4.1685>
- Gentilucci, M., & Campione, G. C. (2011). Do Postures of Distal Effectors Affect the Control of Actions of Other Distal Effectors? Evidence for a System of Interactions between Hand and Mouth. *PLoS ONE*, 6(5), e19793. <https://doi.org/10.1371/journal.pone.0019793>
- Gibson, J. J. (1979). *The ecological approach to visual perception*. Boston, MA, US.
- Goodall, C. (1991). *Procrustes Methods in the Statistical Analysis of Shape*. Source: *Journal of the Royal Statistical Society. Series B (Methodological)* (Vol. 53). Retrieved from <https://www.jstor.org/stable/pdf/2345744.pdf?refreqid=excelsior%3Ab258dd9131eaa821be58292fda87cc59>
- Gray, R. (2013). Being selective at the plate: Processing dependence between perceptual variables relates to hitting goals and performance. *Journal of Experimental Psychology: Human Perception and Performance*, 39(4), 1124–1142. <https://doi.org/10.1037/a0030729>
- Hardwick, R. M., Caspers, S., Eickhoff, S. B., & Swinnen, S. P. (2018). Neural correlates of action: Comparing meta-analyses of imagery, observation, and execution. *Neuroscience & Biobehavioral Reviews*, 94, 31–44. <https://doi.org/10.1016/J.NEUBIOREV.2018.08.003>
- Ishai, A., Ungerleider, L. G., & Haxby, J. V. (2000). for the Generation of Visual Images. *Neuron*, 28, 979–990.
- JASP. (2018). JASP Team.
- Jeannerod, M. (2001). Neural Simulation of Action: A Unifying Mechanism for Motor Cognition. *NeuroImage*, 14(1), S103–S109. <https://doi.org/10.1006/NIMG.2001.0832>
-

- Karniel, A. (2011). Open Questions In Computational Motor Control. *Journal of Integrative Neuroscience*, 10(03), 385–411. <https://doi.org/10.1142/S0219635211002749>
- Kikinis, R., Pieper, S. D., & Vosburgh, K. G. (2014). 3D Slicer: A Platform for Subject-Specific Image Analysis, Visualization, and Clinical Support. In *Intraoperative Imaging and Image-Guided Therapy* (pp. 277–289). New York, NY: Springer New York. https://doi.org/10.1007/978-1-4614-7657-3_19
- Klingenberg, C. P. (2011). MORPHOJ: an integrated software package for geometric morphometrics. <https://doi.org/10.1111/j.1755-0998.2010.02924.x>
- Kriegeskorte, N., Simmons, W. K., Bellgowan, P. S. F., & Baker, C. I. (2010). Circular Analysis in Neuroscience Double Dipping. *NeuroImage*, 52(2), 535–540. <https://doi.org/10.1038/nm.2303.Circular>
- Kuling, I. A., Brenner, E., & Smeets, J. B. J. (2013). Proprioception Is Robust under External Forces. *PLoS ONE*, 8(9), e74236. <https://doi.org/10.1371/journal.pone.0074236>
- Kuling, I. A., van der Graaff, M. C. W., Brenner, E., & Smeets, J. B. J. (2017). Matching locations is not just matching sensory representations. *Experimental Brain Research*, 235(2), 533–545. <https://doi.org/10.1007/s00221-016-4815-1>
- Lange, F. P. de, Hagoort, P., & Toni, I. (2005). Neural Topography and Content of Movement Representations. *Journal of Cognitive Neuroscience*, 17(1), 97–112. <https://doi.org/10.1162/0898929052880039>
- Lass, N. J., Kotchek, C. L., & Deem, J. F. (1972). Oral Two-Point Discrimination: Further Evidence of Asymmetry on Right and Left Sides of Selected Oral Structures. *Perceptual and Motor Skills*, 35(1), 59–67. <https://doi.org/10.2466/pms.1972.35.1.59>
- Linkenauger, S. A., Geuss, M. N., Stefanucci, J. K., Leyrer, M., Richardson, B. H., Proffitt, D. R., ... Mohler, B. J. (2014). Evidence for Hand-Size Constancy. *Psychological Science*, 25(11), 2086–2094. <https://doi.org/10.1177/0956797614548875>
- Linkenauger, S. A., Witt, J. K., & Proffitt, D. R. (2011). Taking a hands-on approach: Apparent grasping ability scales the perception of object size. *Journal of Experimental Psychology: Human Perception and Performance*, 37(5), 1432–1441. <https://doi.org/10.1037/a0024248>
- Linkenauger, S. A., Wong, H. Y., Geuss, M., Stefanucci, J. K., McCulloch, K. C., Bühlhoff, H. H., ... Proffitt, D. R. (2015). The perceptual homunculus: The perception of the relative proportions of the human body. *Journal of Experimental Psychology: General*, 144(1), 103–113. <https://doi.org/10.1037/xge0000028>
- Longo, M. R. (2014). The effects of immediate vision on implicit hand maps. *Experimental Brain Research*, 232(4), 1241–1247. <https://doi.org/10.1007/s00221-014-3840-1>
- Longo, M. R. (2015a). Implicit and explicit body representations. *European Psychologist*, 20(1), 6–15. <https://doi.org/10.1027/1016-9040/a000198>
- Longo, M. R. (2015b). Intuitive anatomy: Distortions of conceptual knowledge of hand structure. *Cognition*, 142, 230–235. <https://doi.org/10.1016/j.cognition.2015.05.024>
- Longo, M. R. (2015c). Posture modulates implicit hand maps. *Consciousness and Cognition*, 36, 96–102. <https://doi.org/10.1016/J.CONCOG.2015.06.009>
- Longo, M. R., & Haggard, P. (2010). An implicit body representation underlying human position sense. *Proceedings of the National Academy of Sciences of the United States of America*, 107(26), 11727–11732. <https://doi.org/10.1073/pnas.1003483107>
- Longo, M. R., & Haggard, P. (2011). Weber's illusion and body shape: Anisotropy of tactile size perception on the hand. *Journal of Experimental Psychology: Human Perception and Performance*, 37(3), 720–726. <https://doi.org/10.1037/a0021921>
- Longo, M. R., & Haggard, P. (2012a). A 2.5-D representation of the human hand. *Journal of Experimental Psychology: Human Perception and Performance*, 38(1), 9–13. <https://doi.org/10.1037/a0025428>
- Longo, M. R., & Haggard, P. (2012b). Implicit body representations and the conscious body image. *Acta Psychologica*, 141(2), 164–168. <https://doi.org/10.1016/j.actpsy.2012.07.015>

- Longo, M. R., Mattioni, S., & Ganea, N. (2015). Perceptual and Conceptual Distortions of Implicit Hand Maps. *Frontiers in Human Neuroscience*, 9, 656. <https://doi.org/10.3389/fnhum.2015.00656>
- Longo, M. R., Schüür, F., Kammers, M. P., Tsakiris, M., & Haggard, P. (2008). What is embodiment? A psychometric approach. *Cognition*, 107(3), 978–998.
- Lunghi, C., Lo Verde, L., & Alais, D. (2017). Touch Accelerates Visual Awareness. *I-Perception*, 8(1), 204166951668698. <https://doi.org/10.1177/2041669516686986>
- Mancini, F., Bauleo, A., Cole, J., Lui, F., Porro, C. A., Haggard, P., & Iannetti, G. D. (2014). Whole-body mapping of spatial acuity for pain and touch. *Annals of Neurology*, 75(6), 917–924. <https://doi.org/10.1002/ana.24179>
- Marotta, A., Tinazzi, M., Cavedini, C., Zampini, M., & Fiorio, M. (2016). Individual Differences in the Rubber Hand Illusion Are Related to Sensory Suggestibility. *PLOS ONE*, 11(12), e0168489. <https://doi.org/10.1371/journal.pone.0168489>
- Mattioni, S., & Longo, M. R. (2014). The effects of verbal cueing on implicit hand maps. *Acta Psychologica*, 153, 60–65. <https://doi.org/10.1016/J.ACTPSY.2014.09.009>
- Mechelli, A., Price, C. J., Friston, K. J., & Ishai, A. (2004). Where bottom-up meets top-down: Neuronal interactions during perception and imagery. *Cerebral Cortex*, 14(11), 1256–1265. <https://doi.org/10.1093/cercor/bhh087>
- Medina, J., & Coslett, H. B. (2010). From maps to form to space: Touch and the body schema. *Neuropsychologia*, 48(3), 645–654. <https://doi.org/10.1016/j.neuropsychologia.2009.08.017>
- Medina, J., & Duckett, C. (2017). Domain-General Biases in Spatial Localisation: Evidence Against a Distorted Body Model Hypothesis. <https://doi.org/10.1037/xhp0000397>
- Miall, R. C., & Wolpert, D. M. (1996). Forward Models for Physiological Motor Control. *Neural Networks*, 9(8), 1265–1279. [https://doi.org/10.1016/S0893-6080\(96\)00035-4](https://doi.org/10.1016/S0893-6080(96)00035-4)
- Miller, K. J., Leuthardt, E. C., Schalk, G., Rao, R. P. N., Anderson, N. R., Moran, D. W., ... Ojemann, J. G. (2007). Spectral Changes in Cortical Surface Potentials during Motor Movement. *Journal of Neuroscience*, 27(9), 2424–2432. <https://doi.org/10.1523/jneurosci.3886-06.2007>
- Moutsiana, C., De Haas, B., Papageorgiou, A., Van Dijk, J. A., Balraj, A., Greenwood, J. A., & Schwarzkopf, D. S. (2016). Cortical idiosyncrasies predict the perception of object size. *Nature communications*, 7, 12110.
- Munari, C., Hoffmann, D., Fracione, S., Kahane, P., Tassi, L., Russo, G. Lo, & Benabid, A. L. (1994). Stereo-electroencephalography methodology: advantages and limits. *Acta Neurologica Scandinavica*, 89(S152), 56–67. <https://doi.org/10.1111/j.1600-0404.1994.tb05188.x>
- Narizzano, M., Arnulfo, G., Ricci, S., Toselli, B., Tisdall, M., Canessa, A., ... Cardinale, F. (2017). SEEG assistant: a 3DSlicer extension to support epilepsy surgery. *BMC Bioinformatics*, 18(1), 124. <https://doi.org/10.1186/s12859-017-1545-8>
- Neuper, C. C., & Pfurtscheller, G. G. (1997). Motor imagery activates primary sensorimotor area in humans. *Neuroscience Letters*, 239(2–3), 65–68.
- Nolan, M. F. (1985). Quantitative measure of cutaneous sensation. Two-point discrimination values for the face and trunk. *Physical Therapy*, 65(2), 181–185. <https://doi.org/10.1093/ptj/65.2.181>
- Ocklenburg, S., Rüter, N., Peterburs, J., Pinnow, M., & Güntürkün, O. (2011). Laterality in the rubber hand illusion. *Laterality: Asymmetries of Body, Brain and Cognition*, 16(2), 174–187. <https://doi.org/10.1080/13576500903483515>
- Oldfield, R. C. (1971). The assessment and analysis of handedness: The Edinburgh inventory. *Neuropsychologia*. [https://doi.org/10.1016/0028-3932\(71\)90067-4](https://doi.org/10.1016/0028-3932(71)90067-4)
- Oostenveld, R., Fries, P., Maris, E., & Schoffelen, J.-M. (2011). FieldTrip: Open Source Software for Advanced Analysis of MEG, EEG, and Invasive Electrophysiological Data. *Computational Intelligence and Neuroscience*, 2011, 1–9. <https://doi.org/10.1155/2011/156869>
- Paillard, J. (1999). *Motor Control, Today and Tomorrow*. Retrieved from
-

- http://www.nyu.edu/gsas/dept/philo/courses/mindsandmachines09/papers/Paillard_1999.pdf
- Parsons, L. M. (1987). Imagined spatial transformations of one's hands and feet. *Cognitive Psychology*, 19(2), 178–241. [https://doi.org/10.1016/0010-0285\(87\)90011-9](https://doi.org/10.1016/0010-0285(87)90011-9)
- Parsons, L. M. (1994). Temporal and kinematic properties of motor behavior reflected in mentally simulated action. *Journal of Experimental Psychology: Human Perception and Performance*, 20(4), 709–730. <https://doi.org/10.1037/0096-1523.20.4.709>
- Penfield, W., & Rasmussen, T. (1950). *The cerebral cortex of man; a clinical study of Localisation of function* (Macmillan). Oxford, England. Retrieved from <http://psycnet.apa.org/record/1951-01483-000>
- Peviani, V., & Bottini, G. (2018). The distorted hand metric representation serves both perception and action. *Journal of Cognitive Psychology*, 30(8), 880–893. <https://doi.org/10.1080/20445911.2018.1538154>
- Peviani, V., Magnani, F. G., Ciricugno, A., Vecchi, T., & Bottini, G. (2018). Rubber Hand Illusion survives Ventral Premotor area inhibition: A rTMS study. *Neuropsychologia*, 120, 18–24. <https://doi.org/10.1016/j.neuropsychologia.2018.09.017>
- Peviani, V., Melloni, L., & Bottini, G. (2019). Visual and somatosensory information contribute to distortions of the body model. *Scientific Reports*. DOI: 10.1038/s41598-019-49979-0
- Pfurtscheller, G. (2000). Chapter 26 Spatiotemporal ERD/ERS patterns during voluntary movement and motor imagery. *Supplements to Clinical Neurophysiology*, 53(C), 196–198. [https://doi.org/10.1016/S1567-424X\(09\)70157-6](https://doi.org/10.1016/S1567-424X(09)70157-6)
- Pfurtscheller, G., Graimann, B., Huggins, J. E., Levine, S. P., & Schuh, L. A. (2003). Spatiotemporal patterns of beta desynchronization and gamma synchronization in corticographic data during self-paced movement. *Clinical Neurophysiology*, 114(7), 1226–1236. [https://doi.org/10.1016/S1388-2457\(03\)00067-1](https://doi.org/10.1016/S1388-2457(03)00067-1)
- Pinheiro, J., Bates, D., DebRoy, S., Sarkar, D., & Team, R. C. (2012). nlme: Linear and nonlinear mixed effects models. R package version, 3(0).
- Prins, N., & Kingdom, F. A. A. (2018). Applying the Model-Comparison Approach to Test Specific Research Hypotheses in Psychophysical Research Using the Palamedes Toolbox. *Frontiers in Psychology*, 9, 1250. <https://doi.org/10.3389/fpsyg.2018.01250>
- R Development Core Team. (2008). R: A language and environment for statistical computing. Vienna, Austria: R Foundation for Statistical Computing. Retrieved from <http://www.r-project.org>.
- Rath, E. M., & Essick, G. K. (1990). Perioral somesthetic sensibility: do the skin of the lower face and the midface exhibit comparable sensitivity? *Journal of Oral and Maxillofacial Surgery : Official Journal of the American Association of Oral and Maxillofacial Surgeons*, 48(11), 1181–1190. [https://doi.org/10.1016/0278-2391\(90\)90534-9](https://doi.org/10.1016/0278-2391(90)90534-9)
- Ray, S., & Maunsell, J. H. R. (2011). Different Origins of Gamma Rhythm and High-Gamma Activity in Macaque Visual Cortex. *PLoS Biology*, 9(4), e1000610. <https://doi.org/10.1371/journal.pbio.1000610>
- Riemer, M., Bublatzky, F., Trojan, J., & Alpers, G. W. (2015). Defensive activation during the rubber hand illusion: Ownership versus proprioceptive drift. *Biological Psychology*, 109, 86–92. <https://doi.org/10.1016/J.BIOPSYCHO.2015.04.011>
- Rohde, M., Di Luca, M., & Ernst, M. O. (2011). The Rubber Hand Illusion: Feeling of Ownership and Proprioceptive Drift Do Not Go Hand in Hand. *PLoS ONE*, 6(6), e21659. <https://doi.org/10.1371/journal.pone.0021659>
- Rouder, J. N., Speckman, P. L., Sun, D., Morey, R. D., & Iverson, G. (2009). Bayesian t tests for accepting and rejecting the null hypothesis. *Psychonomic Bulletin & Review*, 16(2), 225–237. <https://doi.org/10.3758/PBR.16.2.225>
- Rumiati, R. I., Tomasino, B., Vorano, L., Umiltà, C., & De Luca, G. (n.d.). *SELECTIVE DEFICIT OF IMAGINING FINGER CONFIGURATIONS*. Retrieved from <http://wexler.free.fr/library/files/rumiati> (2001) selective deficit of imagining finger configurations.pdf
-

- Sadibolova, R., Ferrè, E. R., Linkenauger, S. A., & Longo, M. R. (2019). Distortions of perceived volume and length of body parts. *Cortex*, 111, 74–86. <https://doi.org/10.1016/J.CORTEX.2018.10.016>
- Sakreida, K., Effnert, I., Thill, S., Menz, M. M., Jirak, D., Eickhoff, C. R., ... & Binkofski, F. (2016). Affordance processing in segregated parieto-frontal dorsal stream sub-pathways. *Neuroscience & Biobehavioral Reviews*, 69, 89–112.
- Saulton, A., Bühlhoff, H. H., & de la Rosa, S. (2017). Conceptual biases explain distortion differences between hand and objects in Localisation Tasks. *Journal of Experimental Psychology: Human Perception and Performance*, 43(7), 1444–1453. <https://doi.org/10.1037/xhp0000396>
- Saulton, A., Dodds, T. J., Bühlhoff, H. H., & de la Rosa, S. (2015). Objects exhibit body model like shape distortions. *Experimental Brain Research*, 233(5), 1471–1479. <https://doi.org/10.1007/s00221-015-4221-0>
- Saulton, A., Longo, M. R., Wong, H. Y., Bühlhoff, H. H., & de la Rosa, S. (2016). The role of visual similarity and memory in body model distortions. *Acta Psychologica*, 164, 103–111. <https://doi.org/10.1016/J.ACTPSY.2015.12.013>
- Schady, W. J. L., & Torebjörk, H. E. (1983). Projected and receptive fields: A comparison of projected areas of sensations evoked by intraneural stimulation of mechanoreceptive units, and their innervation territories. *Acta Physiologica Scandinavica*, 119(3), 267–275. <https://doi.org/10.1111/j.1748-1716.1983.tb07337.x>
- Schwarzkopf, D. S. (2015). Where is size in the brain of the beholder?. *Multisensory research*, 28(3-4), 285–296.
- Soechting, J. F., & Flanders, M. (1992). Moving in three-dimensional space: frames of reference, vectors, and coordinate systems. *Annual Review of Neuroscience*, 15, 167–191. <https://doi.org/10.1146/annurev.neuro.15.1.167>
- Stevens, J. C., & Choo, K. K. (1996). Spatial Acuity of the Body Surface over the Life Span. *Somatosensory & Motor Research*, 13(2), 153–166. <https://doi.org/10.3109/08990229609051403>
- Stone, K. D., Keizer, A., & Dijkerman, H. C. (2018). The influence of vision, touch, and proprioception on body representation of the lower limbs. *Acta Psychologica*, 185, 22–32. <https://doi.org/10.1016/J.ACTPSY.2018.01.007>
- Suffczynski, P., Crone, N. E., & Franaszczuk, P. J. (2014). Afferent inputs to cortical fast-spiking interneurons organize pyramidal cell network oscillations at high-gamma frequencies (60–200 Hz). *Journal of Neurophysiology*, 112(11), 3001–3011. <https://doi.org/10.1152/jn.00844.2013>
- Talairach, J., & Bancaud, J. (1973). *Stereotaxic Approach to Epilepsy* (Vol. 5, pp. 297–354). Karger Publishers. <https://doi.org/10.1159/000394343>
- Taylor-Clarke, M., Kennett, S., & Haggard, P. (2002). Vision Modulates Somatosensory Cortical Processing. *Current Biology*, 12(3), 233–236. [https://doi.org/10.1016/S0960-9822\(01\)00681-9](https://doi.org/10.1016/S0960-9822(01)00681-9)
- Weinstein, S. (1968). Intensive and Extensive Aspects of Tactile Sensitivity as a Function of Body Part, Sex and Laterality. *The Skin Senses*. Retrieved from <https://ci.nii.ac.jp/naid/10000031475/>
- Winlove, C. I. P., Milton, F., Ranson, J., Fulford, J., MacKisack, M., Macpherson, F., & Zeman, A. (2018). The neural correlates of visual imagery: A co-ordinate-based meta-analysis. *Cortex*, 105, 4–25. <https://doi.org/10.1016/j.cortex.2017.12.014>
- Witt, J. K. (2011). Action's Effect on Perception. *Current Directions in Psychological Science*, 20(3), 201–206. <https://doi.org/10.1177/0963721411408770>
- Witt, J. K., & Proffitt, D. R. (2005). *See the Ball, Hit the Ball Apparent Ball Size Is Correlated With Batting Average*. Retrieved from <http://www.baseball-almanac.com/players/>
- Wold, A., Limanowski, J., Walter, H., & Blankenburg, F. (2014). Proprioceptive drift in the rubber hand illusion is intensified following 1 Hz TMS of the left EBA. *Frontiers in Human Neuroscience*, 8, 390. <https://doi.org/10.3389/fnhum.2014.00390>
- Wolpert, D. M., Diedrichsen, J., & Flanagan, J. R. (2011). Principles of sensorimotor learning. *Nature Reviews Neuroscience*, 12(12), 739–751. <https://doi.org/10.1038/nrn3112>
-

Acknowledgements

First, I would like to express my gratitude to Prof. Gabriella Bottini and Prof. Lucia Melloni for their invaluable advice and guide during this research journey.

I have been welcomed and generously supported by the Neuroscience Department of the Max-Planck Institute for Empirical Aesthetics in Frankfurt during my long visiting period. I take the occasion to thank all its members and in particular its director Prof. David Poeppel.

I would like to thank all the colleagues (and friends) who have supported and advised me, and with whom I had the opportunity to entertain enriching discussions, as well as joyful moments. Among the others, a special thank to Martina Gandola, Francesca Magnani, Gabriele de Maio, Pina Scarpa, Gerardo Salvato, Cristian Romaniello and Alessio Toraldo in Pavia; and to Ava Kiai, Dooyoung Kim, Valerie Pu and Martian Gonzalez Vilas in Frankfurt.

I am indebt with the lab managers, the master students and the administrative personnel of the Brain and Behavioural Sciences Department of the University of Pavia and of the Max-Planck Institute for Empirical Aesthetics in Frankfurt. I would particularly like to thank Francesco Nigito, Jessica Liotta, Sara Longo and Luisella Bellavita in Pavia, and Cornelius Abel, Dominik Thiele, Freya Materne, Claudia Lehr, Daniela Van Hinsberg, Cordula Ullah and Anja Tydecks in Frankfurt.

Needless to say, I owe my deepest gratitude to my incredible family and my precious friends from Italy (in detail, from Codogno, Casale, Zorlesco, Morbegno, Maleo, Senna Lodigiana, Montagna in Valtellina, Pavia, Pieve Porto Morone, Casorate Primo, Pietra Ligure) as well as those from Germany, Mexico, China, Turkey, Argentina, Korea and the USA.
